

For Reference

NOT TO BE TAKEN FROM THIS ROOM

Ex LIBRIS
UNIVERSITATIS
ALBERTAENSIS



T H E U N I V E R S I T Y O F A L B E R T A

RELEASE FORM

NAME OF AUTHOR..... Simon A. Barton.....
TITLE OF THESIS..... Vibrational Dynamics of the
..... Hydrogen Bond
.....
.....
DEGREE FOR WHICH THESIS WAS PRESENTED..... Ph.D..
YEAR THIS DEGREE GRANTED..... 1979.....

Permission is hereby granted to THE UNIVERSITY
OF ALBERTA LIBRARY to reproduce single copies of
this thesis and to lend or sell such copies for
private, scholarly or scientific research purposes
only.

The author reserves other publication rights,
and neither the thesis nor extensive extracts from
it may be printed or otherwise reproduced without
the author's written permission.

THE UNIVERSITY OF ALBERTA

VIBRATIONAL DYNAMICS OF THE HYDROGEN BOND

by



SIMON A. BARTON

A THESIS

SUBMITTED TO THE FACULTY OF GRADUATE STUDIES AND
RESEARCH IN PARTIAL FULFILMENT OF THE REQUIREMENTS
FOR THE DEGREE OF DOCTOR OF PHILOSOPHY

IN

CHEMISTRY

EDMONTON, ALBERTA

FALL 1979

THE UNIVERSITY OF ALBERTA
FACULTY OF GRADUATE STUDIES AND RESEARCH

The undersigned certify that they have read, and recommend to the Faculty of Graduate Studies and Research, for acceptance, a thesis entitled VIBRATIONAL DYNAMICS OF THE HYDROGEN BOND submitted by Simon A. Barton in partial fulfilment of the requirements for the degree of Doctor of Philosophy in Chemistry.

ABSTRACT

A general treatment of non-harmonic vibrational dynamics in an isolated hydrogen bond is presented, based on an *adiabatic* mode separation of hydrogenic motions from those of the heavier particles.

The validity of the Stepanov (adiabatic) approximation is examined by including correct non-adiabatic couplings and solving the resultant coupled eigenvalue problem for a model system (HF_2^-) in which the couplings are expected to have a maximum intrinsic strength. Convergence is demonstrated by including up to three coupled protonic states. Comparison with exact results thus obtained shows that the adiabatic approximation gives transition frequencies within 1%, and infrared relative intensities to about 10% - in cases where the coupled protonic levels are not degenerate. Cases of isolated strong coupling, arising from accidental or systematic degeneracies of proton levels, can be accommodated in the theory in a direct way, but do not arise for HF_2^- .

Calculations on the HF_2^- system are based entirely on the *ab initio* potential energy surface of Almløf (Ref. 24), but employ a model form with correct dissociation properties. The close agreement of computed and observed transition frequencies, and IR relative intensities, leads to a convincing assignment (in the adiabatic mode description) for nearly all transitions in the bifluoride spectrum (e.g. in $\text{KHF}_2(\text{s})$), on the basis of an isolated ion model.

ACKNOWLEDGMENTS

This project was conceived by Dr. W.R. Thorson, who has provided essential theoretical direction and computational advice throughout the work.

Dr. J.E. Bertie has also influenced the direction of this work, with much valuable critical comment.

The financial support of a National Research Council Postgraduate Scholarship, for the years 1974-77, is gratefully acknowledged.

TABLE OF CONTENTS

CHAPTER		PAGE
I	INTRODUCTION	1
	A. Purpose	1
	B. Previous Vibrational Calculations	6
	1. General Formulation	6
	2. Direct Two-dimensional Solutions	8
	3. Adiabatic Representations	12
II	GENERAL THEORY	19
	A. Vibrational Coordinates	19
	1. Centre of Mass Motion	19
	2. Jacobi Relative Coordinates	19
	3. Separation of Vibration and Rotation	20
	4. Harmonic and Adiabatic Mode Descriptions	22
	B. Adiabatic Representation	22
	1. Expansion Basis	22
	2. Coupled Equations	23
	3. Stepanov Approximation	25
	C. Separation of Bending and Stretching Potentials	26
	1. Approximations	26
	2. Couplings	29
	3. Equations for Stretching Motion	31

CHAPTER		PAGE
	D. Modified Adiabatic Representation	34
	1. Introduction	34
	2. Coordinates	38
	3. The Non-Linear Transformation	41
	4. Modified Coupled Equations	43
	5. Asymptotic Cancellation of \underline{P} and \underline{A}	45
	E. Summary	47
III	BIFLUORIDE ION POTENTIAL FUNCTION	50
	A. <i>Ab initio</i> and Empirical Results	50
	B. An Asymptotically Reasonable Form	55
	1. The polynomial form of Almløf	55
	2. The Jiang and Anderson form	62
	3. Summary	66
IV	THE VIBRATIONAL BORN-OPPENHEIMER STATES:	68
	A. General Eigenvalue Condition	68
	B. Symmetric Potential	71
	1. Constraints	71
	2. Numerical Method	72
	3. Eigenvalue Initialization	74
	4. Normalization	74
	5. Matrix Elements: P_{ij} ; A_{ij} ; C_{ij} .	75
	C. Results.	78
	1. HF_2^-	78
	2. Deuterium Shifts	87
	3. Asymptotic Values	88

CHAPTER		PAGE
V	SOLUTION OF THE COUPLED EQUATIONS	93
	A. Eigenvalue Condition	93
	B. Open and Closed Channels	97
	1. Zero Coupling	97
	2. Non-zero Coupling	98
	C. Linear Dependence	99
	1. Reorthogonalization	99
	2. Extended Definition	101
	3. Nodes	102
	D. Symmetric Potential Parity Separation	104
	E. Eigenfunctions	104
	1. Construction	104
	2. Three Channel Example	107
	3. Normalization	108
	F. IR Relative Intensities	108
	G. Curve Fits for HF_2^-	111
	1. Matrix Elements	112
	2. $\{U_n\}$ and $\{I_{KJ}\}$	114
VI	RESULTS AND DISCUSSION FOR HF_2^-	116
	A. Eigenvalues and Eigenfunctions:	116
	1. Uncoupled States	116
	2. Coupling Effects	120
	3. Summary	143
	B. Transition Frequencies and Relative Intensities	143

CHAPTER	PAGE
C. Conclusions	153
1. Stepanov Approximation	153
2. Vibrational Spectrum of the Bifluoride Ion	155
REFERENCES	159

LIST OF TABLES

Table	Description	Page
1.	Even Parity Eigenvalues (HF_2^-)	125
2.	Odd Parity Eigenvalues (HF_2^-)	126
3.	Transition Frequencies (cm^{-1})	144
4.	Relative Intensities: B = zero	146
5.	Relative Intensities: B negative	147
6.	Relative Intensities: B positive	148

LIST OF FIGURES

Figure		Page
2.1	Molecular Vibrational Coordinates	21
2.2	Jacobi Coordinates for a Linear Bond	36
3.1	Coordinates for the Linear Bifluoride Ion	57
3.2	$V_2^A(R) \times 10^3$ (a.u.) vs. R (a.u.)	59
3.3	$V_1^A(z;R) \times 10^3$ (a.u.) at $R = 4$ to 5 a.u.	60
3.4	$V_1^A(z;R) \times 10^3$ (a.u.) at $R = 5.6, 5.8$ a.u.	61
4.1	Γ (a.u.) ⁻² vs. R (a.u.)	77
4.2	$U_n \times 10^3$ vs. R (a.u.)	79
4.3	$i/\hbar \cdot P_{02}$ & C_{02} (a.u.) ⁻¹ vs. R (a.u.)	81
4.4	$-i/\hbar \cdot P_{04}$ & $-C_{04}$ (a.u.) ⁻¹ vs. R (a.u.)	82
4.5	$i/\hbar \cdot P_{24}$ & C_{24} (a.u.) ⁻¹ vs. R (a.u.)	83
4.6	$i/\hbar \cdot P_{13}$ & C_{13} (a.u.) ⁻¹ vs. R (a.u.)	84
4.7	$-i/\hbar \cdot P_{15}$ & C_{15} (a.u.) ⁻¹ vs. R (a.u.)	85
4.8	$i/\hbar \cdot P_{35}$ & C_{35} (a.u.) ⁻¹ vs. R (a.u.)	86
6.1	Even Parity Uncoupled Eigenstates	118
6.2	Odd Parity Uncoupled Eigenstates	119
6.3	$W(E) \times 10^2$ vs. $E \times 10$ (a.u.)	124
	2 Channels: $E_{71}; E_{03}$	
6.4	PSI 00	128
6.5	PSI 01	129
6.6	PSI 11	130
6.7	PSI 21	131
6.8	PSI 31	132
6.9	PSI 41	133

Figure		Page
6.10	PSI 51	134
6.11	PSI 61	135
6.12	PSI 71	136
6.13	PSI 03	137
6.14	PSI 81	138
6.15	PSI 13	139
6.16	IR Spectrum of KHF_2 at 90°K (Reference 101)	150

CHAPTER ONE

INTRODUCTION

A. Purpose.

The hydrogen bond has been the subject of much experimental and theoretical investigation. This has been summarized in three volumes edited by Schuster, Zundel, and Sandorfy,¹ in several other texts,²⁻⁶ and in many review articles (surveyed to 1977 by Kollman⁷).

The presence of a hydrogen bond (A-H...B) is strongly indicated by the behaviour, in the infrared (IR) spectrum of the band associated with the stretching mode $\nu(\text{A-H})$. Upon hydrogen bonding, this band is lowered in frequency and greatly broadened, with many well defined peaks.⁸ In addition, the frequencies (ν_2, ν_2') of the deformation modes are progressively increased with increasing hydrogen bond (H-bond) strength, and the bands are also generally broad and structured.⁸ It is now widely accepted that this broadening and structure is largely due to strong anharmonic coupling between the A...B symmetric stretching mode (ν_1), the asymmetric A-H vibration (ν_3), and the deformation modes (ν_2, ν_2'). In general, the potential is a non-separable function of the four vibrational coordinates, and cannot be made separable by any linear transformation.

However, since the frequency of the heavy particle vibration (ν_1) is invariably much less than the frequencies associated with the light protonic motions, an *adiabatic* mode separation was suggested by Stepanov.⁹ In the Stepanov approximation, as in the Born-Oppenheimer^{10,11} separation of nuclear from electronic motions, a set of "protonic" eigenstates is defined for each configuration of the heavy nuclei (A...B). These states depend parametrically upon the "heavy particle" coordinate, and each protonic eigenvalue defines an effective potential curve for the heavy particle vibration (ν_1). The curves may be quite different for each protonic state, so that much of the breadth and complexity of the spectrum may be attributed to Franck-Condon^{12,13} progressions in the ν_1 mode, as was pointed out by Sheppard.⁸

This thesis presents a general theoretical treatment of the vibrational dynamics of an isolated H-bond, using adiabatic protonic states as the basis for a representation of the exact vibrational wavefunctions. In this representation (discussed in Chapter Two) there results a set of coupled second order linear differential equations in the heavy particle coordinate, the solutions to which define the total vibrational eigenstates of the system. The Stepanov approximation is a "zero order" description in this representation: the *non-adiabatic coupling* between the adiabatic states is taken to be negligible.

It is necessary to distinguish between non-adiabatic coupling and the "anharmonic coupling" which arises because the H-bond potential function is non-separable. The latter is *not* negligible, and produces a strong dependence in the protonic potential curves on the heavy particle coordinate, and a reciprocally strong dependence in the ν_1 dynamics on the protonic quantum state. These effects may be accurately described in the Stepanov approximation if the non-adiabatic couplings are negligible.

This work examines the effects of non-adiabatic couplings on the validity of the Stepanov approximation. Calculations have been performed for a physically realistic model system in which these couplings are *intrinsically* as strong as they are ever likely to be in a hydrogen bond. The conclusion is that for most purposes the non-adiabatic couplings are indeed intrinsically negligible.

The emphasis on *intrinsic* strength is made for the following reason: in cases where the adiabatic states are degenerate, or nearly so, even very weak non-adiabatic couplings may cause the states to be strongly mixed. The corresponding strong vibronic coupling effects are well known in the Born-Oppenheimer separation (e.g. the Jahn-Teller effect). In hydrogen bonds, the accidental degeneracy, or near degeneracy, of the protonic levels ' $2\nu_2$ ' and ' ν_3 ' would be such a case; the strong coupling ("Fermi resonance"¹⁴) arising in this situation has been

discussed by Witkowski and Wojcik.¹⁵ In this thesis the effects of non-adiabatic couplings are examined for cases where the coupled protonic levels are *not* degenerate.

The non-adiabatic couplings have a coordinate system dependence. In the usual system appropriate to a molecular (H-bonded) situation, they have an undesirable property: they do not vanish as the H-bond dissociates. This defect has been corrected by applying the non-linear coordinate transformation technique of Thorson and Delos¹⁶ (Chapter Two, section D3). A degree of approximation is introduced, but the dominant effects of extending a calculation *beyond the Stepanov description* are retained.

The system used to examine non-adiabatic coupling effects is a realistic model for the (ν_3, ν_1) stretching dynamics in the strongly hydrogen-bonded bifluoride ion (HF_2^-). Calculations were carried out using a model potential surface based entirely on *ab initio* calculations. This model is described in Chapter Three.

It is also necessary to establish techniques for the accurate numerical solutions of (a) the Schroedinger equation describing essentially proton motion at a fixed heavy nuclear configuration (yielding "vibrational Born-Oppenheimer" states, Chapter Four), and (b) the set of coupled equations (Chapter Five). Techniques which are applicable to a linear symmetric system (A-H...A) are described. This is not a restriction imposed by the

general theory, but it does allow a great reduction in computation time.

For HF_2^- , the calculated IR and Raman transition frequencies, and IR relative intensities, allow assignments of lines in the experimental spectrum of crystalline KHF_2 to quantum states defined within the Stepanov description (Chapter Six). This crystal spectrum can be well understood using the isolated ion model.

The theoretical calculation shows, quite independently of the experimental agreement, that with an *adiabatic separation* (Stepanov description) the useful concept of mode excitations may be retained, while accurately including the effects of a non-separable, strongly anharmonic interaction. However, many of the predictions of a simple *harmonic* mode description must be abandoned: overtone frequencies are not integer multiples of fundamentals, the frequency of the heavy particle mode (ν_1) depends strongly on the protonic state, and intensities may differ greatly from those predicted using a harmonic basis; yet the common idea is that each level can be assigned distinct quantum numbers for each of a collection of separate modes. A simple, yet general picture of the vibrational dynamics of an isolated hydrogen bond thus emerges.

B. Previous Vibrational Calculations.

1. General Formulation.

Janoschek¹⁷ has reviewed the methods which have been used in vibrational calculations to date. The usual procedure is:

- (a) centre of mass motion is extracted and ignored;
- (b) the Born-Oppenheimer separation of nuclear and electronic motions is assumed to be valid;
- (c) vibration-rotation interactions are ignored;
- (d) the equilibrium configuration is taken to be linear.

At this point the internal motion of the three nuclei (A-H..B) may be expressed in terms of four vibrational coordinates which correspond, in the harmonic approximation, to "proton stretching" and "A...B stretching" modes, and the degenerate "bending modes". A further approximation is then introduced:

- (e) bending and stretching modes are assumed to be separable.

Coulson and Robertson¹⁸ have pointed out that, since accurate experimental frequencies for the bending modes are not generally available, it is of interest to see what progress can be made by ignoring them.

In the absence of an accurate four-dimensional potential function, some approximate separation of bending and stretching is clearly necessary.

In Chapter Two it is assumed that the bending and stretching motions of the proton are approximately separable at any fixed heavy nuclear separation (R). The separate potentials are then *both* taken to be parametrically dependent on R . It follows that the adiabatic curves for heavy nuclear motion are dependent upon both bending and stretching "vibrational Born-Oppenheimer" eigenstates of the proton. Any Fermi resonances between bending and stretching modes of the proton¹⁵ can be treated by introducing their interaction as a perturbation within the manifold of near-degenerate proton states.

There is evidence¹⁹ that the R -dependence of the potential function for ν_2 is much weaker than that for ν_3 , which implies that an approximate treatment ignoring bending interactions may yield useful results. This is the approach taken here for the specific study of the bifluoride ion.

The main focus of attention, in past calculations and in this thesis, is then upon the two stretching coordinates, and the non-separable two-dimensional potential surface which describes their interaction.

If a pair (q_1, q_3) of generalized Jacobi coordinates (discussed in detail in Chapter Two) is used (corresponding to the stretching modes (ν_1, ν_3) , with associated reduced masses (m_1, m_3)), the vibrational Schroedinger equation contains no cross-terms in the kinetic energy

operator:

$$\{- (\hbar^2/2m_1) \partial^2 / \partial q_1^2 - (\hbar^2/2m_3) \partial^2 / \partial q_3^2 + V(q_3, q_1) - E\} \psi(q_3, q_1) = 0 \quad (1.1)$$

The solution of (1.1), with $V(q_3, q_1)$ from *ab initio* calculation, or from empirical data, or both, has been the main subject of recent vibrational calculations.¹⁷ The methods which have been used fall into two classes:

- (a) "direct" solutions of the two-dimensional equation by expansion in products of harmonic oscillator functions;
- (b) adiabatic representations.

A brief discussion of these methods follows.

2. Direct Two-Dimensional Solutions.

An eigenfunction $\psi_n(q_3, q_1)$, which satisfies (1.1) under appropriate boundary conditions, may be expressed as a linear combination of binary products of harmonic oscillator (ho) functions in q_1 and q_3 :

$$\psi_n(q_3, q_1) = \sum_{i,j} C_{nij} \cdot X_i(q_3) \cdot X_j(q_1) \quad ; \quad (1.2)$$

where

$$X_i(q_k) = H_i(\eta_k q_k) \cdot \exp(-0.5\eta_k^2 \cdot q_k^2), \quad (k = 1 \text{ or } 3) \quad (1.3)$$

and $\{H_i\}$ are normalized Hermite polynomials.

The coefficients $\{C_{nij}\}$ are obtained, for a given basis size N , by application of the variational principle.

Diagonalization of the resulting $N \times N$ matrix yields upper bounds on the first N eigenvalues. The exponents (η_1, η_3) may initially be fixed using either the transition frequencies ν_1 and ν_3 (as Ibers,²⁰ and Singh and Wood²¹), or the curvature at the minimum of the potential surface (as Janoschek *et al.*^{22,23}), or they may be treated as further variational parameters (as Almløf²⁴). In principle, the values for $\{\eta_k\}$ are not critical, because the functions $\{X_i(q_k); i = 1, 2, \dots, \infty\}$ are complete in q_k space, but a judicious choice will speed the convergence of (1.2).

The problems of convergence and interpretation are the main difficulties with this approach to the solution of (1.1).

Without exception, those who have applied this "matrix expansion" method have used a polynomial form for the representation of the potential surface:

$$V(q_3, q_1) = \sum_{k, \ell} a_{k\ell} q_1^k q_3^\ell \quad (1.4)$$

The coefficients $\{a_{k\ell}\}$ are then obtained either from experimental data,^{20,21} or by least-squares fit to *ab initio* data points.²²⁻²⁴ The number of terms used in (1.4) varies greatly: the form of Ibers²⁰ is limited to four (with anharmonic coupling arising only through a term in $q_1 q_3^2$), whereas Almløf²⁴ included eight terms.

The polynomial representation for the potential function is used with good reason: matrix elements $\{H_{ij}\}$,

arising in the secular equations, are readily calculated. Unfortunately, it has been found necessary to use large basis sets in order to ensure convergence for the lower eigenvalues: Singh and Wood²¹ required $N = 144$, and Almløf²⁴ had $N = 160$.

Janoschek *et al.*^{22,23} have used non-orthogonal basis sets for double-minimum surfaces (with the h_o functions localized at the minima: a two centre expansion), in order to provide more rapid convergence ($N = 32$). This introduces overlap integrals $\{S_{ij}\}$ into the secular equations, and consequently the possibility of over-completeness for the higher eigenstates (as N increases, or as the minima coalesce, the matrix \underline{S} becomes singular).

The question of convergence to an accurate eigenvalue is particularly disturbing with a polynomial representation for the potential surface. The surface given by (1.4) may be accurate in the region of the equilibrium configuration (where *ab initio* or empirical data have been used to define the coefficients), but as the hydrogen bond dissociates the representation inevitably becomes very poor.

In addition, having achieved convergence with many h_o products, it may become difficult to interpret the associated eigenfunctions in a conceptually useful manner.

Previous vibrational calculations for the bifluoride ion^{20,24} have used this approach, and will be further

discussed in Chapter Three. Other systems which have been investigated using this two-dimensional treatment are H_5O_2^+ ,^{22,25} and H_3Cl_2^+ .²³

The work of Singh and Wood²¹ is of particular relevance to this thesis, as they have made a quantitative estimation of the validity of the Stepanov approximation for the lower lying levels of a model H-bonded system. Their four term polynomial representation of the potential function (Ibers form²⁰) was chosen to approximate the symmetric double minimum function appropriate to O-H...O systems. Coefficients a_{10} , a_{01} and a_{04} (equation (1.4)) were fixed by requiring $\nu_1 \simeq 175 \text{ cm}^{-1}$, $\nu_3 \simeq 3000 \text{ cm}^{-1}$, and a barrier height $\simeq 5000 \text{ cm}^{-1}$, while the anharmonic coupling parameter a_{12} was related to an equilibrium configuration. Their results show very close agreement (within 1% for the lower levels) between eigenvalues calculated by the two-dimensional matrix expansion method, and the corresponding Stepanov approximation values (which they obtained by first solving the one-dimensional Schroedinger equation (ho basis in q_3) for m_3 , at fixed q_1 values, yielding protonic eigenvalue curves, and then solving the one-dimensional equations (ho basis in q_1) using these curves as potential surfaces for m_1).

With this model they have convincingly shown that the Stepanov approximation is very good for H-bonds of weak to medium strength, involving for example, oxygen

and nitrogen, but they have not quantitatively investigated the energy levels for a strong bond such as the bifluoride ion.

In a later paper²⁶ Singh and Wood have studied the Stepanov approximation for the bifluoride ion, but only in relation to the contraction (ΔR) in equilibrium F-F distance upon deuteration.^{20,28-30} Again using a four term polynomial representation (with the coefficients of Ibers and Delaplane,²⁷ empirically estimated for HF_2^-) for the potential function, they found that a Stepanov calculation accurately reproduces the isotope contraction, and have suggested that the lower energy states are therefore well approximated.

3. Adiabatic Representations.

The Hamiltonian of (1.1) may be written:

$$H(q_3, q_1) = (p_1^2/2m_1) + h(q_3; q_1) \quad , \quad (1.5)$$

where

$$h(q_3; q_1) = (p_3^2/2m_3) + V(q_3; q_1) \quad , \quad (1.6)$$

and p_j is the momentum operator, $-i\hbar \partial/\partial q_j$ ($j = 1, 3$).

Recall that q_1 and q_3 are a pair of generalized Jacobi coordinates with associated relatively heavy and light reduced masses (m_1 and m_3) respectively. There are three possible choices for this pair (described in

Chapter Two), each of which is appropriate for a particular configuration (A-H....B, A-H-B, A....H-B). There is an important significance to this choice, which will be discussed in detail in Chapter Two, in connection with the asymptotic behaviour of the non-adiabatic coupling terms. For any choice, however, the adiabatic representation employs eigenfunctions of the "protonic" Hamiltonian $h(q_3; q_1)$ (calculated at any fixed value of q_1) as basis states for an expansion of the total wavefunction:

$$\psi_j(q_3, q_1) = \sum_{\ell}^N f_{j\ell}(q_1) \phi_{\ell}(q_3; q_1) \quad , \quad (1.7)$$

with $\{\phi_{\ell}\}$ defined by:

$$h(q_3; q_1) \phi_{\ell}(q_3; q_1) = U_{\ell}(q_1) \phi_{\ell}(q_3; q_1) \quad (1.8)$$

It is shown in Chapter Two that substitution of (1.7) into (1.1) results in an $N \times N$ set of coupled equations for the functions $\{f_{j\ell}\}$ in q_1 space. The coupling arises from terms:

$$P_{k\ell}(q_1) \equiv \int_{-\infty}^{+\infty} \phi_k^* p_1 \phi_{\ell} dq_3 \quad . \quad (1.9)$$

The adiabatic (Stepanov) *approximation* neglects these terms (i.e., assumes the protonic states change "slowly" with respect to q_1). The equations which result in the adiabatic approximation are then very simple:

$$[p_1^2/2m_1 + U_{\ell}(q_1)] f_{j\ell}(q_1) = E_{j\ell} f_{j\ell}(q_1) \quad . \quad (1.10)$$

Equation (1.10) describes the motion of a mass m_1 on a proton-state-dependent potential curve U_ℓ (ℓ gives the state of excitation of the proton). For each protonic curve there are associated eigenvalues $\{E_{j\ell}; j = 0, 1, 2, \dots\}$, and so the *adiabatic separation* has retained the concept of a *mode description*: total eigenstates may be labelled by a double index: $|j, \ell\rangle$. Changes in ℓ (for fixed j) refer to excitation of the "A-H stretching mode" (ν_3), and changes in j (for fixed ℓ) refer to excitation of the "A..B mode" (ν_1). Of course, these are not excitations of any "pure mode" in the sense of a harmonic separation, but it is a useful concept. Because of a shift in the minima and form of the excited state curves $\{U_\ell\}$, a Franck-Condon effect is expected: the combination bands " $m\nu_3$ " \pm " $n\nu_1$ " will have significant intensities.

The adiabatic description has been extensively employed by Marechal, Witkowski, and numerous co-workers.^{15,31-45} As they were concerned with asymmetric H-bonds of weak to medium strength, they have treated the potential function in the following empirical manner: the proton motion is assumed to be harmonic, but with force constant and equilibrium position parametrically dependent upon the A...B separation. They write:

$$V(q, Q) = 1/2 \cdot m\omega^2(Q) [q - q_0(Q)]^2 + 1/2 \cdot M\Omega^2 (Q - Q_0)^2 \quad (1.11)$$

(where q is to be identified with q_3 , Q with q_1 , and (m, M)

with (m_3, m_1) ; w and Ω are protonic and heavy particle frequencies respectively).

By expanding $w(Q)$ and $q_0(Q)$ about the equilibrium value Q_0 , in powers of Q , and retaining only linear terms, they have related the principal anharmonic coupling to the parameter $(dw/dQ)_{Q_0}$. By a quantitative examination of the potential surfaces of Reid⁴⁶ (which are based on the empirical potential function of Lippincott and Schroeder,⁴⁷ for O-H...O systems) they concluded that $(dq_0/dQ)_{Q_0}$ and higher terms are of much less importance.

In their model the ground state protonic curve $U_0(Q)$ is harmonic:

$$U_0(Q) \simeq \text{const.} + 1/2 \cdot M\Omega^2 (Q - Q_0)^2, \quad (1.12)$$

whereas the curve for the first excited state of the proton is vertically displaced and linearly distorted:

$$U_1(Q) \simeq U_0(Q) + r + bQ, \quad (1.13)$$

where r is the "vertical excitation energy"¹⁵ (essentially ν_3), and b is related to $(dw/dQ)_{Q_0}$. In practice b is altered to give a good spectral fit (it is an empirical parameter in their theory).

Within this model, they have estimated³³ the effect of non-adiabatic coupling as a perturbation of harmonic functions in Q space. They find the perturbation energy to be about $1/300$ of the proton quantum energy, $\hbar w(Q_0)$,

and consequently discard the non-adiabatic coupling terms.

Assuming, then, the validity of the Stepanov approximation within an isolated H-bond, and introducing empirical forms for the surfaces $\{U_\ell\}$, their work then explores couplings between identical A-H..B units, (e.g., in carboxylic acid dimers³³) which have degenerate Stepanov eigenstates in zero order.

Similar adiabatic/harmonic models have been used to study interactions between many bonds (e.g., in the lattice), and have been reviewed by Hofacker, Marechal, and Ratner.⁴⁸

A similar approach is also taken by Sokolov and Savel'ev,⁴⁹ who have shown that the main characteristics of the H-bond spectra of asymmetric (A-H..B) and symmetric (A-H..A) systems may be understood within the adiabatic approximation. They have also estimated the adiabatic coupling effects as a perturbation within the adiabatic/harmonic model, and have concluded that even for the strongly bonded bifluoride ion, the effects are small for the low energy states.

Coulson and Robertson⁵⁰ have assumed the validity of the adiabatic approximation in their detailed study of MeOHX (X = Cl, F) systems. Their potential function model is very simple, consisting of the sum of either a quadratic or a Morse function in the X-H bond length (they consider both cases), and a Morse function in the

O-H distance. Even with such a simple function, for which the anharmonicity of the X-H stretching mode is *unaffected* by H-bond formation, the potential is *non-separable* in an appropriate Jacobi coordinate system, and gives rise to substantial combination band intensities. Robertson⁵¹ extended the calculation to include a potential term explicitly dependent upon both X-H and O-H distances (effectively allowing the potential for the X-H mode to be X-O dependent), but he still calculated line positions and relative intensities within the adiabatic approximation.

Finally, Anderson and Lippincott,⁵² and Jiang and Anderson⁵³⁻⁵⁵ (using modified Lippincott and Schroeder⁴⁷ forms for the potential) have numerically calculated the protonic eigenvalue curves for several systems. They estimated "vertical transition frequencies" between these curves, but have not discussed non-adiabatic couplings. The functional form of Jiang and Anderson⁵³ for the potential in HF_2^- , has been adapted in this thesis to give a reasonable fit to the *ab initio* data points of Almløf,²⁴ and will be discussed in detail in Chapter Three.

Evidently the adiabatic separation of heavy nuclear and protonic motions is widely accepted in the literature, for both weak and strong hydrogen bonds. However, none of these studies in the adiabatic representation have explicitly investigated the form of the non-adiabatic

couplings, or have included them in any extension of a calculation beyond the Stepanov approximation.

CHAPTER TWO

GENERAL THEORY

A. Vibrational Coordinates.

1. Centre of Mass Motion.

For a system of N particles of total mass M , upon which no external forces act, the motion of the centre of mass (CM) is separable from the relative motions of the particles, and is just the free translation of a particle of mass M . In the following treatment this motion has been extracted and ignored (in a crystal environment (e.g., KHF_2) this degree of freedom is associated with lattice modes). The internal motion of the system is then described using $N-1$ relative vectors.

2. Jacobi Relative Coordinates.

The use of N generalized Jacobi vectors, one of which is the vector position of the CM, leads to a diagonal kinetic energy operator (containing no cross terms). A detailed account is given by Blokhintsev.⁵⁶ For three particles (nine degrees of freedom), a Jacobi system consists of 3 *external* coordinates (defining the position of CM), and 6 *internal* coordinates (two relative vectors). One internal vector connects any chosen pair of the particles, and the other gives the position of the third particle from the centre of mass of the chosen pair.

The definition of a Jacobi system does not specify any preferred pair, and the three different sets are each appropriate in a different physical configuration (section D2 of this Chapter).

3. Separation of Vibration and Rotation.

Under the assumption that the vibration of a molecular system does not significantly alter the equilibrium inertial axes and moments (i.e., the molecular frame is essentially rigid) the approximate separation of rotation and vibration is well established.⁵⁷ If the H-bond is not isolated the rotational degrees of freedom may appear as lattice modes (e.g., in the bifluoride salts), or as "rocking modes" (e.g. in the gas phase ether-HCl systems⁵⁸⁻⁶⁰). Interactions with such modes will not be considered here. It will be assumed that the H-bond has a *linear* equilibrium configuration, and the free rotation of the inertial axis will be removed and ignored. This axis then defines the reference frame for the four (3N-5) vibrational coordinates.

Using Jacobi coordinates R and \vec{r} (Figure 2.1) appropriate to the "molecular" configuration, the vibrational Schroedinger equation is:

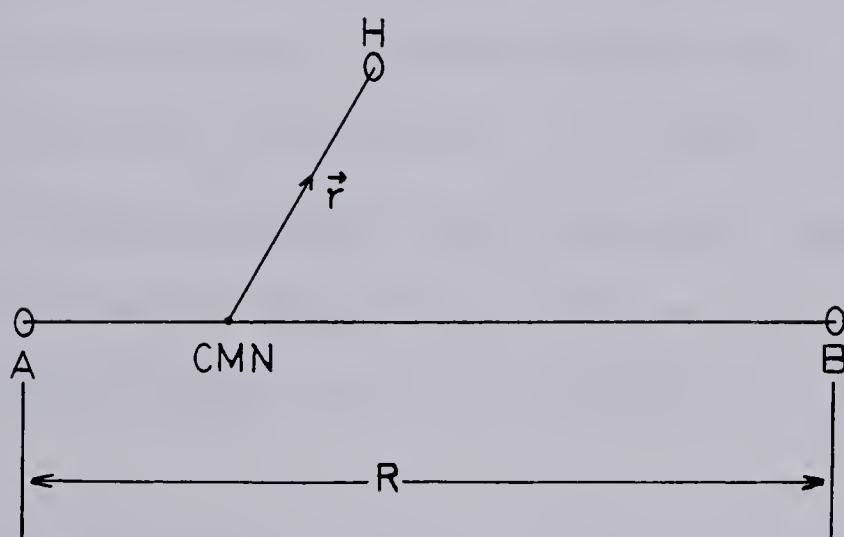
$$\{- (\hbar^2/2\mu) \partial^2 / \partial R^2 - (\hbar^2/2m) \vec{\nabla}_r^2 + V(\vec{r}, R) - E\} \psi(\vec{r}, R) = 0 ; \quad (2.1)$$

where μ is a "heavy particle" reduced mass:

$$\mu = M_A M_B / (M_A + M_B) \quad , \quad (2.2)$$

FIGURE 2.1

MOLECULAR VIBRATIONAL COORDINATES



CMN = CENTRE OF MASS OF A, B

and m is the "molecular" proton reduced mass:

$$m = M_H (M_A + M_B) / M_T \quad . \quad (2.3)$$

M_A , M_B , M_H are the atomic masses, and M_T is their sum.

The solution of (2.1), with appropriate boundary conditions, yields vibrational eigenvalues $\{E_j\}$ and corresponding eigenfunctions $\{\psi_j(\vec{r}, R)\}$.

4. Harmonic and Adiabatic Mode Descriptions.

One may strictly refer to isolated vibrational modes only if the potential surface $V(\vec{r}, R)$ is a separable function of the four coordinates. In such a case there would be two stretching modes (symmetric and asymmetric), and two bending modes (degenerate for an isolated linear bond). These modes might be harmonic in a first approximation.

The H-bond potential is certainly non-separable; but if an *adiabatic* separation is shown to be possible, then a mode description may nevertheless be retained (as discussed in Chapter One, section B3).

B. Adiabatic Representation.

1. Expansion Basis.

If at any point R_i , in R space, there exists a complete set of functions $\{\phi_\ell(\vec{r}; R_i)\}$ which span the \vec{r} space, then any function of \vec{r} , defined at R_i , may be expanded in this

set. With the assumption of continuity in R , for each member of $\{\phi_\ell\}$, the wavefunction $\psi_j(\vec{r}, R)$ may be written:

$$\psi_j(\vec{r}, R) = \sum_{\ell} f_{j\ell}(R) \cdot \phi_\ell(\vec{r}; R). \quad (2.4)$$

In the adiabatic representation, the complete set $\{\phi_\ell\}$ is chosen to be the set of eigenfunctions of the Hamiltonian for the reduced mass m (i.e., essentially protonic vibrational Born-Oppenheimer states):

$$h(\vec{r}; R) \phi_\ell(\vec{r}; R) = U_\ell(R) \phi_\ell(\vec{r}; R) \quad , \quad (2.5a)$$

where

$$h(\vec{r}; R) \equiv -(\hbar^2/2m) \vec{\nabla}_r^2 + V(\vec{r}; R) \quad . \quad (2.5b)$$

In equations (2.5), the semi-colon indicates that R is treated as a fixed parameter. At any R , the functions $\{\phi_\ell\}$ are eigenfunctions of an Hermitian operator in \vec{r} , and therefore form a complete set in \vec{r} , with corresponding eigenvalues $\{U_\ell\}$.

2. Coupled Equations.

Using the expansion (2.4), with $\{\phi_\ell\}$ defined by (2.5), the Schroedinger equation (2.1) gives:

$$\sum_{\ell} \{ -(\hbar^2/2\mu) \partial^2 / \partial R^2 + [U_\ell(R) - E_j] \} f_{j\ell}(R) \phi_\ell(\vec{r}; R) = 0 \quad . \quad (2.6)$$

For any operator A , the bracket notation shall be defined by:

$$\langle k|A|\ell\rangle \equiv \int \phi_k^*(\vec{r};R) A \phi_\ell(\vec{r};R) d\vec{r} \quad , \quad (2.7)$$

so that (2.6) becomes:

$$\sum_{\ell} \{ -(\hbar^2/2\mu) [\langle k|\partial^2/\partial R^2|\ell\rangle f_{j\ell}(R) + f_{j\ell}''(R) \delta_{k\ell} + 2\langle k|\partial/\partial R|\ell\rangle f_{j\ell}'(R)] + [U_\ell(R) - E_j] f_{j\ell}(R) \delta_{k\ell} \} = 0 \quad . \quad (2.8)$$

A coupling matrix $\underline{P}(R)$ is now defined, with elements:

$$P_{k\ell}(R) \equiv -i\hbar \langle k|\partial/\partial R|\ell\rangle \quad , \quad (2.9)$$

which leads to the identity:

$$-\hbar^2 \langle k|\partial^2/\partial R^2|\ell\rangle = -i\hbar P_{k\ell}'(R) + [\underline{P}^2(R)]_{k\ell} \quad ; \quad (2.10)$$

and (2.8) may be written:

$$\sum_{\ell} \{ -\hbar^2/2\mu) [(i/\hbar) P_{k\ell}' \cdot f_{j\ell} - (1/\hbar^2) (\underline{P}^2)_{k\ell} \cdot f_{j\ell} + f_{j\ell}'' \cdot \delta_{k\ell} + (2i/\hbar) P_{k\ell} \cdot f_{j\ell}'] + [U_\ell - E_j] f_{j\ell} \cdot \delta_{k\ell} \} = 0 \quad (2.11)$$

This takes the simple matrix form:

$$\{ (1/2\mu) [-i\hbar \cdot d/dR \cdot \underline{I} + \underline{P}(R)]^2 + [\underline{U}(R) - E_j \underline{I}] \} \underline{f}_j(R) = \underline{0} \quad (2.12)$$

$\underline{f}_j(R)$ is a column vector with components $\{f_{j\ell}\}$,

\underline{I} is the unit matrix, and $U(R)$ is diagonal with elements $\{U_\ell\}$.

These coupled equations were originally derived, for a general adiabatic representation, by Born and Huang.⁶¹

In principle, an exact solution to the vibrational eigenvalue problem may be obtained by solving the two sets

of equations, (2.5) and (2.12), with sufficient terms in the expansion (2.4).

3. Stepanov Approximation.

The matrix equation (2.12), resulting from the adiabatic representation, shows that negligible coupling situations ($\underline{P} \approx 0$) lead to the Born-Oppenheimer separation of fast and slow relative motions. The motion of the "slow" heavy reduced mass μ is then determined by one of the protonic energy curves $\{U_\ell(R)\}$ through the uncoupled differential equation:

$$\{-(\hbar^2/2\mu)d^2/dR^2 + U_\ell(R) - E_{j\ell}\}f_{j\ell}(R) = 0 \quad (2.13)$$

These equations (one for each eigenstate of the proton: $\ell = 0, 1, 2, \dots$) provide the basis for the Stepanov approximation (cf. equation (1.10)).

In this case the total eigenfunctions have a single product form:

$$\psi_{j\ell}(\vec{r}, R) = f_{j\ell}(R) \cdot \phi_\ell(\vec{r}; R) \quad (2.14)$$

(one term in expansion (2.4)), and together with eigenvalues $\{E_{j\ell}\}$, may be indexed by " ℓ ", to indicate the protonic state with which they are associated.

A description invoking excitation of the "protonic modes" ν_3 and ν_2 (for which ℓ changes), and the "A...B stretching mode" ν_1 (for which j changes) may be retained,

and their strong interaction will be indicated by shifts in the minima and "force constants" of the curves $\{U_\ell\}$. The intensities of "combination bands" (e.g., $\nu_3 \pm \nu_1$) may be significant, as predicted by the Franck-Condon principle.

The validity of the Stepanov approximation is a major concern of this thesis.

If the coupling between one or more *degenerate or nearly degenerate* levels is not zero, then the Stepanov approximation breaks down, and the wavefunction must be represented by an expansion (2.4), with the sum including all the (near-)degenerate states. An important case is the possible near-degeneracy of the stretching fundamental (ν_3) and the bending overtone ($2\nu_2$). This case has been discussed by Witkowski and Wojcik.¹⁵

This possible degeneracy represents a "special case" in the Stepanov approximation, and does not occur in the HF_2 - system considered here as a test problem for the "normal" validity of the approximation.

C. Separation of Bending and Stretching Potentials.

1. Approximations.

In attempting a solution of (2.5):

$$\{-(\hbar^2/2m)\nabla_{\vec{r}}^2 + V(\vec{r};R)\}\phi_\ell(\vec{r};R) = U_\ell(R)\phi_\ell(\vec{r};R) \quad , \quad (2.5)$$

the following approximate separation of the potential

will be made:

$$V(\vec{r};R) \simeq V_z(z;R) + V_{xy}(x,y;R) \quad , \quad (2.15)$$

where the z coordinate of \vec{r} is defined to be collinear with R .

For an isolated linear H-bond, the potential energy will not be dependent on the cylindrical polar angle ϕ (cylindrical symmetry), and (2.15) may be written:

$$V(\vec{r};R) \simeq V_z(z;R) + V_\rho(\rho;R) \quad (2.16a)$$

where $\rho = x^2 + y^2$.

It may be further assumed that V_ρ is approximately harmonic, but with an R -dependent force constant, giving:

$$V(\vec{r};R) \simeq V_z(z;R) + 1/2 \cdot K_\rho(R) \rho^2 \quad . \quad (2.16b)$$

With (2.16b) the Schroedinger equation is separable in cylindrical polar coordinates. The details are given by Pauling and Wilson.⁶²

The bending motion has been reduced to that of a two-dimensional isotropic oscillator in the x,y (ρ,ϕ) plane.

[If it is observed ($v_2 \neq v_2'$) that environmental effects lift the degeneracy of the bending modes (removing the cylindrical symmetry), V_{xy} can be approximately separated as the sum of harmonic functions with different force constants ($V_{xy} \simeq 1/2 \cdot K_x(R)x^2 + 1/2 \cdot K_y(R)y^2$), and

the development which follows is easily modified].

An eigenstate of (2.5) must now be specified by three quantum numbers: ℓ , n , m . An eigenfunction is:

$$\phi_{\ell nm}(\vec{r}; R) = \alpha_{\ell}(z; R) \beta_{nm}(\rho; R) e^{im\phi} \cdot (2\pi)^{-1/2} \quad , \quad (2.17)$$

with eigenvalue

$$U_{\ell n}(R) = a_{\ell}(R) + b_n(R) \quad , \quad (2.18)$$

where

$$b_n(R) = (n+1)\hbar[k_{\rho}(R)/m]^{1/2} \quad . \quad (n = 0, 1, 2, \dots) \quad (2.19)$$

The eigenvalues $\{b_n\}$ are $(n+1)$ -fold degenerate, corresponding to the possible values of m :

$$\begin{aligned} m &= 0, \pm 2, \pm 4, \dots \pm n && (n \text{ even}) \\ m &= \pm 1, \pm 3, \pm 5, \dots \pm n && (n \text{ odd}) \end{aligned} \quad (2.20)$$

(Note that in (2.19) m is the reduced mass, equation (2.3). No confusion can arise from this dual use of m ; it is always clear from the context).

The $\{\beta_{nm}\}$ satisfy:

$$\begin{aligned} \{ (-\hbar^2/2m) [\partial^2/\partial \rho^2 + (1/\rho)\partial/\partial \rho - m^2/\rho^2] + 1/2 \cdot K_{\rho}(R) \rho^2 \} \beta_{nm} \\ = b_n(R) \beta_{nm} \quad , \end{aligned} \quad (2.21)$$

and are related to the Laguerre polynomials.⁶²

The "stretching mode" eigenfunctions $\{\alpha_\ell\}$ obey the equation

$$\{(-\hbar^2/2m)\partial^2/\partial z^2 + V_z(z;R)\}\alpha_\ell = a_\ell(R)\alpha_\ell, \quad (2.22)$$

where $V_z(z;R)$ is so far unspecified.

2. Couplings.

Consider the effect of (2.17) on the coupled equations (2.12). The expansion (2.4) becomes:

$$\psi_j(\vec{r}, R) = \sum_{\ell, n, m} f_{j, \ell n m}(R) \phi_{\ell n m}(z, \rho, \phi; R), \quad (2.23)$$

and an element of the matrix \underline{P} (equation (2.9)) is:

$$\begin{aligned} -i\hbar \langle \ell' n' m' | \partial/\partial R | \ell n m \rangle = & -i\hbar \delta_{m' m} \left\{ \delta_{n' n} \int_{-\infty}^{\infty} \alpha_{\ell'} \partial/\partial R \alpha_{\ell} dz \right. \\ & \left. + \delta_{\ell' \ell} \int_0^{\infty} \beta_{n' m'} \partial/\partial R \beta_{n m} \rho d\rho \right\} \quad (2.24) \end{aligned}$$

Since, however, the two integrals of (2.24) vanish for $\ell' = \ell$, and $n' = n$, respectively, the only non-zero matrix elements are:

$$-i\hbar \langle \ell' n m | \partial/\partial R | \ell n m \rangle = -i\hbar \int_{-\infty}^{\infty} \alpha_{\ell'} \partial/\partial R \alpha_{\ell} dz \quad (2.25a)$$

and

$$-i\hbar \langle \ell n' m | \partial/\partial R | \ell n m \rangle = -i\hbar \int_0^{\infty} \beta_{n' m} \partial/\partial R \beta_{n m} \rho d\rho \quad (2.25b)$$

That is: vibrational Born-Oppenheimer states of different "stretching" quantum number ℓ are coupled (2.25a), and states of different "bending" quantum number n are

coupled (2.25b), but states of different ℓ and n are not coupled.

This is *not*, however, the same as saying that the bending and stretching modes do not interact.

An interaction arises because an element $U_{\ell n}(R)$, of the diagonal matrix \underline{U} of equation (2.12), is now a sum of independent contributions from both proton stretch and bend eigenvalues (through equation (2.18)), $a_{\ell}(R) + b_n(R)$.

In the *Stepanov approximation*, Franck-Condon progressions $v_3 + "jv_1"$ and $v_2 + "jv_1"$ may both appear, and the *spacing* in each progression will be dependent on both ℓ and n . A "stretching" transition from a curve $U_{\ell n}$ to $U_{\ell', n}$ is therefore dependent on the form of $b_n(R)$, and similarly "bending" transitions from $U_{\ell n}$ to $U_{\ell n'}$ depend on $a_{\ell}(R)$.

It has been observed (a review is given by Hadzi and Bratos¹⁹) that in a series of hydrogen bonded systems with varying bond lengths, the frequencies of the deformation modes increase with increasing bond strength (decreasing R), but "that the increase of the deformation vibration wavenumber is certainly much less"¹⁹ than the decrease in wavenumber for the stretching vibration. That is, $K_{\rho}(R)$ changes much more slowly with R than does $V_z(z; R)$; hence $\{b_n(R)\}$ are more slowly varying than $\{a_{\ell}(R)\}$, and the couplings (2.25b) are likely to be weaker than those given by (2.25a).

An accurate solution for the vibrational dynamics of an isolated hydrogen bond is therefore expected to be obtained with the following procedure:

- (i) assume the separation of bending and stretching potentials as in (2.16);
- (ii) calculate bending eigenstates in the Stepanov approximation (retaining R-dependence of K_ρ , and hence $b_n(R)$);
- (iii) solve the (z,R) dynamics with inclusion of non-adiabatic coupling terms, in order to estimate the validity of the Stepanov approximation;
- (iv) for isolated cases of bending/stretching near-degeneracy, allow for strong coupling¹⁵ by inclusion of any non-separable part of $V(\vec{r},R)$.

This is essentially the treatment which has been applied to the HF_2^- system, except that dependence of the (z,R) motion on the bending quantum number n is ignored. Inclusion of this weak dependence merely redefines the potential curves for heavy particle motion, and does not influence the estimation of the validity of the Stepanov approximation (with which this calculation is mainly concerned).

3. Equations for Stretching Motion.

With the *Stepanov approximation for the bending motion* the total wavefunctions have the form:

$$\psi_j^{(nm)}(\vec{r}, R) = \psi_j^{(n)}(z, R) \beta_{nm}(\rho; R) e^{im\phi}, \quad (2.26)$$

and (2.1) may be reduced to a two-dimensional equation for $\psi_j^{(n)}$:

$$\begin{aligned} \{ -(\hbar^2/2\mu) \partial^2/\partial R^2 - (\hbar^2/2m) \partial^2/\partial z^2 + V_z(z, R) \\ + b_n(R) - E_j^{(n)} \} \psi_j^{(n)} = 0 \end{aligned} \quad (2.27)$$

The effect of $b_n(R)$ is to redefine the heavy particle potential curves. The index n is suppressed (assuming $b_n(R) \sim \text{constant}$ in the region of equilibrium configuration) in the following development of the equations which have been solved for the HF_2^- system.

It is then of interest to solve the vibrational dynamics of the HF_2^- system, considering motion only in the (z, R) coordinates. The two-dimensional Schroedinger equation is:

$$\{ -(\hbar^2/2\mu) \partial^2/\partial R^2 - (\hbar^2/2m) \partial^2/\partial z^2 + V(z, R) - E_j \} \psi_j(z, R) = 0 \quad (2.28)$$

The adiabatic representation then uses

$$\psi_j(z, R) = \sum_{\ell} f_{j\ell}(R) \alpha_{\ell}(z; R), \quad (2.29)$$

where $\{\alpha_{\ell}\}$ satisfy

$$\{ -(\hbar^2/2m) \partial^2/\partial z^2 + V(z; R) \} \alpha_{\ell}(z; R) = U_{\ell}(R) \alpha_{\ell} \quad (2.30)$$

and in this approximation $U_{\ell}(R) \equiv a_{\ell}(R)$.

The coupled equations which result from the substitution of (2.29) into (2.28) are again those shown in equation (2.12), but the elements of the matrix \underline{P} are now just given by (2.25a):

$$P_{\ell, \ell} \equiv -i\hbar \int_{-\infty}^{+\infty} \alpha_{\ell}(z;R) \cdot (\partial/\partial R)_z \cdot \alpha_{\ell}(z;R) \cdot dz \quad . \quad (2.31)$$

The procedure for the solution of the problem now appears to be straightforward:

- (i) define a potential $V(z;R)$;
- (ii) solve equation (2.30) for protonic eigenvalues $\{U_{\ell}(R)\}$ and eigenfunctions $\{\alpha_{\ell}(z;R)\}$;
- (iii) calculate coupling matrix elements $\{P_{\ell, \ell}\}$ using (2.31);
- (iv) solve the coupled equations (2.12) for vibrational eigenvalues $\{E_j\}$, with enough terms in expansion (2.29) to ensure convergence.

Unfortunately, any attempt to carry the calculation "*beyond Stepanov*" encounters an immediate difficulty: the matrix elements $P_{\ell, \ell}(R)$ *do not vanish* as $R \rightarrow \infty$. This behaviour does not result from any approximation in the potential function or the computation; it is inherent in the usual adiabatic representation, and it is the *representation* which must be modified.

D. Modified Adiabatic Representation.

1. Introduction.

In the adiabatic representation described in sections B and C, the total wavefunction $\psi(z,R)$ is expanded in terms of vibrational Born-Oppenheimer (BO) functions *defined on surfaces of constant R*. On each surface the BO functions are *complete* in z space, but the resultant coupled equations (in R space) have undesirable properties. The most significant defect, from the point of view of this thesis, is that the matrix \underline{P} does not vanish asymptotically.

The expansion (2.29) is formally correct, and the coupled equations (2.12) are mathematically exact. However, though formally true, this fact is not of practical use. Problems arise because individual terms in (2.29) do *not* correspond in a one-to-one way with exact eigenstates of the dissociated systems $A-H + B$, and $A + H-B$. This point has been discussed in detail by Thorson and Delos.^{16,64}

The magnitudes of the coupling matrix elements $\{P_{\ell,\ell}\}$ depend, through equation (2.31), upon the rate of change of the states $\{\alpha_{\ell}\}$ with R (holding z fixed). Now the eigenfunctions $\{\alpha_{\ell}\}$, being generated by the Hamiltonian for the reduced mass m , must asymptotically ($R \rightarrow \infty$) approach vibrational eigenfunctions of the diatomics AH

and HB (apart from small reduced mass errors, of order (m/μ) , in both energies and wavefunctions). For the symmetric case A-H-A, the asymptotically degenerate (g,u) states are merely linear combinations of the degenerate pair of diatomic states. In either case, the functions are *constant in form*, since the potential is assumed to take the dissociated form:

$$V(z,R) \xrightarrow{R \rightarrow \infty} V_A(z_A) + V_B(z_B) + V_{AB}(R) \quad (2.32)$$

(z_A and z_B are defined in figure 2.2).

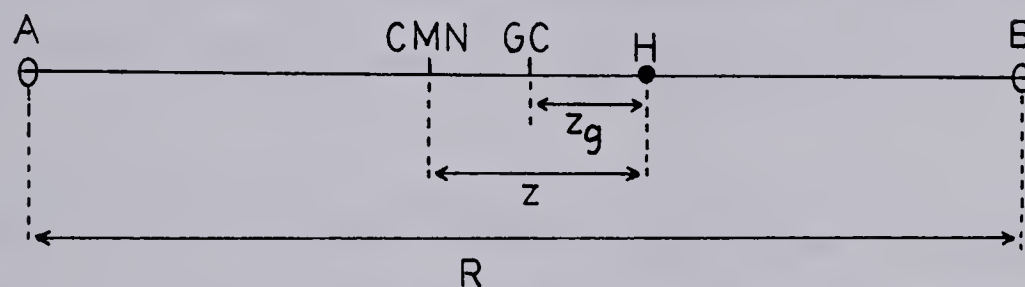
Asymptotically, a state α_ℓ merely translates with respect to CMN (defined in figure 2.1), from which z is measured, and the partial derivative of this function with respect to R , keeping z fixed, is obviously *not* zero, but a constant. Simple displacement of states without distortion cannot give physically real coupling. There is, therefore, no physical basis for coupling between asymptotic states in any reasonable representation of the problem.

In the adiabatic representation the elements $\{P_{\ell,\ell}(R)\}$ approach constant values, the magnitudes of which (relative to their maxima) are not at all negligible (see figures 4.3 to 4.8 for examples of $\{P_{\ell,\ell}(R)\}$ calculated using a realistic potential for HF_2^-).

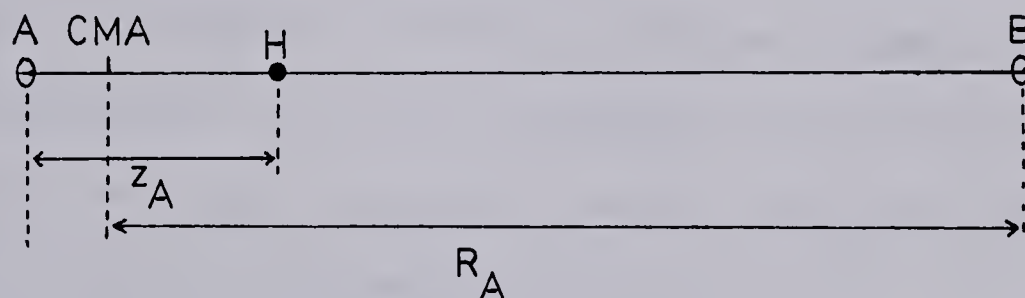
This phenomenon (and other defects, e.g., non-vanishing velocity dependent couplings between g and u states of

Figure 2.2

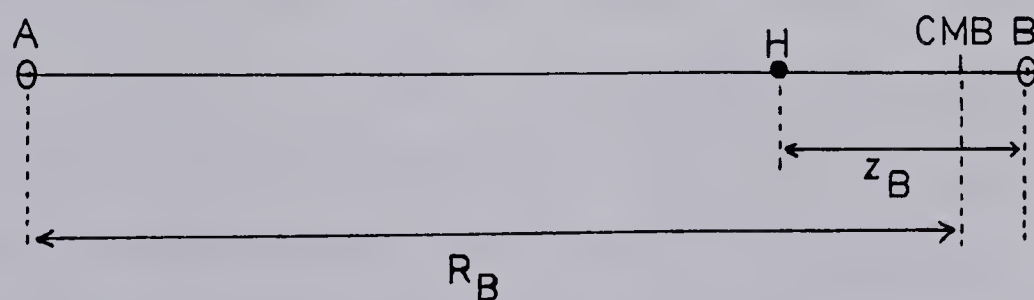
Jacobi Coordinates for a Linear Bond

(2.2a) 'Molecular Configuration'.

$$\mu = M_A M_B / (M_A + M_B); \quad m = M_H (M_A + M_B) / M_T$$

(2.2b) 'A Configuration'.

$$\mu_A = (M_H + M_A) M_B / M_T; \quad m_A = M_H M_A / (M_H + M_A)$$

(2.2c) 'B Configuration'.

$$\mu_B = (M_H + M_B) M_A / M_T; \quad m_B = M_H M_B / (M_H + M_B)$$

$\text{HD}^{+16,63-65}$) is well known in atomic collision theory (a detailed discussion is given by Thorson and Delos^{16,64}), and is the result of translation without deformation of the wavefunctions (this translational origin is demonstrated explicitly for the HF_2^- system in Chapter Four, section C3). The phenomenon does not appear to have been discussed in the literature in the context of the hydrogen bond.

Thorson and Delos¹⁶ have shown that a better representation may be constructed if the basis functions are defined on surfaces of a constant coordinate ξ , related to z and R by a non-linear transformation (originally suggested by Mittleman⁶⁶⁻⁶⁸). ξ is chosen to be essentially a "heavy particle coordinate", which is uniquely specified by the proton position. In the dissociated situations AH or HB, it reduces to the appropriate heavy particle Jacobi coordinate (to be described below).

In the Thorson-Delos¹⁶ (TD) formulation, a wavefunction $\psi_j(z, \xi)$ now satisfies the transformed form of the Schroedinger equation (2.28), and may be expanded in a series of the same *form* as (2.29), with ξ replacing R , since the set of BO states is complete for any *parameter* $\xi \equiv R$. The set of coefficients $\{f_{j\ell}(\xi)\}$ now satisfy a different set of coupled differential equations (*not* (2.12)), and it is the purpose of this section to exhibit these equations.

In order to understand the motivation for the TD choice of transformation, it is necessary to examine the three sets of Jacobi coordinates and their relationships.

2. Coordinates.

Figure 2.2 shows the three possible sets of Jacobi coordinates for a linear hydrogen bond, and their associated reduced masses.

It will also be convenient to use the position (z_g) of H from the geometric centre (GC) of the heavy nuclei A,B (shown in figure 2.2a). z_g is related to z and R by:

$$z_g = z - 1/2 \cdot \lambda R \quad , \quad (2.33)$$

where

$$\lambda \equiv (M_A - M_B) / (M_A + M_B) \quad ; \quad 0 \leq \lambda \leq 1 \quad (2.34)$$

λ is called the "mass asymmetry parameter". Without loss of generality it has been assumed: $M_A \geq M_B$.

Using any one of these sets of coordinates, the kinetic energy operator contains no cross terms:

$$T = -(\hbar^2/2\mu) \partial^2/\partial R^2 - (\hbar^2/2m) \partial^2/\partial z^2 \quad ; \quad (2.35a)$$

$$\text{or } T = -(\hbar^2/2\mu_J) \partial^2/\partial R_J^2 - (\hbar^2/2m_J) \partial^2/\partial z_J^2 \quad , \quad (2.35b)$$

where, in (2.35b), J may be A or B.

Now the defects of the unmodified adiabatic representation originate in the fact that asymptotically the AH or HB subsystems are merely translating with respect to the other atom (B or A respectively). This "free particle motion" is appropriately described using either R_A or R_B , depending on the position of H, which is specified by the value of z . That is, the translational motion associated with a dissociated diatomic JH is properly described in the R_J system, not the R system (this is the concept expressed by TD,¹⁶ p. 152).

A transformation is therefore required which gives (z, R_J) asymptotically, and essentially (z, R) in the "molecular" region.

Using coordinates (z, R_J) , the kinetic energy operator is, however, no longer diagonal:

$$T = -\frac{\hbar^2}{2\mu_J} \cdot \frac{\partial^2}{\partial R_J^2} - \frac{f_J \cdot \hbar^2 M_H}{m(M_J + M_H)} \cdot \frac{\partial}{\partial R_J} \cdot \frac{\partial}{\partial z} - \frac{\hbar^2}{2m} \cdot \frac{\partial^2}{\partial z^2}, \quad (2.36)$$

where f_J is a device introduced for convenience.⁶⁴ It is defined by:

$$f_J = \begin{cases} -1 & ; \quad J = A \\ +1 & ; \quad J = B. \end{cases} \quad (2.37)$$

(2.36) is derived from the relationships:

$$R_J = \frac{M_J + 1/2 \cdot (1 - f_J \lambda) M_H}{M_J + M_H} \cdot R + \frac{f_J M_H}{M_J + M_H} \cdot z \quad (2.38)$$

The transformations to z_J are given by:

$$z_J = z - 1/2 \cdot (\lambda + f_J) R \quad (2.39)$$

It is well known^{69,70} that by using *mass scaled* coordinates, the motion of two masses in three-dimensional space may be expressed as that of a single particle of unit mass on a six-dimensional surface. For the linear coordinates used here, the relationships (2.38), (2.39) may be expressed as *rotations* (orthogonal transformations) in a two-dimensional space. Thus with mass scaled coordinates:

$$\tilde{z} \equiv (m)^{1/2} \cdot z \quad ; \quad \tilde{R} \equiv (\mu)^{1/2} \cdot R \quad , \quad (2.40a)$$

$$\tilde{z}_J \equiv (m_J)^{1/2} \cdot z_J \quad ; \quad \tilde{R}_J \equiv (\mu_J)^{1/2} \cdot R_J \quad , \quad (2.40b)$$

equations (2.38) to (2.40) give:

$$\begin{bmatrix} \tilde{z}_J \\ \tilde{R}_J \end{bmatrix} = \begin{bmatrix} \cos \sigma_J & -\sin \sigma_J \\ \sin \sigma_J & \cos \sigma_J \end{bmatrix} \begin{bmatrix} \tilde{z} \\ \tilde{R} \end{bmatrix} \quad ; \quad (2.41)$$

where

$$\begin{aligned} \tan \sigma_J &= 1/2 \cdot (\lambda + f_J) (m/\mu)^{1/2} \\ &= f_J (M_H/M_T) (M_{J'} / M_J)^{1/2} \quad ; \quad (J' \neq J) \end{aligned} \quad (2.42a)$$

$$\begin{aligned} \cos \sigma_J &= (m_J/m)^{1/2} \\ &= (\mu_J/\mu)^{1/2} [(M_J + 1/2 \cdot (1-f_J \lambda) M_H) / (M_J + M_H)] \end{aligned} \quad (2.42b)$$

$$\begin{aligned}
\sin \sigma_J &= 1/2 \cdot (\lambda + f_J) (m_J/\mu)^{1/2} \\
&= f_J (\mu_J/m)^{1/2} [M_H/(M_J + M_H)]
\end{aligned}
\tag{2.42c}$$

(2.41) represents two possible rotations: the "molecular" coordinates (\tilde{z}, \tilde{R}) may be transformed into either the 'A configuration' set $(\tilde{z}_A, \tilde{R}_A)$, or the 'B configuration' set $(\tilde{z}_B, \tilde{R}_B)$. In particular, the second line of (2.41) suggests the definition of an angle $\sigma(z; R)$ with the property that it becomes either σ_A or σ_B (depending on the value of z) at large R , for then a "heavy particle coordinate" $\tilde{\xi}(\tilde{z}; \tilde{R})$ may be constructed which asymptotically becomes the desired coordinate \tilde{R}_J .

3. The Non-Linear Transformation.

The preceding discussion is intended to provide an insight into the choice by TD¹⁶ of the following non-linear transformation:

$$\tilde{\xi} = \tilde{R} \cos \sigma(z; R) + \tilde{z} \sin \sigma(z; R) \tag{2.43}$$

The required boundary conditions on σ are met by use of a *switching function* $f(z; R)$ (introduced by Schneiderman and Russek⁷¹), which is defined only through its asymptotic properties:

$$\begin{aligned}
\text{Lim } [f(z; R)] &= -1 = f_A \quad ; \tag{2.44a} \\
(R \rightarrow \infty, z_A \text{ finite})
\end{aligned}$$

and

$$\text{Lim } [f(z;R)] = +1 = f_B \quad . \quad (2.44b)$$

($R \rightarrow \infty$, z_B finite)

$\sigma(z;R)$ is now defined, by analogy with (2.42a):

$$\tan \sigma(z;R) = 1/2 \cdot [f(z;R) + \lambda] (m/\mu)^{1/2} \quad (2.45)$$

$\tilde{\xi}$ is uniquely specified, at all R , by the local proton position. In particular, at large R , when the proton is travelling with nucleus J , $\tilde{\xi}$ becomes the appropriate coordinate \tilde{R}_J . For the symmetric system ($\lambda = 0$) HF_2^- , the switching function shall be chosen (Chapter 4, section B5) to vanish in the small R region. $\tilde{\xi}$ then reduces to \tilde{R} . If the *unscaled* coordinate ξ is defined by:

$$\xi \equiv \tilde{\xi}/\mu^{1/2} \quad , \quad (2.46)$$

it can be seen that ξ becomes R in the case $f = 0$, $\lambda = 0$.

Using (2.43) and (2.45), an expansion for the unscaled coordinate, in powers of (m/μ) , gives:

$$\xi = R + (m/\mu) S(z;R) + O(m/\mu)^2 \quad , \quad (2.47)$$

where

$$S(z;R) = 1/2 \cdot [f(z;R) + \lambda] z - [f(z;R) + \lambda]^2 \cdot R/8 \quad (2.48)$$

$S(z;R)$ is only constrained by its asymptotic behaviour, and since $f^2 = 1$ in that region, (2.48) may be written in a more convenient form:

$$S(z;R) = 1/2 \cdot [f(z;R) + \lambda] z_g - (1 - \lambda^2) R/8 \quad (2.49)$$

(z_g is defined in equation (2.33)).

Two problems remain. Firstly, the Hamiltonian must be transformed to the variables (z, ξ) , and then new coupled equations must be derived for the ξ -dependent coefficients of a BO basis (defined on surfaces of fixed ξ) expansion for $\psi(z, \xi)$.

Thorson and Delos¹⁶ obtained the transformed Hamiltonian, retaining terms to order (m/μ) , and have shown that their form gives correct asymptotic kinetic energy operators (equation (2.36)), within errors of order $(m/\mu)^2$.

4. Modified Coupled Equations.

The coupled equations, which result from the application of the transformed Hamiltonian to a wavefunction expanded in the BO basis:

$$\psi_j(z; \xi) = \sum_{\ell} f_{j\ell}(\xi) \alpha_{\ell}(z; \xi) \quad , \quad (2.50)$$

are shown by TD to be:

$$\begin{aligned} & \{ (2\mu)^{-1} [-i\hbar(d/d\xi) + \underline{P}(\xi) + \underline{A}(\xi)]^2 + \underline{U}(\xi) \} \underline{f}_j(\xi) \\ & + \{ \underline{\Delta}(\xi) - (2\mu)^{-1} \underline{A}^2(\xi) \} \underline{f}_j(\xi) + (2\mu)^{-1} (m/\mu) \underline{D}(\xi) (-i\hbar d/d\xi)^2 \underline{f}_j(\xi) \\ & = E_j \underline{f}_j(\xi) \end{aligned} \quad (2.51)$$

The functions $\{\alpha_{\ell}\}$ of equation (2.50), and the elements $\{U_{\ell}\}$ of the matrix \underline{U} of equation (2.51), satisfy equation (2.30) with the *replacement* $R = \xi$ being understood.

Now, in the final coupled differential equations (2.51), the symbol ' ξ ' is merely a dummy variable, and shall be replaced by the more familiar ' R ', in order to clarify a comparison with the unmodified equations (2.12). Evidently there are additional terms arising from the matrices \underline{A} , $\underline{\Delta}$, and \underline{D} . With the ' R ' notation, these have the following definitions:

$$A_{\ell n}(R) = (im/\hbar) [U_{\ell}(R) - U_n(R)] \langle \ell | S | n \rangle ; \quad (2.52)$$

$$D_{\ell n}(R) = 1/4 \cdot \langle \ell | f^2 - 1 | n \rangle ; \quad (2.53)$$

$$\Delta_{\ell n}(R) = \langle \ell | V[z; R - (m/\mu)S] - V(z; R) | n \rangle ; \quad (2.54)$$

TD^{16,64} have shown that the dominant modification to the coupled equations is in the replacement of the matrix \underline{P} by $(\underline{P} + \underline{A})$ in the 'momentum operator'. The smaller terms are:

- (i) $\{\underline{\Delta}(R) - (2\mu)^{-1} \underline{A}^2(R)\} \underline{f}_j(R)$, giving reduced mass corrections to the proton binding energies ($\sim (m/\mu) U_n$);
- (ii) $(2\mu)^{-1} (m/\mu) \underline{D}(R) (-i\hbar d/dR)^2 \underline{f}_j(R)$, the diagonal elements of which give a short range correction ($\sim (m/\mu) E$) to the 'heavy particle' kinetic energy (\underline{D} vanishes as R increases); the off-diagonal elements give couplings which are an order of magnitude smaller than the $(\underline{P} + \underline{A})$ terms.

Neglecting the smaller terms, the coupled equations to be solved are:

$$\{(2\mu)^{-1}[(-i\hbar d/dR) + \underline{P}(R) + \underline{A}(R)]^2 + \underline{U}(R)\}\underline{f}_j(R) = E_j \underline{f}_j(R). \quad (2.55)$$

To repeat, terms neglected in arriving at (2.55) are:

(a) of order $(m/\mu)^2$, and higher, in the transformed Hamiltonian;^{16,64}

(b) much less significant in the resulting coupled equations than the non-adiabatic coupling $(\underline{P}+\underline{A})$.

Higher order terms could, in principle, be retained, but the solution of (2.55) for a specific hydrogen bonded system is expected to give an accurate indication of the effects of non-adiabatic coupling on vibrational line positions and intensities. If these effects were large, a higher order calculation may be justified, but for the case of the strongly hydrogen bonded system HF_2^- (Chapters three to six) they are not.

The purpose of the TD transformation is to produce equations in which the principal couplings vanish asymptotically. It will now be shown that the term $(\underline{P}+\underline{A})$ satisfies this requirement.

5. Asymptotic Cancellation of \underline{P} and \underline{A} .

Asymptotically, the vibrational BO states $\{\alpha_\ell(z;R)\}$ are functions only of z_j , and not explicitly of R . Thus:

$$\alpha_\ell \stackrel{R \rightarrow \infty}{\sim} \alpha_\ell(z_J) \quad (2.56)$$

where $z_J(z, R)$ is given by (2.39).

Now consider the general transformation $(z, R) \rightarrow (z_J, R)$:

$$\left(\frac{\partial}{\partial R} \right)_z \cdot g(z_J(z, R), R) = \left(\frac{\partial g}{\partial R} \right)_{z_J} + \left(\frac{\partial g}{\partial z_J} \right)_R \cdot \left(\frac{\partial z_J}{\partial R} \right)_z, \quad (2.57)$$

and

$$\left(\frac{\partial}{\partial z} \right)_R \cdot g(z_J, R) = \left(\frac{\partial g}{\partial z_J} \right)_R \cdot \left(\frac{\partial z_J}{\partial z} \right)_R, \quad (2.58)$$

where g is an arbitrary (well behaved) function.

$$\text{Thus, } \left(\frac{\partial}{\partial R} \right)_z \alpha_n \stackrel{R \rightarrow \infty}{\sim} -1/2 \cdot (f_J + \lambda) \left(\frac{\partial}{\partial z_J} \right)_R \alpha_n \quad (2.59)$$

and

$$\left(\frac{\partial}{\partial z} \right)_R \alpha_n \stackrel{R \rightarrow \infty}{\sim} \left(\frac{\partial}{\partial z_J} \right)_R \alpha_n \quad (2.60)$$

The \underline{P} matrix, defined by (2.31), becomes:

$$P_{\ell n} = -i\hbar \langle \ell | (\partial/\partial R)_z | n \rangle$$

i.e.,

$$P_{\ell n} \stackrel{R \rightarrow \infty}{\sim} + 1/2 \cdot i\hbar (f_J + \lambda) \langle \ell | (\partial/\partial z_J)_R | n \rangle \quad (2.61)$$

Also, the \underline{A} matrix, equation (2.52), has elements:

$$\begin{aligned} A_{\ell n} &= (im/\hbar) \langle \ell | S | n \rangle \cdot (U_{\ell} - U_n) \\ &= (im/\hbar) \langle \ell | [h, S] | n \rangle, \end{aligned} \quad (2.62)$$

where $h(z; R)$ is the protonic Hamiltonian of (2.30).

$$\text{Thus, } [h, S] = -\hbar^2/2m \left\{ 2 \cdot \left(\frac{\partial S}{\partial z} \right)_R \cdot \left(\frac{\partial}{\partial z} \right)_R + \left(\frac{\partial^2 S}{\partial z^2} \right)_R \right\} \quad (2.63)$$

and from (2.48):

$$S \sim 1/2 \cdot (f_J + \lambda) z - 1/8 \cdot (f_J + \lambda)^2 R, \quad (2.64)$$

giving $\partial^2 S / \partial z^2 = 0$, and $\partial S / \partial z = 1/2 \cdot (f_J + \lambda)$

(2.62) then yields:

$$A_{\ell n} \xrightarrow{R \rightarrow \infty} -1/2 \, i\hbar (f_J + \lambda) \langle \ell | (\partial / \partial z)_J | n \rangle. \quad (2.65)$$

The required result is shown by (2.61) and (2.65):

$$P_{\ell n} + A_{\ell n} \xrightarrow{R \rightarrow \infty} 0. \quad (2.66)$$

E. Summary.

To a good approximation, vibrational eigenvalues $\{E_j\}$ and eigenvectors $\{\underline{f}_j\}$ satisfy (2.55), which may be written in real form as:

$$\{ -(\hbar^2/2\mu) [(d/dR) \underline{I} + \underline{C}(R)]^2 + \underline{U}(R) - E_j \underline{I} \} \underline{f}_j(R) = \underline{0}; \quad (2.67)$$

where \underline{C} is the real matrix defined by:

$$C_{\ell n}(R) = i/\hbar \cdot (P_{\ell n} + A_{\ell n}) \quad (2.68)$$

For a symmetric system ($\lambda = 0$), $A_{\ell n}$ (defined in general by (2.52)) takes the simple form:

$$A_{\ell n}(R) = (im/\hbar) (U_{\ell} - U_n) \langle \ell | 0.5f(z;R) \cdot z | n \rangle \quad (2.69)$$

$P_{\ell n}$ is defined by (2.31), and the eigenstates $\{U_{\ell}; \alpha_{\ell}\}$ satisfy (2.30).

The switching function $f(z;R)$ has not yet been defined. It is not uniquely specified by the theory: providing it meets the boundary conditions (2.44) it may be chosen arbitrarily, and the coupling matrix \underline{C} will have correct asymptotic behaviour. The choice of a switching function for the HF_2^- system is discussed in Chapter 4, section B5. In this case the function is chosen to *vanish* for R values at which the potential $V(z,R)$ has a single minimum (i.e., in the "molecular" region, for which appropriate coordinates are z and R), and to become essentially a "step function" (in z space) as the barrier to protonic motion becomes significant.

The procedure for the solution of the vibrational problem which was outlined in section C3 (page) may now be adopted, with the following modifications: in item (iii) the integrals $\{C_{\ell, \ell}\}$ defined by equation (2.68) are required, and in item (iv) the coupled equations (2.67) are to be solved.

The remaining chapters of this thesis describe a solution of this system of equations for the case of the

isolated bifluoride ion, for which a reasonable potential function (Chapter Three) has been constructed from purely *ab initio* data in the "molecular" region, and empirical data in the dissociated situation ($\text{F}^- + \text{HF}$). That the solution is convergent is demonstrated by increasing the number of vibrational BO states in the expansion (2.50).

CHAPTER THREE

BIFLUORIDE ION POTENTIAL FUNCTION

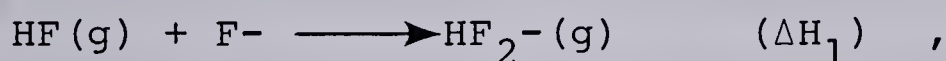
A. *Ab initio* and empirical results.

Early (1957-62) investigations of the electronic structure of the bifluoride ion include valence bond^{72,73} and SCF⁷⁴⁻⁷⁶ (Slater basis) estimates of the total energy for a fixed F-F distance (2.26 \AA), but no attempt was made to calculate the H-bond energy. McLean and Yoshimine⁷⁷ performed SCF (Slater basis) calculations for 21 geometries of HF_2^- , and found that the minimum energy occurred with the H atom at the centre of an F-F bond of length 2.25 \AA . They also did not estimate the hydrogen bond energy.

Later SCF calculations^{24,78,79} (Gaussian basis) have shown good agreement in the general form of the bifluoride ion potential surface: the minimum energy occurs for a linear configuration, with the proton at the centre of the F-F bond, and interfluorine distance $2.25\text{--}2.285 \text{ \AA}$ (experimental values for salts of HF_2^- are $2.26\text{--}2.29 \text{ \AA}$).^{28,80-83} At this F-F distance, the potential function for the proton is a fairly flat-bottomed, single minimum well (in good agreement with the assessment by Ibers²⁰ of the diffraction and spectroscopic data; Williams and Schneemeyer⁸⁴ have, however, found that in p-toluidinium bifluoride the proton is asymmetrically placed, with F-H distances of 1.025 \AA

and 1.235 \AA , but have attributed this to the asymmetry of the crystal environment). As the F-F distance increases, a barrier grows at the center of the bond, and a symmetric double minimum potential is formed. Hydrogen bond energy estimates range from 40 to 52 kcal/mole. Configuration interaction has not been included in any of these calculations.

At the time of writing, there have been no entirely reliable experimental estimates of the hydrogen bond energy. In order to obtain the enthalpy change for the gas phase reaction:



an estimate of the lattice energy for the salt (MHF_2) has been required (Tuck⁸⁵ has reviewed the situation to 1967).

Waddington⁸⁶ calculated $U(\text{MHF}_2)$ ($M = \text{K, Rb, Cs}$), assuming a solid composed of ionic spheres, and concluded $\Delta H_1 = -58 \pm 5 \text{ kcal/mole}$. Harrell and McDaniel⁸⁷ determined the enthalpy of reaction for:



They found $\Delta H_2 = -37 \text{ kcal/mole}$, and assumed the change in lattice energy would be small, concluding $\Delta H_1 = \Delta H_2 \pm 2 \text{ kcal/mole}$.

Dixon *et al.*⁸⁸ then repeated lattice energy calculations for a series of metal salts ($M = \text{Li, Na, K, Rb, Cs}$) and

found an average $\Delta H_1 = 60.2$ kcal/mole. Neckel *et al.*⁸⁹ did a similar calculation ($M = K, Rb, Cs$), but used the wavefunction of Clementi and McLean⁷⁵ to calculate the quadrupole moment, and found $\Delta H_1 \simeq 56$ kcal/mole.

The "experimental" bond energy estimates for HF_2^- are thus about as theoretical as those obtained directly from *ab initio* calculation, and have about the same range of values (37-60 vs. 40-52 kcals/mole).

The general description of the two-dimensional potential surface which has emerged from the *ab initio* calculations is, however, intuitively very satisfactory: for a general bond $A-H...A$, at large $A-A$ distance, the proton may be visualized as sitting in either of two identical Morse-like curves; this is a double minimum potential, the barrier height being the dissociation energy D_e , for the diatomic $A-H$. As the two A nuclei approach, the barrier height must decrease to zero (although, of course, the minimum energy does not necessarily occur when there is no barrier), for at very small $A-A$ distance, a barrier to protonic motion is physically inconceivable.

Ibers²⁰ proposed an empirical form for the potential function governing the stretching motions of the bifluoride ion. In his polynomial representation, the coupling of the two modes (Q_1 for symmetric, Q_3 for asymmetric, normal coordinates) is included through a term $dQ_1Q_3^2$:

$$V(Q_1, Q_3) = aQ_1^2 + bQ_3^2 + cQ_3^4 + dQ_1Q_3^2 \quad (3.1)$$

Ibers obtained solutions to the Schroedinger equation with this potential, by using an expansion of products of harmonic oscillator functions (Chapter One, section B2); the four parameters (a,b,c,d) were varied to give agreement with the following four experimental values: ν_1 (symmetric stretch, 600 cm^{-1}); ν_3 (asymmetric stretch, 1450 cm^{-1}); a value assigned to the second overtone, $3\nu_3$ (5090 cm^{-1}); and an estimation of the contraction Δ , in the equilibrium F-F distance upon deuteration (0.0024 \AA). A computational error in the first estimation of these 'force constants' was later corrected by Ibers and Delaplane.²⁷

Kollman and Allen,⁷⁸ and Noble and Kortzeborn⁷⁹ have attempted to fit their *ab initio* data points, and those of McLean and Yoshimine,⁷⁷ to the form of Ibers. The resultant force constants are quite dissimilar. Noble and Kortzeborn have obtained coefficients for a higher order polynomial representation (including Q_1^3 and Q_1^4), and have compared these coefficients with those obtained using the data of McLean and Yoshimine. Again the agreement is very poor, and the correspondence between coefficients of different polynomial representations is even worse.

Janoschek¹⁷ has summarized the situation: "the potential parameters for different analytical representations

of an energy surface are only of little importance... furthermore the same analytical representations are unable to be compared... only the calculated frequencies are able to yield a global judgement for the accuracy of the representation."

Almløf²⁴ has performed a calculation of the potential surface and the associated vibrational levels. His MO-LCAO-SCF (Gaussian basis) calculation is the most extensive of those discussed, involving 27 linear geometries of the bifluoride ion. Again, a polynomial representation for the vibrational potential surface was used, and the coefficients were obtained by least-squares fit of his *ab initio* points. The minimum of this surface occurs at an F-F distance of 2.246 Å, in a single minimum region. The vibrational problem was also solved by expanding the wavefunction in products of linear harmonic functions, and convergence to $\pm 5 \text{ cm}^{-1}$ was obtained with 160 products (!). The frequencies reported by Almløf are in good agreement with experimental data. For the lower energy transitions, at least, the polynomial representation appears to be a reasonable potential surface. No calculation of relative intensities was performed.

For the purpose of the calculation described in this thesis, all polynomial representations of the function $V(z, R)$ have a serious fundamental defect: they take no account of dissociation in the coordinate R . Furthermore,

beyond a fairly small region of R (in which they are, in various ways, constrained to be reasonable representations), they may exhibit wildly non-physical behaviour (polynomial oscillations), for which the vibrational Born-Oppenheimer eigenvalues, and matrix elements $\{(i/\hbar)P_{mn}(R)\}$, will be completely unreliable.

An analytic form for the potential function of a general hydrogen bond, involving the superposition of Morse-like curves, was proposed by Lippincott and Schroeder,⁴⁷ and modified by later workers.^{46,52-55} This model is purely empirical, requiring information from experiment, and/or *ab initio* calculation, in order to establish the values of several parameters for a particular bond. It does, however, have the essential characteristics of reasonable form in the dissociation limit, and decreasing barrier height in the interaction region. The *form* (but not the parameters) of Jiang and Anderson,⁵³ for this representation of the H-bond potential function, has been adopted for the calculation described herein.

B. An Asymptotically Reasonable Form.

1. The Polynomial Form of Almløf.²⁴

Before discussing the final form for the potential used in this study, it is necessary to describe the polynomial obtained by Almløf, and its characteristics, because the free parameters in the Jiang and Anderson form

have been fixed using this *ab initio* data.

Figure 3.1 shows the relationships between the coordinates used by Almløf (Q_1, Q_2), Jiang and Anderson (s, t), and this work (z, R).

Almløf's polynomial is a more general form of that of both Ibers²⁰ (equation (3.1)), and Noble and Kortzeborn.⁷⁹ It is:

$$V(Q_1, Q_2) = \sum_{m,n} C_{mn} Q_1^m Q_2^n \quad (3.2)$$

(Note that here Q_2 is used in place of Q_3 for the asymmetric coordinate).

The paper by Almløf contains several errors: in his definition of Q_2 , the factor of $1/2$ is missing (see figure 3.1); in 'figure 1' of Almløf's paper, both axes are incorrectly labelled (this is a contour diagram for the potential surface; the axis labelled ' Q_1 (a.u.)', should be ' $Q_1 + R_e$ (Å)', and the other, labelled ' Q_2 (a.u.)', should be ' $2Q_2$ (Å)'). These errors have been resolved by private communication with Dr. Almløf.

It is convenient to express $V(Q_1, Q_2)$ in a form which emphasizes the non-separable part. The full expansion is:

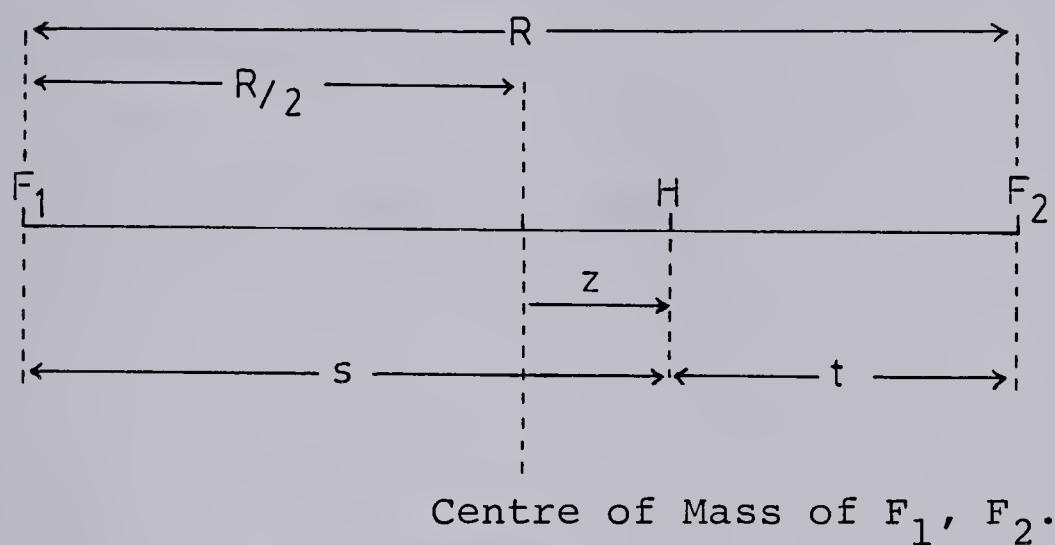
$$\begin{aligned} V(Q_1, Q_2) = & Q_1^2 (C_{20} + C_{30} Q_1) \\ & + Q_2^2 \{ (C_{02} + C_{12} Q_1 + C_{22} Q_1^2) + Q_2^2 (C_{04} + C_{14} Q_1) + Q_2^4 \cdot C_{06} \} \end{aligned} \quad (3.3)$$

Now defining:

$$Q \equiv Q_1 = R - R_e \quad ; \quad z = Q_2 \quad , \quad (3.4)$$

Figure 3.1

Coordinates for the Linear Bifluoride Ion



The subscript 'e' is used to denote 'equilibrium values', that is, values for the coordinates at the minimum of the potential surface.

Thus:

$$R_e = 2.246 \text{ \AA} \text{ (4.244 a.u.)}$$

$$s_e = t_e = 1.123 \text{ \AA}$$

$$z_e = 0.0$$

Almløf coordinates:

$$Q_1 = R - R_e = (s - s_e) + (t - t_e)$$

$$Q_2 = (s - t)/2 = z.$$

Jiang and Anderson coordinates:

$$s(z, R) = R/2 + z$$

$$t(z, R) = R/2 - z$$

(3.3) may be written:

$$V(Q, z) = V_2^A(R) + V_1^A(z, R) \quad (3.5)$$

with:

$$V_2^A(R) \equiv Q^2 (C_{20} + C_{30} \cdot Q) \quad (3.6a)$$

$$V_1^A(z, R) \equiv Az^6 + B(Q)z^4 + C(Q)z^2 \quad (3.6b)$$

and:

$$A \equiv C_{06}$$

$$B(Q) \equiv C_{04} + C_{14} \cdot Q \quad (3.7)$$

$$C(Q) \equiv C_{02} + C_{12}Q + C_{22}Q^2$$

Clearly, $V_1^A(z, R)$ is symmetric in the z coordinate, at any R . It is the variation in the coefficients of this sixth degree polynomial which causes the growth of a barrier as R increases. The partial derivative, $\partial V_1^A / \partial R$, will influence the form of the matrix elements $\{ (i/\hbar) P_{mn}(R) \}$.

Figures 3.2 to 3.4 show the functions $V_2^A(R)$, and $V_1^A(z, R)$ over a range of values of R .

In the region $R = 3.8$ to 5.2 a.u., where Almløf has *ab initio* data points, the polynomials V_2^A , and V_1^A have reasonable physical behaviour. Beyond $R = 5.2$ a.u. the cubic behaviour of V_2^A is evident in figure 3.2, and the

FIGURE 3.2

 $V_2^A(R) \times 10^3 \text{ (a.u.) vs } R \text{ (a.u.)}$ 

FIGURE 3.3

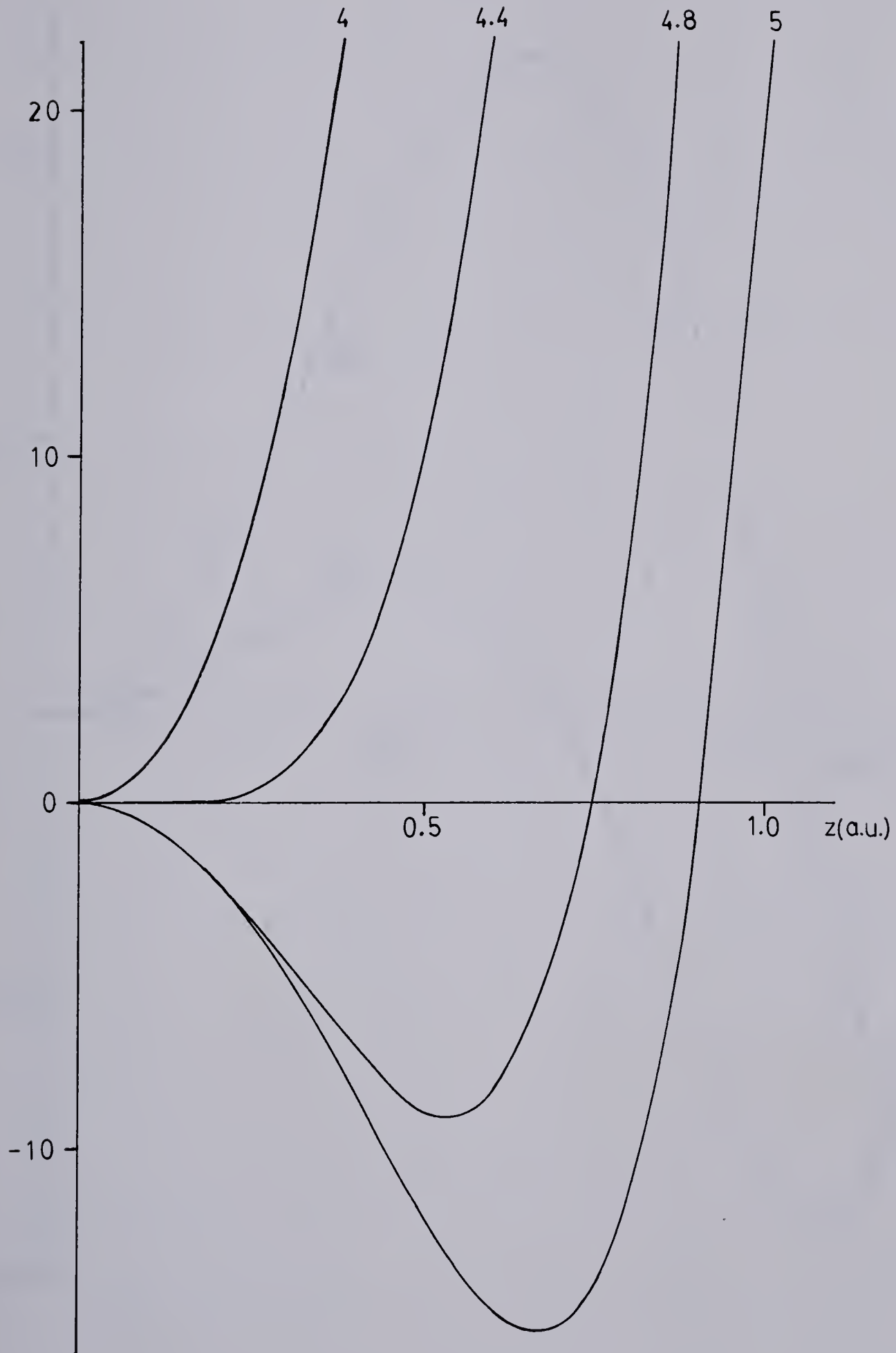
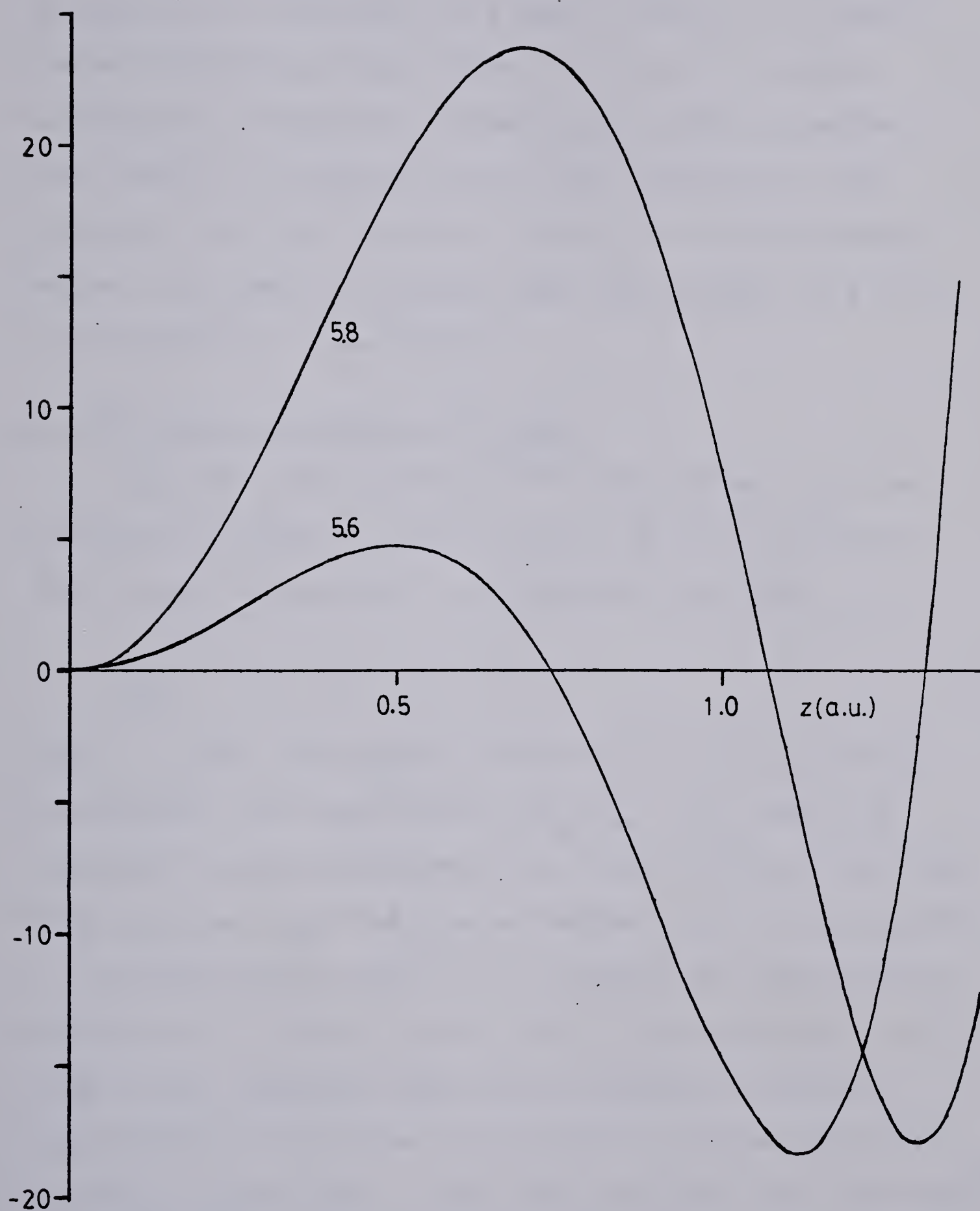
 $V_1^A(z;R) \times 10^3 \text{ (a.u.)}$ at $R = 4$ to 5 a.u.

FIGURE 34

$V_1^A(z;R) \times 10^3$ (a.u.) at $R = 5.6, 5.8$ a.u.



oscillations of the sixth degree polynomial v_1^A , become apparent in figure 3.4.

To summarize, the Almløf polynomial representation is physically reasonable in a small region of R , about the equilibrium position ($R_e = 4.244$ a.u.), but has unacceptable asymptotic (dissociation in R) character. That Almløf's calculated vibrational frequencies are accurate, for lower energies (within 5% of experimental values), is taken to indicate that the surface is a *good* representation in this region.

2. The Jiang and Anderson⁵³ Form.

Lippincott and Schroeder^{90,91} have shown that the vibrational potential function for a diatomic molecule (AB) is well represented by the Morse-like form:

$$V_{AB}(r) = D_e(1 - \exp(-n\Delta r^2/2r)) \quad (3.8)$$

where r is the internuclear distance, $\Delta r = r - r_e$ is the displacement from equilibrium ($V_{AB}(r_e) \equiv 0$), and n is obtained from the curvature at r_e (empirically, using the force constant k_{AB} from the IR fundamental, $n = k_{AB} \cdot r_e / D_e$).

Attempts were made^{46,47,52} to simulate the potential function for a linear H-bond, A-H...A, by superposition of forms (3.8), together with terms intended to include electrostatic attraction ($-C_2(R_e/R)^m$), and Van der Waals repulsion ($C_1 \exp(-bR)$). Thus the Lippincott and Schroeder⁴⁷

(LS) form for the H-bond potential is:

$$V_{LS} = D(1 - y(s) - y(t) + C_1 e^{-bR} - C_2 (R_e/R)^m) \quad (3.9)$$

where:

$$y(u) = \exp(-n(u-u_{e\infty})^2/2u) \quad (3.10)$$

$u_{e\infty}$ = equilibrium bond length for free diatomic A-H.

$$(s_{e\infty} = t_{e\infty} = 0.917 \text{ \AA} \text{ for HF})$$

$$n = k_{HA} \cdot u_{e\infty}/D$$

$$(k_{HF} = 9.655 \text{ mdyn. \AA}^{-1}, D = 51,300 \text{ cm}^{-1},$$

dissociation energy⁵³ for H-F bond)

R_e = equilibrium H-bond length.

$$(R_e = 2.246 \text{ \AA}, \text{ from Alml\o f, has been used})$$

C_1 , C_2 , b and m must also be fixed empirically.

In attempting to fit the *ab initio* data of Kollman and Allen,⁷⁸ and Alml\o f,²⁴ Jiang and Anderson⁵³ have found the form (3.9) to be insufficiently flexible, and have introduced an additional repulsive term $g \cdot y(s) \cdot y(t)$:

$$V_{JA}(z, R) = D(1 - y(s) - y(t) + g y(s) y(t) + C_1 e^{-bR} - C_2 (R_e/R)^m) \quad (3.11)$$

There are now five undetermined parameters: C_1 , C_2 , g , b , and m .

C_1 , and C_2 may be fixed from the following equilibrium conditions:

$$V_{JA}(0, R_e) \equiv V_e = \text{hydrogen bond energy} \quad (3.12a)$$

(-51 kcal/mole, from Alml\o f, was used)

and,

$$\left. \frac{\partial V_{JA}}{\partial s} \right|_{s_e, t_e} = \left. \frac{\partial V_{JA}}{\partial t} \right|_{s_e, t_e} = 0 \quad (3.12b)$$

giving:

$$C_2 = (Ve/D - 1 - y(s_e)(g \cdot y(s_e) - 2) - y'(s_e)(gy(s_e) - 1)/b) / (m/bR_e - 1) \quad (3.13)$$

$$C_1 = e^{bR_e} (mC_2/R_e + y'(s_e)(g \cdot y(s_e) - 1)) / b \quad (3.14)$$

Thus, *given* the parameters m , g , and b , the equilibrium conditions (3.12) have been used to determine the coefficients C_1 , and C_2 .

Jiang and Anderson have assigned values ($m = 6$, $g = 0.64$, $b = 3.2009 \text{ \AA}^{-1}$) by fitting the form (3.11) to *ab initio* data,^{78,24} and "observed infrared frequency".

In this study, the surface of Almløf alone has been used to define the parameters.

First, the parameter g is fixed using $V_1^A(z, R)$ (equation (3.6b), and figure 3.3). For comparison, $V_1(z, R)$ is defined by:

$$V_1(z, R) \equiv V_{JA}(z, R) - V_{JA}(0, R) \quad (3.16)$$

This merely sets $V_1(0, R) = 0$, for all R (as $V_1^A(z, R)$), and using (3.11) this becomes:

$$V_1(z, R) = D(g(y(s)y(t) - y^2(\xi)) + 2y(\xi) - y(s) - y(t)) \quad (3.17)$$

where,

$$\xi \equiv s(0, R) = t(0, R) = R/2 \quad (3.18)$$

Hence, $V_1(z, R)$ is *only* dependent on g (not on m or b). With a value $g = 0.55$, equation (3.17) has been found to give curves which are in good agreement with those of figure 3.3, in the region $R = 3.8-4.8$ a.u.

Now $V_2(R)$ is also defined to be consistent with the Almløf function (equation (3.6a), and figure 3.2) $V_2^A(R)$:

$$V_2(R) \equiv V_{JA}(0, R) - V_{JA}(0, R_e) \quad (3.19)$$

so that $V_2(R_e) = 0$.

The complete potential surface is now:

$$V(z, R) = V_2(R) + V_1(z, R) \quad (3.20a)$$

i.e.,

$$V(z, R) = V_{JA}(z, R) - V_{JA}(0, R_e) \quad (3.20b)$$

(3.20b) simply defines the potential to be zero at the equilibrium position for the bifluoride ion (as Almløf), rather than at an equilibrium configuration for the dissociated fragments, $F^- + HF$, or $FH + F^-$ (as Jiang and Anderson).

Having fixed g , the function $V_1(z,R)$ is fixed, and the vibrational Born-Oppenheimer eigenvalues $\{\epsilon_\ell(R)\}$ may be calculated by the method of Chapter four. The curves $\{U_\ell(R)\}$ may then be constructed ($U_\ell(R) = \epsilon_\ell(R) + V_2(R)$) for a given pair of the parameters m and b . The values of these parameters were varied (only integer values of m were considered) until the curves $\{U_\ell(R)\}$ agreed closely with those calculated using the Almløf surface in the physically reasonable region, $R = 3.8-5.2$ a.u. In this way, the values $m = 4$, $b = 2.35 \text{ \AA}^{-1}$, have been assigned.

3. Summary.

A potential function $V(z,R)$ has been defined (equations (3.10), (3.11) and (3.20b)) using the representation of Jiang and Anderson,⁵³ with parameters:

$$m = 4$$

$$b = 2.35 \text{ \AA}^{-1}$$

$$g = 0.55.$$

This representation gives a potential surface which matches that of the polynomial form of Almløf²⁴ very well in the region $3.8-5.2$ a.u., and in addition gives good behaviour as $R \rightarrow \infty$.

It should be noted, however, that at *small* R , the function V_{JA} is dominated by the attractive term $-C_2(R_e/R)^m$. Thus,

$$\lim_{R \rightarrow 0} V_2(R) = -\infty,$$

and the H-bond collapses. The Jiang and Anderson representation breaks down at small R . This does not, however, present any difficulty in practice, because the matrix elements $\{(i/\hbar)P_{mn}(R)\}$, and curves $\{U_n(R)\}$ may be numerically extrapolated without difficulty for $R < 3.8$ a.u., in a manner which avoids this false behaviour (Chapter 5, section G).

CHAPTER FOUR

VIBRATIONAL BORN-OPPENHEIMER STATES

A. General Eigenvalue Condition.

This chapter describes a method for the numerical solution of the eigenvalue problem (at fixed R) posed by equation (2.30), with $V(z;R) = V_1(z;R) + V_2(R)$, and $U_\ell(R) = \varepsilon_\ell(R) + V_2(R)$, as described in Chapter 3.

For an arbitrary energy ε , there exist solutions to the differential equation:

$$\{\partial^2/\partial z^2 + (2m/\hbar^2)[\varepsilon - V_1(z;R)]\}\alpha(z;R) = 0 \quad . \quad (4.1)$$

Unless ε is an eigenvalue, however, $\alpha(z;R)$ will not be everywhere 'regular', that is, will not satisfy the boundary conditions:

$$\alpha(z;R) \xrightarrow{z \rightarrow \pm\infty} 0 \quad . \quad (4.2)$$

An eigenfunction $\alpha_\ell(z;R)$ is everywhere continuous, obeys (4.2), and satisfies (4.1), for which the corresponding energy is an eigenvalue $\varepsilon_\ell(R)$. R is here considered to be a fixed parameter (indicated by the semi-colon), and so the quantum states $\{\alpha_\ell\}$ of the reduced mass m are essentially vibrational Born-Oppenheimer states of the proton.

The JWKB⁹² approximation guarantees that, in classically forbidden regions of z far from the turning points, the

form of $\alpha(z;R)$ for an arbitrary energy ϵ , is:

$$\alpha(z;R) \simeq c \cdot p^{-1/2} \cdot \exp(\pm \int^z p(z') dz') \quad ; \quad (4.3a)$$

where c is an arbitrary constant, and

$$p(z;R) \equiv \{(2m/\hbar^2) [V_1(z;R) - \epsilon]\}^{1/2} \quad (4.3b)$$

There is, therefore, one solution which is exponentially growing and one which is exponentially decreasing in a direction away from either turning point. Growing solutions are clearly forbidden by (4.2).

At any point in z space, z_i , a solution to (4.1) is uniquely defined by the values:

$$\alpha_i \equiv \alpha(z_i;R),$$

$$\text{and } \alpha_i' \equiv \alpha'(z_i;R). \quad (4.4)$$

If z_i^R is in the right asymptotic region (RAR: $z \rightarrow +\infty$), and α_i^R is any arbitrary value, then the derivative is related to this by (4.3):

$$\alpha_i^{R'} = -p(z_i^R;R) \alpha_i^R \quad (4.5a)$$

Similarly, in the left asymptotic region (LAR: $z \rightarrow -\infty$):

$$\alpha_i^{L'} = +p(z_i^L;R) \alpha_i^L \quad (4.5b)$$

In obtaining (4.5) from (4.3), the JWKB criterion⁹²

$$\left| \frac{1}{p} \frac{\partial p}{\partial z} \right| \ll |p| \quad (4.6)$$

has been used.

The different signs in (4.5a) and (4.5b) ensure the correct asymptotic exponential decay of the solution.

Solutions to (4.1) may then be accurately numerically propagated from either of the points z_i^L or z_i^R towards the left and right turning points respectively. In fact, the initial values assigned to α_i and α_i' are quite unimportant (providing they are not both zero) because any non-zero pair of numbers may be considered to be a linear combination of the two solution forms. Propagation towards the turning points *ensures* the decay of the unacceptable form, and the process is self-purifying.

Thus, if solutions α^L and α^R are generated regular in LAR and RAR respectively, they may be accurately propagated to a suitable matching point z_m . z_m must be chosen in the classically allowed region, because a solution which is regular in one region cannot be propagated into the other classically forbidden region without the undesirable exponential growth occurring.

The condition that ϵ be an eigenvalue is clearly that the two solutions, generated from LAR and RAR, be identical, for then, and only then, is the function regular on $-\infty$ to $+\infty$. Thus, functions and derivatives must match at z_m .

The eigenvalue condition is:

$$a\alpha^L + b\alpha^R = 0 \quad ;$$

$$\text{and } a\alpha^{L'} + b\alpha^{R'} = 0 \quad . \quad (4.7)$$

That is, the constants a and b must exist, which requires:

$$\begin{vmatrix} \alpha^L & \alpha^R \\ \alpha^{L'} & \alpha^{R'} \end{vmatrix} = 0 \quad (4.8)$$

This is the well known property of the Wronskian of two linearly dependent solutions to a second order linear differential equation: the Wronskian vanishes at any point.⁹³

If the function $W(\varepsilon)$ is defined:

$$W(\varepsilon) \equiv \alpha^L \alpha^{R'} - \alpha^R \alpha^{L'} \quad (4.9)$$

the eigenvalue condition becomes:

$$W(\varepsilon_\ell) = 0 \quad (4.10)$$

$W(\varepsilon)$ is to be calculated at the matching point z_m .

These concepts will be extended, in Chapter 5, for the case of N *coupled* second order differential equations.

(B). Symmetric Potential:

1. Constraints:

$V_1(z;R)$ has been defined such that:

$$V_1(0;R) = 0 \quad ;$$

and

$$V_1(z;R) = V_1(-z;R) . \quad (4.11)$$

This leads to the eigenfunction conditions:

Even parity:

$$\begin{aligned} \alpha_\ell'(0;R) &= 0 \\ \alpha_\ell(0;R) &= C \quad (\ell = 0, 2, 4, \dots) \end{aligned} \quad (4.12a)$$

Odd parity:

$$\begin{aligned} \alpha_\ell(0;R) &= 0 \\ \alpha_\ell'(0;R) &= d \quad (\ell = 1, 3, 5, \dots) \end{aligned} \quad (4.12b)$$

c and d are arbitrary initial values (eventually fixed by normalization).

2. Numerical Method:

The conditions (4.12) lead to a great reduction of numerical computation, particularly for cases in which $V_1(z;R)$ has a single minimum, or the top of the barrier is below the eigenvalue being calculated.

Numerical calculation of an eigenvalue falls, then, into two classes.

(i) $\varepsilon \geq 0$:

In this case the matching point is chosen at $z = 0$. It is only necessary to propagate a solution from one of the asymptotic regions, the other solution being fixed by (4.12).

Arbitrarily choosing to propagate from RAR, (4.9)

becomes:

$$\begin{aligned} W(\varepsilon) &= \alpha^{R'} && \text{even parity} \\ W(\varepsilon) &= \alpha^R && \text{odd parity} \end{aligned} \tag{4.13}$$

Values of ε are sought such that either the wave-function vanishes at $z = 0$ (odd parity eigenvalues), or the derivative vanishes there (even parity eigenvalues).

The fourth-order Runge-Kutta procedure has been used to integrate (4.1) from RAR to $z = 0$. The Newton-Raphson method was used to find the zeros of $W(\varepsilon)$.

Eigenvalues have been calculated to eight significant figures by this method, and are completely stable on halving the Runge-Kutta integration stepsize and varying the starting point in RAR.

(ii) $\varepsilon < 0$:

$z = 0$ is not a suitable matching point if the distance of the energy from the minimum of the potential well is less than the barrier height. This is always the case for bound states at sufficiently large R . The problem is that, in order to reach $z = 0$, the solution propagated from RAR must penetrate a classically forbidden region in a direction *away* from a turning point, and then exponential growth of the forbidden solution occurs. This is overcome by propagating a solution *from* $z = 0$, with initial values defined by (4.12), *towards* the RAR solution. The solutions are then matched in a classically allowed region, at

$z_m = z_0$ (the position of the potential minimum), and zeros are sought for $W(\varepsilon)$ defined by the full equation (4.9).

3. Eigenvalue Initialization :

In seeking a zero of $W(\varepsilon)$, the value of ε must initially be chosen close to the required eigenvalue ε_ℓ , and must be limited by high and low bounds, so that computational effort is minimized and convergence to an undesired eigenvalue is avoided. This is achieved by starting the calculation of $\{\varepsilon_\ell(R); \alpha_\ell(z; R)\}$ in a region of R where the potential has a single minimum and non-zero curvature at $z = 0$. A harmonic approximation then yields a good approximation to ε_0 , and subsequent eigenvalues are initialized from the spacing of the previous ones. Providing the step to the next R point is sufficiently small, $\varepsilon_\ell(R_{i+1})$ is approximately $\varepsilon_\ell(R_i)$ and the process continues.

Alternatively, the procedure may be initiated in a region of large R , where the double minimum gives effectively harmonic oscillator states of the non-hydrogen bonded A-H molecule.

4. Normalization:

The wavefunctions $\{\alpha_\ell(z; R)\}$ are stored pointwise in z space, and (after suitable matching of magnitudes at z_m for the case $\varepsilon_\ell < 0$) each is numerically integrated (Simpson's rule is found to be quite adequate for six figure accuracy in the subsequently calculated \underline{P} and \underline{A}

matrix elements) to find the scaling factors C_ℓ , such that:

$$2 \cdot \int_0^\infty (\alpha_\ell \cdot C_\ell^{-1/2})^2 dz = 1 \quad (4.14)$$

The functions are thus redefined as the normalized set $\{\alpha_\ell\}$.

5. Matrix elements: P_{ij} , A_{ij} , C_{ij} .

(i) P_{ij} :

The Hellmann-Feynman theorem⁹⁴ gives:

$$(i/\hbar) \cdot P_{\ell n}(R) \cdot [\epsilon_n(R) - \epsilon_\ell(R)] = \int_{-\infty}^{+\infty} \alpha_\ell(z; R) \left(\frac{\partial V_1}{\partial R} \right)_z \alpha_n(z; R) dz. \quad (4.15)$$

V_1 , using the Jiang and Anderson⁵³ form, has been defined (equation (3.17)) by:

$$V_1(z; R) = D\{g \cdot (y(s)y(t) - y(\xi)^2) + 2y(\xi) - y(s) - y(t)\} \quad (4.16)$$

with $\xi = R/2$.

Any part of $\partial V_1 / \partial R$ which is only a function of R gives zero contribution to (4.15). Now:

$$[\partial V_1 / \partial R]_z = (D/2) \cdot d(z; R) + \text{function of } R \quad (4.17)$$

where:

$$d(z; R) \equiv y'(s)\{g \cdot y(t) - 1\} + y'(t)\{g \cdot y(s) - 1\} \quad (4.18)$$

and (4.15) becomes

$$(i/\hbar) P_{\ell n}(R) \cdot (\epsilon_n - \epsilon_\ell) / D = \int_0^\infty \alpha_\ell(z; R) d(z; R) \alpha_n(z; R) dz \quad (4.19)$$

This integral is calculated numerically at each R point using the stored normalized $\{\alpha_\ell\}$. It is evident from (4.15) that there is *no coupling between states of opposite parity* ($\partial V_1/\partial R$ is an even function).

(ii) A_{ij} :

From equation (2.69), the matrix elements required to correct for proton translation, are given by:

$$(-i\hbar)A_{\ell n}(R) = m(\varepsilon_\ell - \varepsilon_n) \cdot 1/2 \cdot \int_{-\infty}^{+\infty} \alpha_\ell \cdot z \cdot f(z;R) \alpha_n dz \quad (4.20)$$

The form:

$$f(z;R) = \tanh(\gamma(R) \cdot z_0(R) \cdot z) \quad (4.21)$$

has been chosen. This has the property that when there is no barrier ($z_0 = 0$) the switching function vanishes.

$\gamma(R)$ has been chosen in such a way that all elements of the matrix $\underline{C}(R)$ remain smooth while asymptotically going to zero.

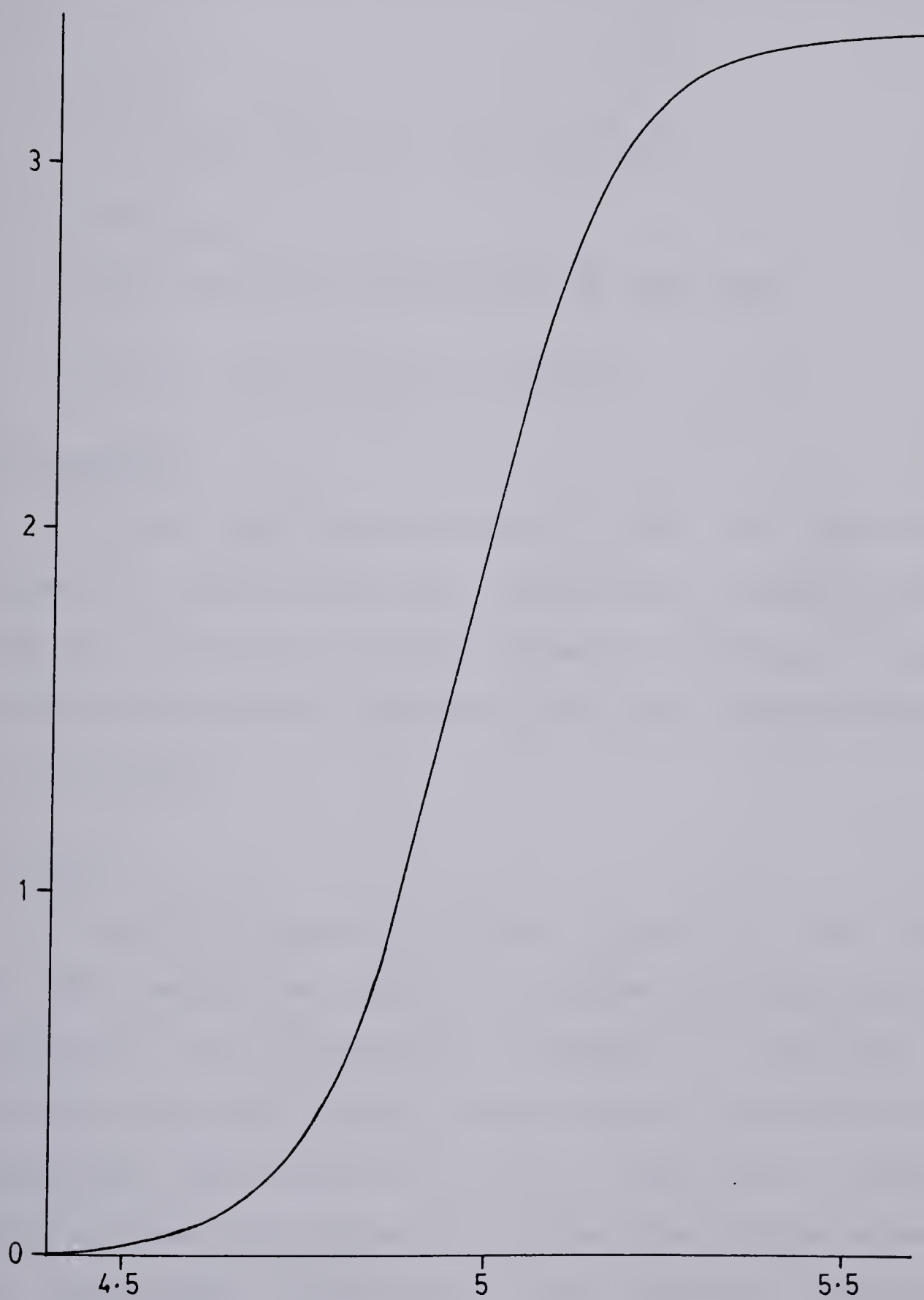
The following form (shown in figure 4.1) was found to be suitable:

$$\gamma(R) = a\{1 + \tanh(b(R-R_C))\} \quad (4.22)$$

with: $a = 1.7 \text{ a.u.}^{-2}$; $b = 5.0 \text{ a.u.}^{-1}$; $R_C = 4.97 \text{ a.u.}$

It is not claimed that the parameters a , b , R_C are unique. They are merely convenient in defining a switching function which grows rapidly from zero, in the single

FIGURE 4.1

 GAMMA (a.u.)^{-2} vs. $R \text{ (a.u.)}$ 

minimum molecular situation, to ± 1 in the high barrier (dissociated) situation. The form (4.22) provides a continuous transformation between these two limiting situations.

From (4.20) the integrals to be numerically evaluated are:

$$(-i\hbar)A_{\ell n}/(m(\epsilon_{\ell}-\epsilon_n)) = \int_0^{\infty} \alpha_{\ell} z f \alpha_n dz \quad (4.23)$$

(iii) C_{ij} :

The \underline{C} matrix is defined to be real, by:

$$C_{\ell n}(R) = (i/\hbar)(P_{\ell n}(R) + A_{\ell n}(R)) \quad (4.24)$$

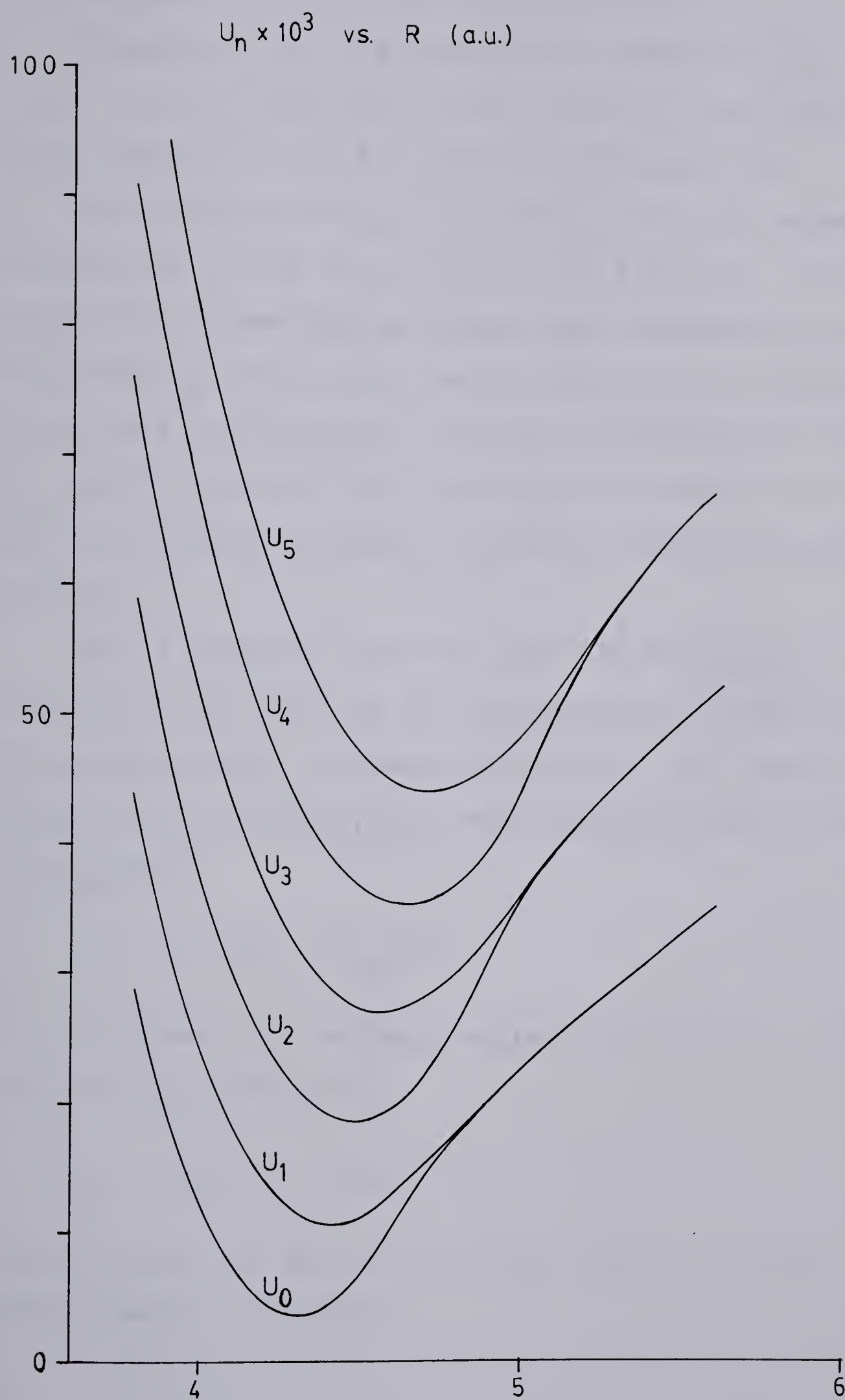
C. Results.

$\{\epsilon_n(R)\}$ are eigenvalues of $V_1(z;R)$, but the full potential, $V(z,R)$, has been written as $V_1(z;R)+V_2(R)$, and so, in order to provide potential surfaces for the complete eigenvalue problem, $\{U_{\ell}(R)\}$ are now defined to be $\{\epsilon_{\ell}(R)+V_2(R)\}$.

1. HF_2^- .

Figure 4.2 shows the curves $\{U_{\ell}(R), \ell = 0,5\}$ obtained for HF_2^- using the potential function, of the Jiang and Anderson⁵³ form, described in Chapter 3. Jiang and Anderson obtained similar curves using a different numerical method for the solution of (4.1). They did not calculate matrix elements or attempt to solve the coupled equations for vibrational eigenvalues. They discussed 'vertical

FIGURE 4.2



transitions' from the minimum of each $U_n(R)$ curve. This is incorrect, and is a poor approximation.

Figures 4.3 to 4.5 show matrix elements $\{P_{ij}\}$, and $\{C_{ij}\}$, coupling the first three states of even parity, while figures 4.6 to 4.8 show the odd parity set.

The maximum of C_{02} is at about 4.75 a.u., whereas the minimum of the curve $U_0(R)$ is at 4.30 a.u. It is then immediately clear that a ground state wavefunction in the curve U_0 will be only weakly coupled to any function associated with curve U_2 . Similar considerations for C_{13} and U_1 indicate that a ground state wavefunction in U_1 will probably be weakly coupled to functions associated with U_3 .

It is therefore expected that the fundamental I.R. transition (ν_3) will be well approximated by the difference in energy between a harmonic oscillator (ho) approximated ground state in $U_1(E_{01}(\text{ho}))$ and a similar ground state in $U_0(E_{00}(\text{ho}))$:

$$\nu_3 \simeq E_{01}(\text{ho}) - E_{00}(\text{ho}) \quad (4.25)$$

Furthermore, the Raman active transition (ν_1) should be well approximated by:

$$\nu_1 \simeq E_{10}(\text{ho}) - E_{00}(\text{ho}) \quad (4.26)$$

where $E_{10}(\text{ho})$ is the first excited state in the ho approximation for $U_0(R)$.

FIGURE 4.3

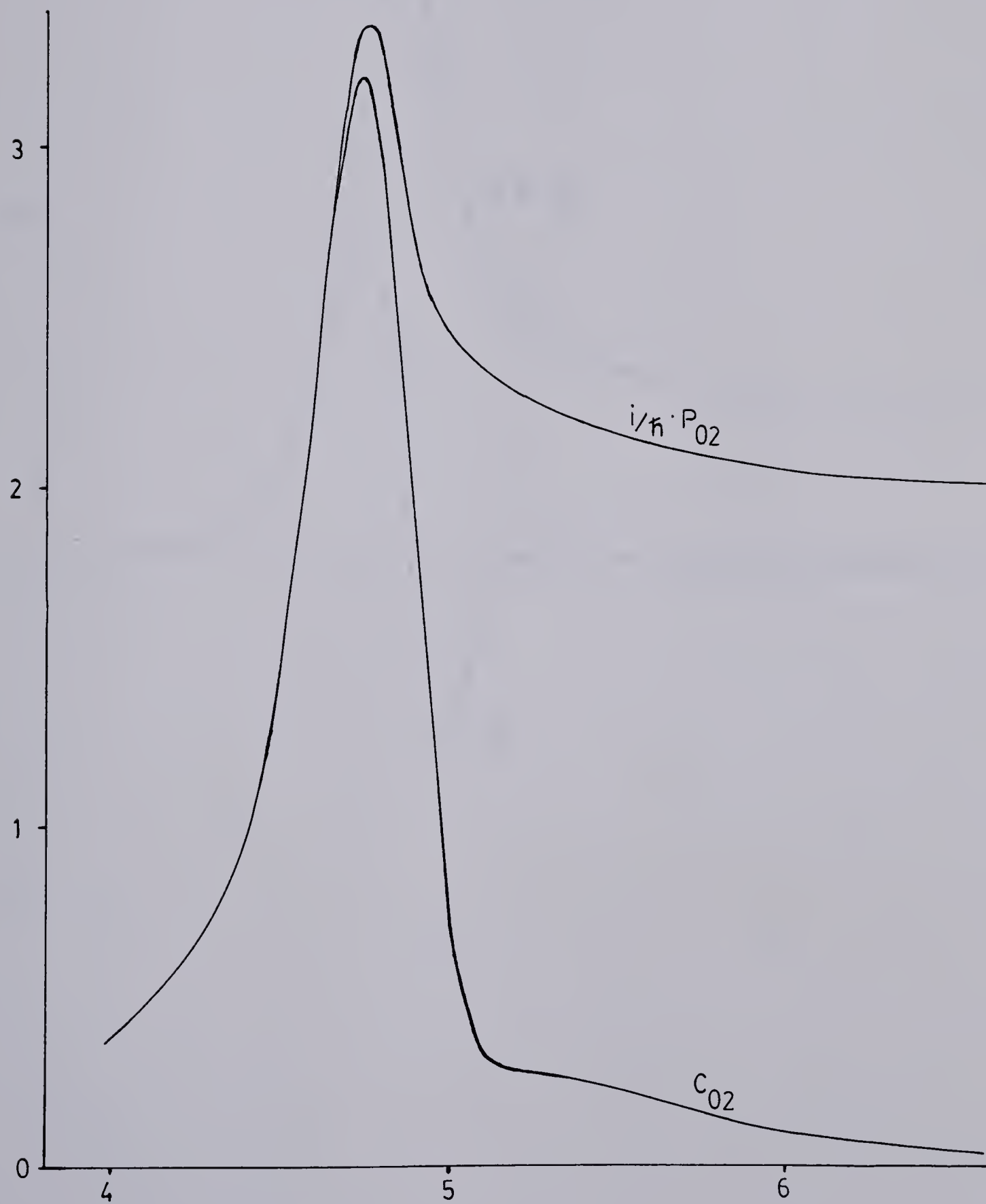
 $i/\hbar \cdot P_{02} \text{ \& } C_{02} \text{ (a.u.)}^{-1} \text{ vs } R \text{ (a.u.)}$ 

FIGURE 4.4

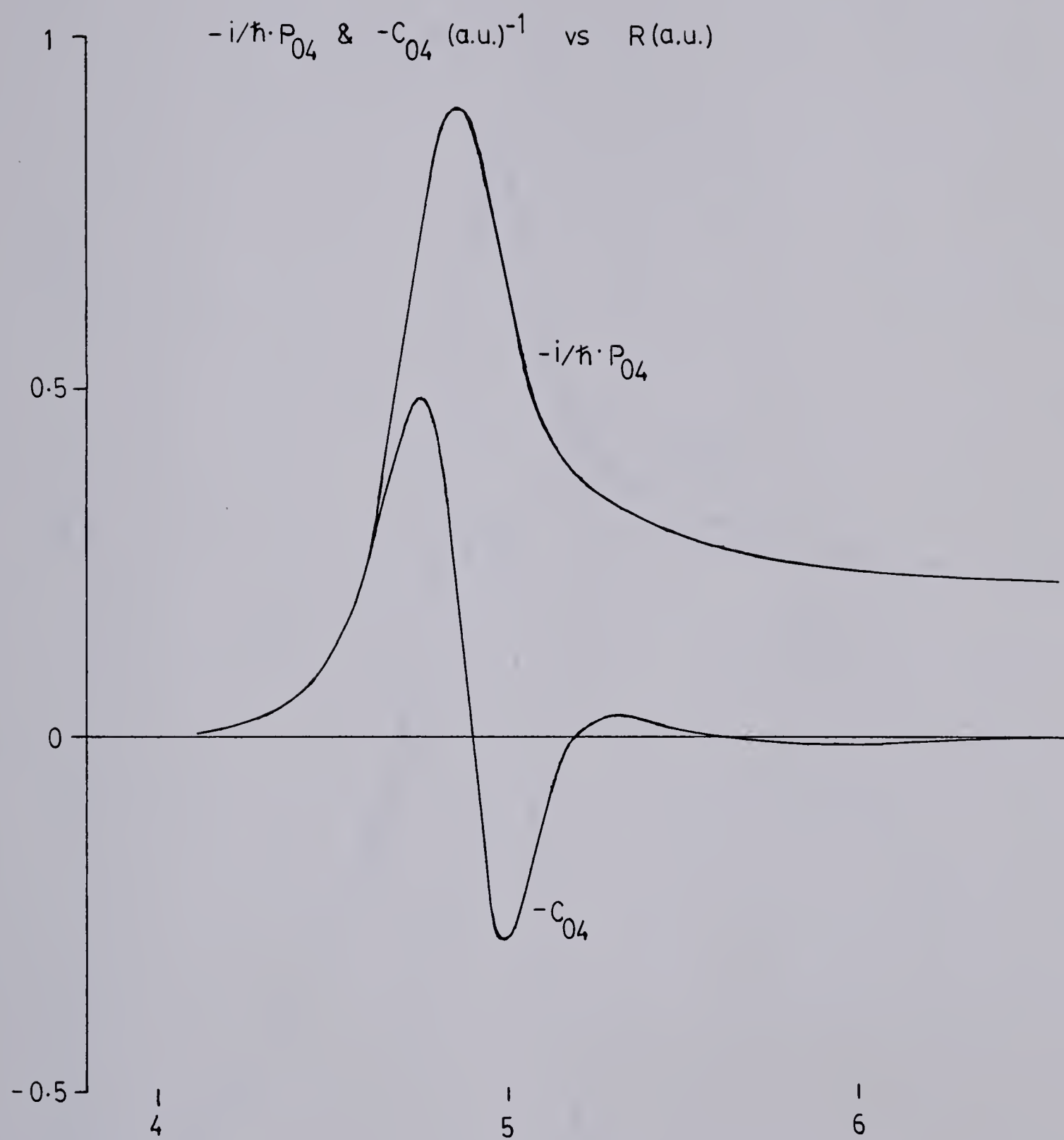


FIGURE 4.5

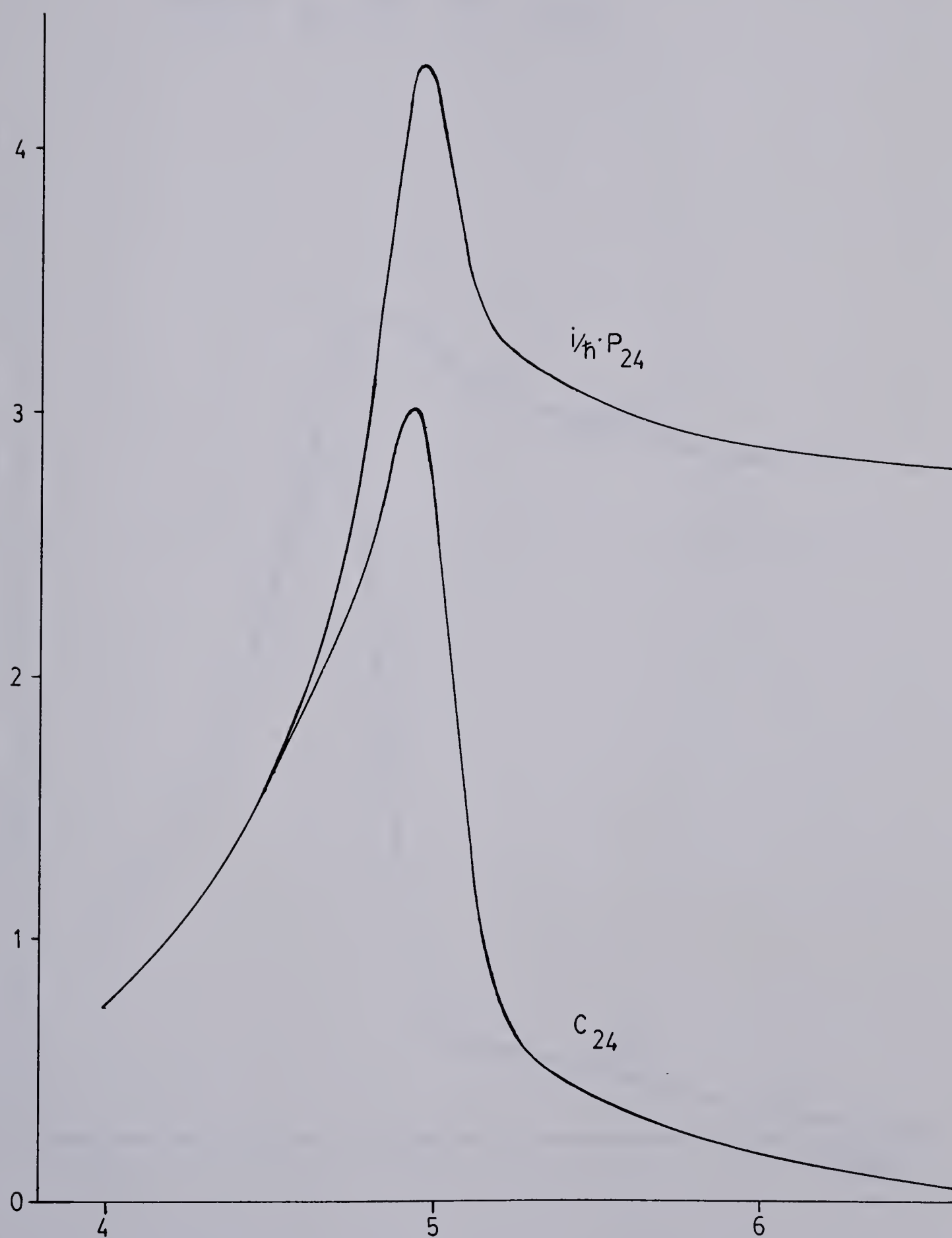
 $i/\hbar \cdot P_{24}$ & C_{24} (a.u.)⁻¹ vs R (a.u.)

FIGURE 4.6

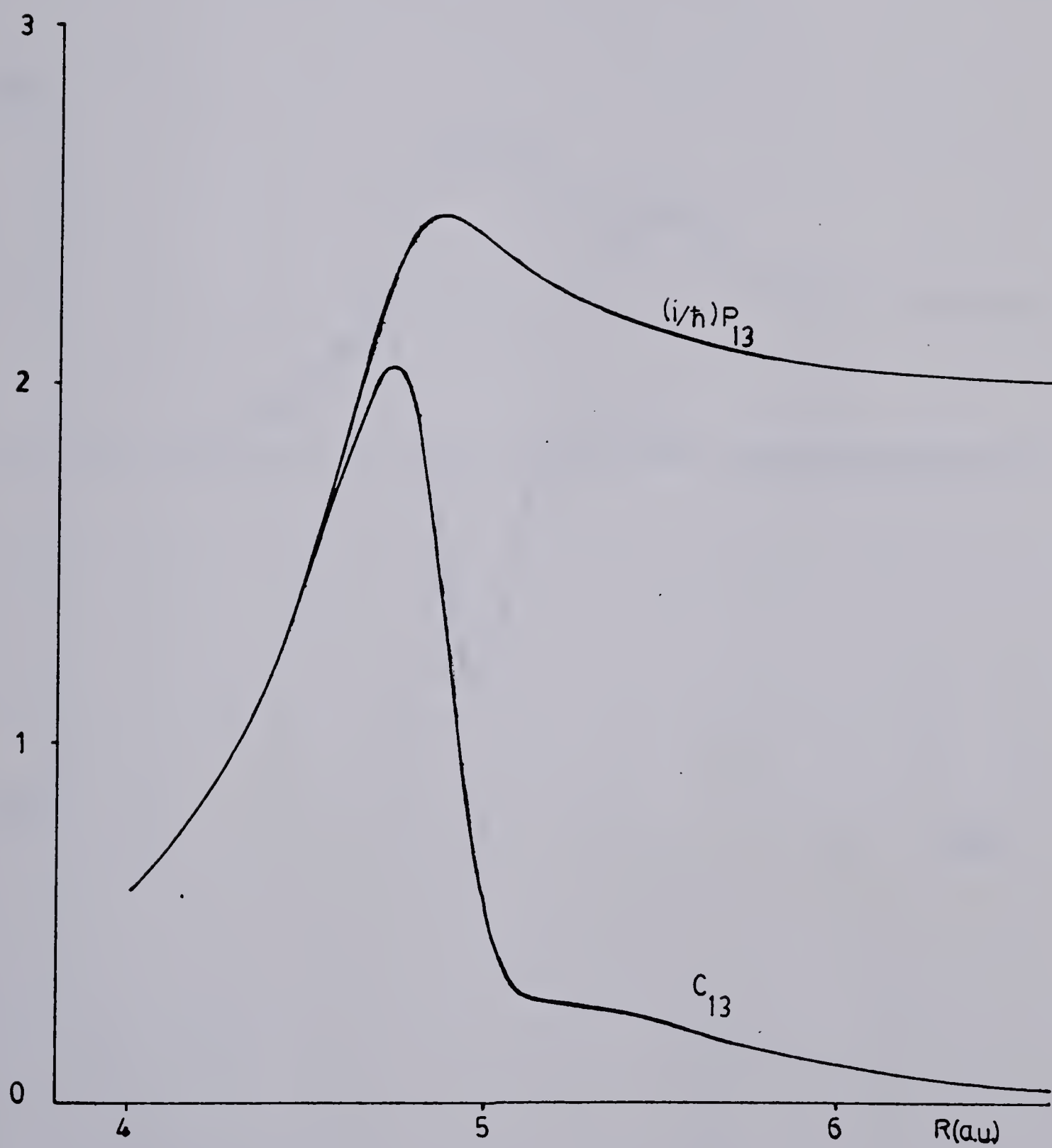
 $(i/\hbar)P_{13}$ & $C_{13} \text{ (a.u.)}^{-1}$ VS. $R \text{ (a.u.)}$ 

FIGURE 4.7

$-(i/\hbar)P_{15}$ & $-C_{15} \text{ (a.u.)}^{-1}$ VS. $R \text{ (a.u.)}$

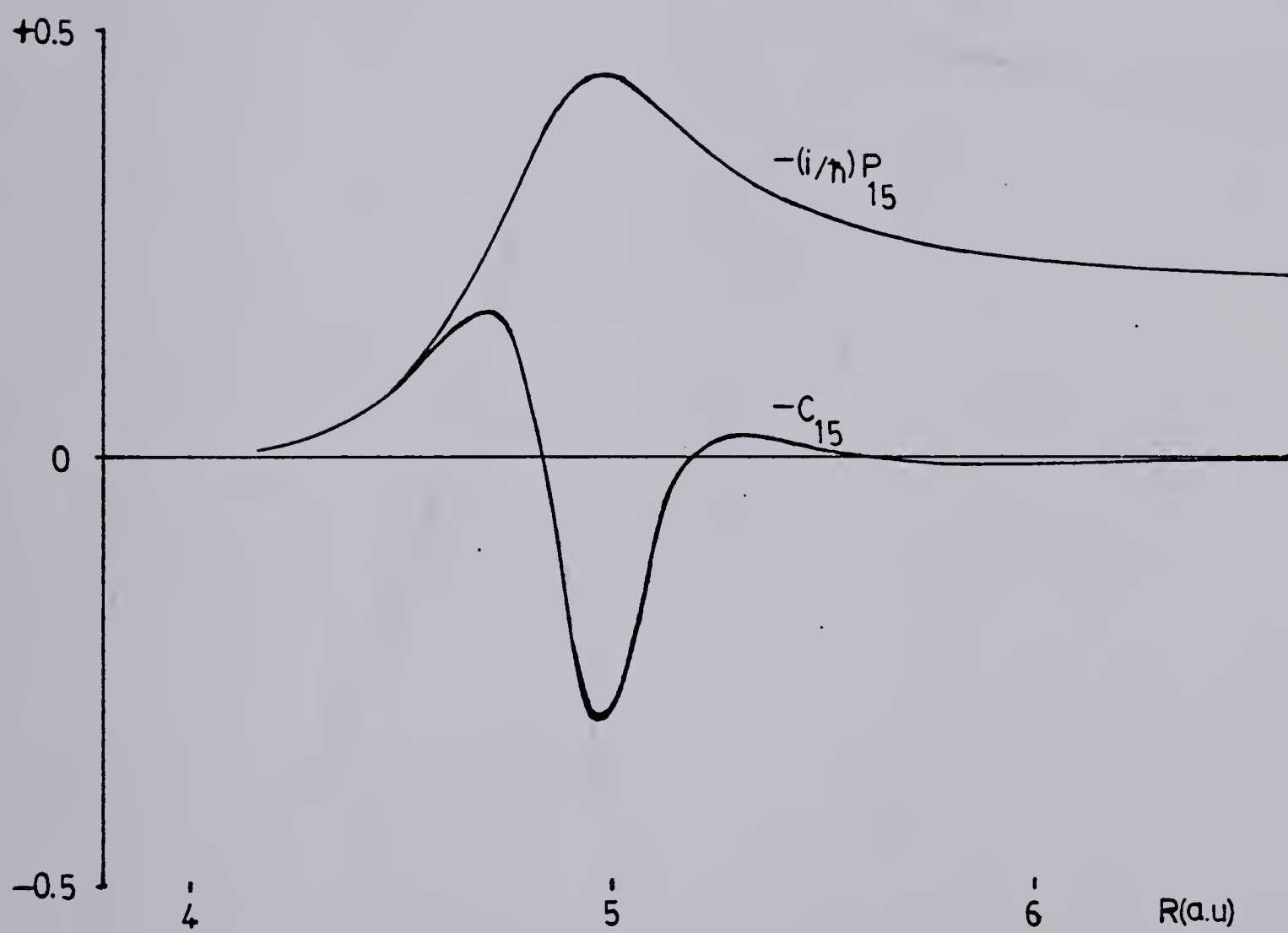
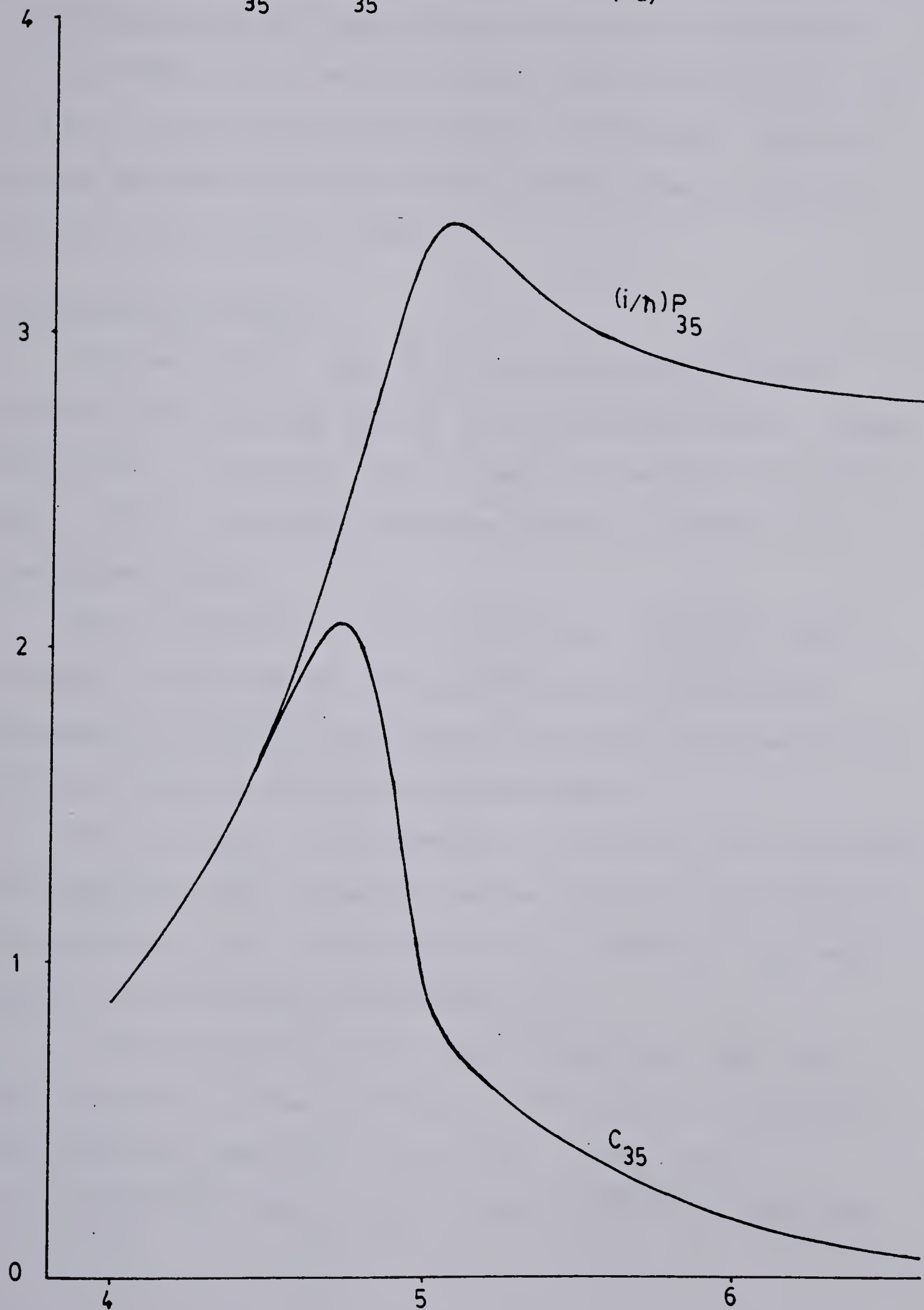


FIGURE 4.8

 $(i/\hbar)P_{35}$ & C_{35} (a.u.)⁻¹ VS R (a.u.)

It is not clear that higher eigenstates of U_1 will have negligible coupling to states of U_3 , for the higher wavefunctions have a considerable region in the classically allowed domain which overlaps the maxima of C_{13} , C_{15} , and C_{35} . The quantitative effects of this are revealed by the accurate solution of the coupled equations, the subject of Chapters 5, and 6.

2. Deuterium Shifts:

Curves $\{U_\ell^D(R)\}$, for DF_2^- are readily obtained by solving (4.1) with M_D for M_H in the reduced mass m . These curves are, of course, more closely spaced than those for HF_2^- , $\{U_\ell^H(R)\}$, but are otherwise similar, and have not been shown here.

The non-adiabatic coupling curves, $\{P_{ij}^D(R)\}$, have slightly higher maxima (as expected from (4.15); the maximum of $(i/\hbar)P_{02}^D$, for example, is about 4.16 (a.u.)^{-1}), but are otherwise similar to those shown.

At this point it is possible to compare the calculated and experimentally observed isotope shifts in equilibrium F-F distance, I.R. active stretching frequency (ν_3), and Raman active stretching frequency (ν_1).

A small negative shift upon deuteration, ΔR_0 , has been observed in the equilibrium F-F distance in crystals of sodium and potassium bifluoride. (KHF_2 , $\Delta R_0 = -0.0024 \text{ \AA}$; $^{20,29}NaHF_2$, $\Delta R_0 = -0.0046 \text{ \AA}$ 20,28). From the

difference between the minima of the curves $U_0^D(R)$ and $U_0^H(R)$, ΔR_0 has been estimated as -0.007 \AA , which is in good agreement with values calculated by Almløf²⁴ (-0.0058 \AA) and Jiang and Anderson⁵³ (-0.006 \AA).

Using the harmonic approximation, ν_3^H and ν_3^D have been estimated:

$$\nu_3^H \simeq 1516 \text{ cm}^{-1} ; \quad \nu_3^D \simeq 1058 \text{ cm}^{-1} ;$$

giving: $\Delta\nu_3 \simeq -458 \text{ cm}^{-1}$; $\nu_3^H/\nu_3^D \simeq 1.43$. Ketelaar and Vedder^{95,96} have measured 1450 cm^{-1} and 1023 cm^{-1} ($\Delta\nu_3 = -427 \text{ cm}^{-1}$; $\nu_3^H/\nu_3^D = 1.42$) for KHF_2 and KDF_2 respectively.

Finally, the Raman active transition is predicted to have a small positive shift:

$$\nu_1^H \simeq 677 \text{ cm}^{-1} ; \quad \nu_1^D \simeq 680 \text{ cm}^{-1} ; \quad \Delta\nu_1 \simeq +3 \text{ cm}^{-1}.$$

The calculation of Almløf²⁴ yielded $\Delta\nu_1 = +6 \text{ cm}^{-1}$. Dawson⁹⁷ has experimentally found $\Delta\nu_1$ to be $+1.25 \text{ cm}^{-1}$ ($\pm 0.25 \text{ cm}^{-1}$) for the potassium salt.

3. Asymptotic Values:

Asymptotically, each of the two wells of the double minimum potential must approach the potential function for a free HF molecule. The fundamental stretching frequency for HF is 3958.4 cm^{-1} ,⁹⁸ from which a harmonic oscillator force constant, $k = 0.56749 \text{ a.u.}$, has been calculated. Because the adiabatic representation uses the reduced mass for HF_2^- , m , (2.6% greater than the HF

reduced mass) a value of 3908 cm^{-1} is expected for the difference between the asymptotic values of ideal curves U_2 and U_0 . At large R values (greater than 7.0 a.u.) this difference actually converges to about 3930 cm^{-1} . The asymptotic curvature of the potential function at each minimum is clearly a little high, but is nevertheless a good representation.

It is also possible to estimate asymptotic values for the matrix elements $\{(i/\hbar)P_{ij}\}$.

At any R point where the potential has a double minimum (at $\pm z_0(R)$) it may be possible to represent the vibrational Born-Oppenheimer wavefunctions by a series of pairs of diatomic molecular vibrational functions (Hermite functions in the harmonic approximation) centred on $+z_0$ and $-z_0$, that is, a two-centre expansion:

$$\alpha_{\mu}^{\text{BO}}(z;R) = \sum_{j=0} a_{\mu j}(R) (\phi_j^-(z) + (-1)^{\mu+j} \phi_j^+(z)) \quad (4.27)$$

where:

$$\begin{aligned} \phi_j^{\mp}(z) &= \exp(-(\eta(z \pm z_0))^2/2) H_j(\eta(z \pm z_0)) \\ &\equiv W_j(u) \end{aligned} \quad (4.28a)$$

$$u \equiv \eta(z \pm z_0); \quad -\int_{-\infty}^{\infty} W_j W_k du = \delta_{jk} \quad (4.28b)$$

$H_j(u)$ is a normalized Hermite polynomial. ϕ_j^- is centred on $-z_0$ and ϕ_j^+ is centred on $+z_0$.

(4.27) contains the term $(-1)^{\mu+j}$ in order that the (g,u) symmetry requirement is met:

$$\alpha_{\mu}^{\text{BO}}(z;R) = (-1)^{\mu} \alpha_{\mu}^{\text{BO}}(-z;R) \quad (4.29)$$

$\eta(R)$ is, in general, a parameter to be chosen for convenience, perhaps defined by the curvature at $z = z_0$.

The expansion basis is non-orthogonal, and as the overlap between the functions $\{\phi_j^{-}; \phi_j^{+}\}$ increases (as $z_0 \rightarrow 0$, the barrier height goes down) it becomes increasingly difficult to uniquely define coefficients $\{a_{\mu j}\}$.

At large R distances, however, the BO states become well defined degenerate (g,u) pairs which directly correspond to HF molecular functions. If the HF functions are approximated by harmonic states, the parameter η is now fixed using the force constant, k , previously calculated:

$$\eta = ((km)^{1/2}/\hbar)^{1/2} \quad (4.30a)$$

which gives

$$\eta = 5.645 \text{ a.u.}^{-1} \text{ (dimension: length}^{-1}\text{)} \quad (4.30b)$$

and the first four Born-Oppenheimer states are:

$$\begin{aligned} \alpha_0^{\text{BO}} &= (\eta/2)^{1/2} (\phi_0^{-} + \phi_0^{+}) \\ \alpha_1^{\text{BO}} &= (\eta/2)^{1/2} (\phi_0^{-} - \phi_0^{+}) \\ \alpha_2^{\text{BO}} &= (\eta/2)^{1/2} (\phi_1^{-} - \phi_1^{+}) \\ \alpha_3^{\text{BO}} &= (\eta/2)^{1/2} (\phi_1^{-} + \phi_1^{+}) \end{aligned} \quad (4.31)$$

$(i/\hbar)P_{02}$ (or P_{13}) may now be estimated. Using the derivative property of the normalized Hermite functions,

(4.28a) gives:

$$\begin{aligned} \partial/\partial R \phi_j^{\mp} &= \pm \eta z_0'(R) [(j/2)^{1/2} \phi_{j-1}^{\mp} - ((j+1)/2)^{1/2} \phi_{j+1}^{\mp}] \\ (i/\hbar) P_{02} &= \langle \alpha_0^{\text{BO}} | \partial/\partial R | \alpha_2^{\text{BO}} \rangle \end{aligned} \quad (4.32)$$

$$\begin{aligned} &\underbrace{R \rightarrow \infty} \int_{-\infty}^{\infty} (\eta/2) (\phi_0^- + \phi_0^+) \eta z_0' [2^{-1/2} (\phi_0^- + \phi_0^+) - (\phi_2^- + \phi_2^+)] dz \\ \text{i.e., } (i/\hbar) P_{02} &\sim 2^{-1/2} \cdot \eta \cdot z_0'(R) \end{aligned} \quad (4.33)$$

However, $z_0(R) \sim R/2$; $\therefore z_0'(R) \sim 0.5$,

$$\text{and: } (i/\hbar) P_{02} \sim 2^{-3/2} \cdot \eta = 1.996 \text{ a.u.}^{-1} \quad (4.34)$$

Figure 4.3 shows that $(i/\hbar) P_{02}$, calculated using numerically generated eigenfunctions (solutions to (4.1)), converges most satisfactorily to the asymptotic value given by equation (4.34).

It is also possible to estimate asymptotic values for the other matrix elements in this way. The one-term harmonic approximation for higher states will, however, give poorer results; for example, in the harmonic approximation $(i/\hbar) P_{04}$ is asymptotically zero, whereas figure 4.4 shows it to be about 0.2 a.u.^{-1} . This merely indicates the asymptotic anharmonicity of α_4^{BO} , which may, however, be represented by a series of the harmonic functions (as in equation (4.27)), the coefficients for which will be asymptotically constant, leading to the constant value for $(i/\hbar) P_{04}$.

The translational origin of the asymptotically non-vanishing constant value for $(i/\hbar)P_{02}$ is evident in equation (4.33). In this derivation the proton translation effect has appeared as the term $z'_0(R)$, the translation of the position of the minimum of the potential with respect to the centre of mass of the heavy nuclei.

It is also possible to obtain an estimate of the "correct tailing" of the modified couplings $\{C_{ij}\}$. This "residual coupling" arises from a distortion of the double minimum wells as the bond dissociates (polarization), and may be estimated by replacing the operator $[\partial V_1/\partial R]_z$ in equation (4.15) by

$[\partial V_1/\partial R]_s$ for $z \leq 0$, and by

$[\partial V_1/\partial R]_t$ for $z \geq 0$ (s and t being the appropriate Jacobi coordinates z_A, z_B in this case: see figures 3.1 and 2.2).

The resulting matrix elements follow the curves $\{C_{ij}(R)\}$ very closely for $R \gtrsim 5.4$ a.u., and by ~ 7.0 a.u. they are virtually identical.

This shows that the switching function corrections are physically reasonable: they remove spurious coupling due only to translation, while retaining coupling due to distortion of the local potential wells.

CHAPTER FIVE

SOLUTION OF THE COUPLED EQUATIONS

A. Eigenvalue Condition.

The eigenvalue problem consists of the search for particular values of E , and the components of a vector $\underline{F}(R)$, which satisfy the matrix equation:

$$\{(-\hbar^2/2\mu)(d/dR)\underline{I} + \underline{C}(R)\}^2 + \underline{U}(R) - E\underline{I}\}\underline{F}(R) = \underline{0} \quad (5.1)$$

where \underline{I} is the unit matrix, \underline{U} is a diagonal matrix with elements $\{U_n(R)\}$, and \underline{C} is a skew-symmetric matrix with elements $\{C_{ij}(R)\}$ (figures 4.2 to 4.8).

In a manner similar to that of Chapter Four (section A), left and right asymptotic regions (LAR, RAR) are defined to be regions of small and large R respectively, far from the turning points of the curves $\{U_n(R)\}$.

In either asymptotic region, $\underline{C}(R)$ approaches zero, and the n th component of a solution vector $\underline{F}(R)$ (for arbitrary E) then behaves as a solution to the uncoupled one-dimensional Schrödinger equation with potential $U_n(R)$. There are, therefore, two linearly independent solutions for each component of a general solution vector $\underline{F}(R)$. This may also be expressed in the following way:

there exist $2N$ linearly independent solution vectors for an arbitrary energy E , where N is the dimension

of the matrix equation. The general solution is a linear combination of this set.

For an eigenvalue E_j , the components of the corresponding vector $\underline{f}_j(R)$, $\{f_{jn}(R); n = 1, 2, \dots, N\}$, must each be continuous and everywhere 'regular', that is they satisfy the boundary conditions:

$$\text{Lim}\{f_{jn}(R)\} = 0 \quad \text{as } R \rightarrow 0 \text{ or } \infty. \quad (5.2)$$

(5.2) eliminates N of the independent solutions (those with components growing exponentially away from the turning points).

For any E , N linearly independent solution vectors may be constructed which are regular in LAR, and N may be constructed which are regular in RAR. The following set may be used at an initial point in either LAR (R_ℓ), or RAR (R_r):

$$\begin{bmatrix} 1 \\ 0 \\ \cdot \\ \cdot \\ 0 \end{bmatrix}, \begin{bmatrix} 0 \\ 1 \\ \cdot \\ \cdot \\ 0 \end{bmatrix} \dots, \begin{bmatrix} 0 \\ 0 \\ \cdot \\ \cdot \\ 1 \end{bmatrix} \quad (5.3)$$

$\underline{F}_1 \qquad \underline{F}_2 \qquad \underline{F}_N$

Clearly this set, $\{\underline{F}_k(R); k = 1, 2, \dots, N\}$, is linearly independent at R_ℓ or R_r . Initial values for derivatives may be fixed by the JWKB criterion discussed

in Chapter Four, although, for the same reasons, the numerical values are unimportant.

The solution vectors, (5.3), may be numerically propagated from an asymptotic region towards the turning points of the curves $\{U_n(R)\}$. Let $\{F_n^l(R); n = 1, 2, \dots, N\}$ and $\{F_n^r(R); n = 1, N\}$ be, respectively, left and right regular linearly independent sets of solution vectors. For a general energy E , no linear combination of the set $\{F_n^r\}$ is identical to any linear combination of the set $\{F_n^l\}$. It is only when E is an eigenvalue that the two sets may be matched.

Thus, the eigenvalue condition is:

$$\sum_{n=1}^N \{d_{n-n}^l F_n^l + d_{n-n}^r F_n^r\} = \underline{0}$$

and

$$\sum_{n=1}^N \{d_{n-n}^l F_n^{l'} + d_{n-n}^r F_n^{r'}\} = \underline{0} \quad (5.4)$$

(5.4) implies the existence of the $2N$ coefficients $\{d_n^l, d_n^r; n = 1, 2, \dots, N\}$, which requires the vanishing of the $2N \times 2N$ determinant:

$$\begin{vmatrix}
 F_{11}^{\ell} & \cdot & \cdot & \cdot & F_{1N}^{\ell} & F_{11}^r & \cdot & \cdot & \cdot & F_{1N}^r \\
 \cdot & & & & \cdot & \cdot & & & & \cdot \\
 \cdot & & & & \cdot & \cdot & & & & \cdot \\
 F_{N1}^{\ell} & \cdot & \cdot & \cdot & F_{NN}^{\ell} & F_{N1}^r & \cdot & \cdot & \cdot & F_{NN}^r \\
 F_{11}^{\ell'} & \cdot & \cdot & \cdot & F_{1N}^{\ell'} & F_{11}^{r'} & \cdot & \cdot & \cdot & F_{1N}^{r'} \\
 \cdot & & & & \cdot & \cdot & & & & \cdot \\
 \cdot & & & & \cdot & \cdot & & & & \cdot \\
 F_{N1}^{\ell'} & \cdot & \cdot & \cdot & F_{NN}^{\ell'} & F_{N1}^{r'} & \cdot & \cdot & \cdot & F_{NN}^{r'}
 \end{vmatrix} \equiv W(E) \quad (5.5)$$

The principle for the solution of the eigenvalue problem is, therefore, merely a generalization of the method of Chapter Four. The energy dependent function $W(E)$, defined by (5.5), may be called a generalized Wronskian (for $N = 1$, it reduces to equation (4.9)).

The problem appears to be trivial: start a numerical integration of the coupled differential equations, (5.1), using initialized linearly independent column vectors given by (5.3); propagate from LAR and RAR to a suitable matching point, in a classically allowed region; calculate $W(E)$ given by (5.5), and numerically determine zeros. The zeros of $W(E)$ are eigenvalues, $\{E_j\}$.

Two main areas of difficulty arise: linear dependency and nodes. Before discussing them it is necessary to introduce the concept of open and closed channels.

B. Open and Closed Channels.

1. Zero Coupling.

If \underline{C} is everywhere zero, (5.1) reduces to N independent one-dimensional Schroedinger equations for the motion of the reduced mass μ in any of the N potential curves $\{U_n(R)\}$. This is precisely the Stepanov (or Born-Oppenheimer) approximation. It may also be called the one-channel approximation, as wavefunctions associated with a particular potential curve evolve independently of functions associated with all other curves.

If eigenvalues are sought for values of E which are less than the minimum of the curve $U_1(R)$, there can only be solutions for the curve $U_0(R)$. There is said to be one OPEN channel, and $(N-1)$ CLOSED channels. If, however, E is greater than the minimum of $U_1(R)$, but less than the minimum of $U_2(R)$, there are now two open channels, and $(N-2)$ closed channels. Eigenvalues associated with $U_1(R)$ and $U_0(R)$ are possible in this case.

In this simple, zero coupling, case it is easy to distinguish between eigenvalues associated with U_0 and U_1 , simply by initializing vectors with a 'signal' (non-zero value) in the appropriate channel; for example, \underline{F}_1 of equation (5.3) could only generate eigenvalues of $U_0(R)$, and \underline{F}_2 could only give eigenvalues of $U_1(R)$.

In the zero coupling case, no signal can ever occur in any channel which is initially zero.

2. Non-Zero Coupling.

Consider a two-channel situation (that is, the expansion basis is limited to two terms; $N=2$) with non-zero coupling. The upper channel is again said to be closed if E is everywhere less than $U_1(R)$. In order to find an eigenvalue, two linearly independent solution vectors must be generated in each asymptotic region, and propagated to a classically allowed region of $U_0(R)$. Although a vector of the form \underline{F}_1 (equation (5.3)) initially has no signal in the closed channel, this component grows exponentially during the numerical integration procedure. As integration continues into the classically allowed region of $U_0(R)$, the closed channel signal begins to dominate the open channel signal. The result is that, despite initializing two linearly independent vectors of the form \underline{F}_1 and \underline{F}_2 , they rapidly become linearly dependent as integration proceeds through a region of non-zero coupling in which at least one channel is closed. This problem *always* occurs for $(N > 1)$ -channel coupling. It has been found that two initially independent vectors may become identical in their components to at least eight significant digits.

The existence of linear dependence among either the members of $\{\underline{F}_n^l\}$, or of $\{\underline{F}_n^r\}$, invalidates the eigenvalue condition (5.4). If there is such a linear dependency, the determinant $W(E)$, (5.5), vanishes for *all* E . This

tendency to linear dependence has been overcome using a reorthogonalization procedure (originated by Riley and Kuppermann;⁹⁹ also described and applied by Wu and Levine¹⁰⁰) which will be described in the next section.

It is worth noting that for the two channel case, with both channels open, it may become difficult, or impossible, to associate any eigenvalue with a particular potential surface. For a weak coupling case, however, it is expected that a one-to-one correspondence of eigenvalues and potential curves will be maintained. This will be discussed in greater detail with reference to the results obtained for the HF_2^- system.

C. Linear Dependence.

1. Reorthogonalization.

The tendency of a set of left or right regular solution vectors, $\{\underline{F}_n; n = 1, 2, \dots, N\}$, to become linearly dependent may be compared to the gradual rotation into one plane of the physical vectors, $\vec{A}, \vec{B}, \vec{C}$, initially chosen to be orthogonal (perpendicular in space). The three vectors may be used to define a parallelepiped, the volume of which is given by the triple product:

$$\vec{A} \cdot \vec{B} \times \vec{C} = \begin{vmatrix} A_x & B_x & C_x \\ A_y & B_y & C_y \\ A_z & B_z & C_z \end{vmatrix} \equiv V \quad (5.6)$$

If the vectors lie in a plane ($V=0$), there is a linear dependency relationship between them. A necessary condition for linear dependence, therefore, is that the determinant V shall vanish. If the three vectors are not orthogonal, but do not lie in a plane, they may be rotated back to a position of mutual perpendicularity. This is the process of reorthogonalization: a particular choice of a linear combination of the vectors.

The linear independence of a set of N N -dimensional solution vectors may be maintained by periodic reorthogonalization at particular points, $\{R_i\}$, in the numerical integration.

The $N \times N$ determinant V (analogous to (5.6)), is constructed, with each column being one of the vectors \vec{F}_n . Each column is 'normalized' by dividing the components of that column by the square root of the sum of the squares. The value of this determinant is initially one (equation (5.3)), and is found to decrease smoothly to zero. There is a complication, due to the presence of 'nodes', which will be discussed later. If the value of V falls below 0.95 (chosen to maintain fairly rigorous

orthogonality), the reorthogonalization procedure is instituted.

Let $\underline{F}(R_i)$ be the *matrix* formed by the columns of the vectors $\{\underline{F}_n(R_i)\}$ at a reorthogonalization point R_i . Reorthogonalization consists of finding the matrix \underline{M} such that:

$$\underline{F}(R_i) \cdot \underline{M}(R_i) = \underline{I} \quad (5.7)$$

where \underline{M} is the inverse of \underline{F} .

At the point R_i , new derivative vectors must also be specified. Although the order of the matrix multiplication in (5.7) is unimportant, it represents a particular linear combination of solutions to the differential equation (5.1), and the correct order must be maintained in redefining the derivatives:

$$\underline{F}'(R_i) \cdot \underline{M}(R_i) \equiv \underline{F}'_{\text{new}}(R_i) \quad (5.8)$$

2. Extended Definition.

In order to define a continuous eigenfunction, it is necessary to apply the rotation matrix $\underline{M}(R_i)$ to all points in the numerical integration which occurred before the reorthogonalization point R_i . That is, for continuity, the same linear combination of solution vectors must be used at all points.

Suppose the matrices $\{\underline{F}_{\text{old}}(R_j)\}$ have been stored (*after* reorthogonalization where applicable) at all integration

points $\{R_j\}$; this set has discontinuities at the reorthogonalization points $\{R_i\}$. A new, continuous, set $\{\underline{F}_{\text{new}}(R_j)\}$ is constructed in the following way:

$$\underline{F}_{\text{new}}(R) = \underline{F}_{\text{old}}(R) \cdot \underline{M}(R_i) \quad (R_{i-1} \leq R < R_i) \quad (5.9)$$

$\underline{F}_{\text{new}}(R_i)$ has *already* been calculated as \underline{I} , and the point R_{i-1} used a different matrix, $\underline{M}(R_{i-1})$, to produce $\underline{F}_{\text{old}}(R_{i-1}) = \underline{I}$, so the definition of $\underline{F}_{\text{new}}(R)$ may now be extended:

$$\underline{F}_{\text{new}}(R) = (\underline{F}_{\text{old}}(R) \cdot \underline{M}(R_{i-1})) \cdot \underline{M}(R_i) \quad (R_{i-2} \leq R < R_{i-1}) \quad (5.10)$$

and

$$\underline{F}_{\text{new}}(R) = (\underline{F}_{\text{old}}(R) \cdot \underline{M}(R_{i-2})) \cdot \underline{M}(R_{i-1}) \cdot \underline{M}(R_i) \quad (R_{i-3} \leq R < R_{i-2}) \quad (5.11)$$

In this way, $\underline{F}(R)$ is redefined (after numerical integration is completed) as a continuous function from the matching point (where a final reorthogonalization is performed) back to the initial point in either asymptotic region.

3. Nodes.

The vanishing of the determinant V is a necessary condition for the linear dependence of N solution vectors. It is not, however, a sufficient condition to *ensure* their linear dependence.

There exist, in general, particular points, $\{R_p\}$, at which some linear combination of the linearly independent vector solutions to equation (5.1) is the null vector. These points are called *nodes*.

The matrices $\{\underline{F}(R_p)\}$ are then singular, but the derivative matrices, $\{\underline{F}'(R_p)\}$, are not. In the region of a node, therefore, the derivative vectors may be reorthogonalized, if necessary.

There are also points, $\{R_q\}$, at which the determinants, $\{VP\}$, of the matrices $\{\underline{F}'(R_q)\}$, vanish. These points may be called 'derivative nodes'.

The situation may be summarized in the following way: in general, three things happen as the numerical integration progresses,

- (i) initially linearly independent solution vectors become dependent; this is indicated by a gradual decrease in both $|V|$ and $|VP|$;
- (ii) 'nodes of V ' occur, in the region of which $|V|$ diminishes rapidly, but $|VP|$ remains stable; derivative vectors may be reorthogonalized;
- (iii) 'nodes of VP ' occur; $|VP|$ diminishes rapidly, but $|V|$ remains stable; vectors may be reorthogonalized.

It is quite often unnecessary to reorthogonalize in the region of either kind of node, as it is only when $|V|$ and $|VP|$ are *simultaneously* small that the solutions are

truly becoming linearly dependent.

D. Symmetric Potential Parity Separation.

If $V_1(z; R)$ is symmetric in z space, it has been shown (Chapter Four, section B5) that there is no coupling between Born-Oppenheimer states of opposite parity. The coupled equations (5.1), may be solved independently for each parity, in this case.

Components $\{F_{nj}; n = 0, 2, 4 \dots\}$, of a vector \underline{F}_j , behave independently of components $\{F_{nj}; n = 1, 3, 5 \dots\}$ (the matrix $\underline{C}(R)$ is block-factored according to parity), and therefore there exists a set of eigenvalues $\{E_m\}$, associated with even parity curves $\{U_n(R); n = 0, 2, \dots\}$, and a completely independent set of eigenvalues associated with odd parity curves, $\{U_n(R); n = 1, 3, \dots\}$.

E. Eigenfunctions.

1. Construction:

An eigenvalue E_j has an associated eigenfunction:

$$\psi_j(z, R) = \sum_{\ell=0}^N f_{j\ell}(R) \alpha_{\ell}(z; R) \quad . \quad (5.12)$$

Let the vector with components $\{f_{j\ell}\}$, be $\underline{f}_j(R)$.

For the symmetric potential case, the eigenfunctions are parity-separated, and (5.12) becomes:

$$\psi_j(z, R) = \sum_{\ell=P, P+2}^{(2N-2+P)} f_{j\ell} \alpha_{\ell} \quad (5.13)$$

where $P = 0, 1$ for even, odd parity.

It is necessary to distinguish between an *eigenvector*, \underline{f}_j , and a set of N linearly independent solution vectors, $\{\underline{F}_k; k = 1, 2, \dots, N\}$. The eigenvector \underline{f}_j must be *constructed* from a set $\{\underline{F}_k^\ell(R)\}$, for $R \leq R_m$, (where R_m is the matching point, at which $W(E_j)$, equation (5.5), has been found to vanish) and a set $\{\underline{F}_k^r(R)\}$, for $R \geq R_m$. It will be shown that reorthogonalization of $\{\underline{F}_k^\ell\}$, and $\{\underline{F}_k^r\}$, at R_m , leads to a simplification in the eigenvector construction, and so R_m is chosen between nodes of the determinant V (section C3 of this chapter). Reorthogonalization at the matching point leads to a matching of the magnitudes of left and right solution vectors.

For $R \leq R_m$, the eigenvector is a particular linear combination of the set $\{\underline{F}_k^\ell\}$, but for $R \geq R_m$ it is, in general, *another* particular linear combination of the set $\{\underline{F}_k^r\}$. That is:

$$\begin{aligned} \underline{f}_j(R) &= \sum_{k=1}^N d_{k-j}^\ell \underline{F}_k^\ell(R) & (R \leq R_m) \\ \underline{f}_j(R) &= \sum_{k=1}^N d_{k-j}^r \underline{F}_k^r(R) & (R \geq R_m) \end{aligned} \tag{5.14}$$

In order to define the (as yet unnormalized) eigenvector $\underline{f}_j(R)$, for all R , the set $\{d_{k-j}^\ell; d_{k-j}^r\}$ must be known.

At R_m :

$$\underline{f}_j(R_m) = \sum_k d_{k-j}^\ell \underline{F}_k^\ell(R_m) = \sum_k d_{k-j}^r \underline{F}_k^r(R_m) \tag{5.15}$$

and the reorthogonalization gives:

$$\begin{aligned}
 \underline{f}_j(R_m) &= d_1^\ell \begin{bmatrix} 1 \\ 0 \\ \cdot \\ \cdot \\ 0 \end{bmatrix} + d_2^\ell \begin{bmatrix} 0 \\ 1 \\ \cdot \\ \cdot \\ 0 \end{bmatrix} + \dots + d_N^\ell \begin{bmatrix} 0 \\ 0 \\ \cdot \\ \cdot \\ 1 \end{bmatrix} \\
 &= d_1^r \begin{bmatrix} 1 \\ 0 \\ \cdot \\ \cdot \\ 0 \end{bmatrix} + d_2^r \begin{bmatrix} 0 \\ 1 \\ \cdot \\ \cdot \\ 0 \end{bmatrix} + \dots + d_N^r \begin{bmatrix} 0 \\ 0 \\ \cdot \\ \cdot \\ 1 \end{bmatrix} \quad (5.16)
 \end{aligned}$$

Thus the simplification:

$$d_k^\ell = d_k^r \equiv d_k \quad (k = 1, 2, \dots, N) \quad (5.17)$$

The coefficients $\{d_k\}$ are now fixed for all R (providing appropriate reorthogonalization matrices are applied in appropriate regions of R).

Derivative matching provides the constraint needed to calculate the $\{d_k\}$:

$$\sum_k d_k (\underline{F}_k^{\ell'} - \underline{F}_k^{r'}) = \underline{0} \quad (5.18)$$

(5.18) may be written in matrix form:

$$\underline{\Delta} \cdot \underline{d} = \underline{0} \quad (5.19)$$

where:

$$\Delta_{ij} = F_{ij}^{\ell'} - F_{ij}^{r'} \quad ; \quad \underline{d} = \begin{bmatrix} d_1 \\ d_2 \\ \vdots \\ d_N \end{bmatrix}$$

(5.19) is an $N \times N$ homogeneous system in the N unknowns, $\{d_k\}$, and can only yield relative values. All the coefficients may, for example, be calculated relative to d_1 :

$$d_i = a_i d_1 \quad (i = 2, 3, \dots, N) \quad (5.20)$$

Now (5.19) provides N ways of defining the $(N-1)$ ratios $\{a_i\}$. In general, for large matrices, $\underline{\Delta}$, this may become a sensitive numerical procedure, but for the maximum dimension used in this study ($N=3$), no significant numerical instability has been found (for $N=3$, all three ways of defining a_2 and a_3 agree to 1 part in 10^5 , in the worst case, over the whole range of eigenvalues calculated).

2. Three Channel Example:

The three channel eigenfunctions may be constructed using (5.14):

$$\underline{f}_j(R) = d_1 \left\{ \begin{bmatrix} F_{11}^{\ell}(R) \\ F_{21}^{\ell}(R) \\ F_{31}^{\ell}(R) \end{bmatrix} + a_2 \begin{bmatrix} F_{12}^{\ell}(R) \\ F_{22}^{\ell}(R) \\ F_{32}^{\ell}(R) \end{bmatrix} + a_3 \begin{bmatrix} F_{13}^{\ell}(R) \\ F_{23}^{\ell}(R) \\ F_{33}^{\ell}(R) \end{bmatrix} \right\} \quad (R \leq R_m) \quad (5.21)$$

$$= d_1 \left\{ \begin{bmatrix} F_{11}^r(R) \\ F_{21}^r(R) \\ F_{31}^r(R) \end{bmatrix} + a_2 \begin{bmatrix} F_{12}^r(R) \\ F_{22}^r(R) \\ F_{32}^r(R) \end{bmatrix} + a_3 \begin{bmatrix} F_{13}^r(R) \\ F_{23}^r(R) \\ F_{33}^r(R) \end{bmatrix} \right\} (R \geq R_m) \quad (5.21)$$

a_2 and a_3 are known from (5.19), and d_1 is to be fixed by normalization.

3. Normalization:

Given that the components $\{f_{j\ell}\}$, of the eigenvector $\underline{f}_j(R)$, are now defined continuously throughout R , the constant d_1 is determined in the usual way. An eigenfunction must satisfy:

$$\int_0^\infty \int_{-\infty}^\infty \psi_j^2(z, R) dz dR = 1 \quad (5.22)$$

or, using (5.12):

$$\int_0^\infty \int_{-\infty}^\infty \left(\sum_{\ell} f_{j\ell} \alpha_{\ell} \right)^2 dz dR = 1 \quad (5.23)$$

Using the orthonormality of the set $\{\alpha_{\ell}\}$ in z space, (5.23) reduces to the requirement:

$$\int_0^\infty \left(\sum_{\ell} f_{j\ell}^2 \right) dR = 1 \quad (5.24)$$

F. IR Relative Intensities:

The integrated absorptivity associated with an IR active transition from the ground state $\psi_0^{(0)}$ (the superscript indicates even parity, $P=0$) to any, odd parity, excited state $\psi_n^{(1)}$, is shown by Wilson, Decius and Cross

(reference 57, p. 163) to be:

$$\int K d\nu = \frac{8\pi^3}{3hc} \nu_{no} (N_0^{(0)} - N_n^{(1)}) (T^{no})^2 \quad (5.25)$$

ν_{no} is the frequency for the transition, $N_j^{(P)}$ the number of molecules per unit volume in state j , and T^{no} is the transition moment defined by (5.26) (see, for example, Pauling and Wilson: reference 62, p. 299):

$$T^{no} \equiv \int_0^\infty \int_{-\infty}^\infty \psi_0^{(0)}(z, R) \mu(z, R) \psi_n^{(1)}(z, R) dz dR; \quad (5.26)$$

$\mu(z, R)$ is the dipole moment.

Transitions from the initial state $\psi_1^{(0)}$ ('hot bands') will not be considered (the occupancy of the first excited state of HF_2^- at 90°K is about 10^{-5} x that of the ground state).

The intensity of the transition $\psi_0^{(0)} \rightarrow \psi_n^{(1)}$, relative to the intensity of the 'fundamental' transition $\psi_0^{(0)} \rightarrow \psi_0^{(1)}$, is therefore given by:

$$RI^{no} \equiv \frac{\nu_{no}}{\nu_{oo}} \left[\frac{T^{no}}{T^{oo}} \right]^2 \quad (5.27)$$

for the case $N_n^{(1)} \ll N_0^{(0)}$.

Using (5.13) the transition moment integrals become:

$$T^{no} = \int_0^\infty \int_{-\infty}^\infty \{ \mu(z, R) \sum_{K=0,2,\dots} f_{0K} \alpha_K \sum_{J=1,3,\dots} f_{nJ} \alpha_J \} dz dR \quad (5.28)$$

or:

$$T^{\text{no}} = \sum_{K,J} \left\{ \int_0^\infty f_{0K}(R) f_{nJ}(R) \left[\int_{-\infty}^\infty \alpha_K(z;R) \mu(z,R) \alpha_J(z;R) dz \right] dR \right\} \quad (5.29)$$

A Taylor expansion of $\mu(z,R)$ about the point $z = 0$, $R = R_0$ (the position of the minimum of $U_0(R)$) is:

$$\begin{aligned} \mu(z,R) = & \mu(0,R_0) + (R-R_0) \partial \mu / \partial R + z \cdot \partial \mu / \partial z \\ & + 1/2 [(R-R_0)^2 \partial^2 \mu / \partial R^2 + 2(R-R_0) z \partial^2 \mu / \partial R \partial z \\ & + z^2 \partial^2 \mu / \partial z^2] \\ & + \text{higher order terms.} \end{aligned} \quad (5.30)$$

(all partial derivatives in (5.30) are evaluated at $z = 0$, $R = R_0$).

For the symmetric case the dipole moment is an odd function of z ($\mu(z,R) = -\mu(-z,R)$), and all coefficients of even powers of z are zero. To second order, the effective dipole moment operator may thus be written:

$$\mu \simeq A(1 + B(R-R_0))z, \quad (5.31)$$

with:

$$A \equiv \partial \mu / \partial z \quad ; \quad A.B \equiv \partial^2 \mu / \partial R \partial z.$$

$|B|$ is expected to be <1 .

A second order estimate of the relative intensities is then given by:

$$R I_{\text{no}}^{\text{no}} \approx \frac{v_{\text{no}}}{v_{\text{oo}}} \left[\frac{\int_0^\infty \left\{ \sum_{K,J} f_{0K} f_{nJ} I_{KJ} \right\} [1+B(R-R_0)] \cdot dR}{\int_0^\infty \left\{ \sum_{K,J} f_{0K} f_{0J} I_{KJ} \right\} [1+B(R-R_0)] \cdot dR} \right]^2 \quad (5.32)$$

where:

$$I_{KJ}(R) \equiv \int_{-\infty}^{+\infty} \alpha_K(z;R) z \alpha_J(z;R) dz \quad (5.33)$$

For three channel coupling, there are nine unique integrals $\{I_{KJ}\}$. These have been calculated numerically (cf. the matrix elements $\{A_{ij}\}$ of Chapter Four).

The effects of electrical anharmonicity may be investigated by taking $|B| > 0$ in equation (5.32). It will be shown (Chapter Six) that, at least for HF_2^- , the relative intensities of combination bands of the fundamental ($v_3 + n'v_1'$) and overtone ($'3v_3' + n'v_1'$), are not strongly dependent upon the value of the parameter B. That is, it is the non-orthogonality of the functions $\{f_{0K}(R), f_{nJ}(R); K = 0, 2, 4, \dots J = 1, 3, 5, \dots\}$ (mechanical anharmonicity and non-adiabatic coupling effects) rather than electrical anharmonicity, which is the principal cause of the broadness and structure of the v_3 band.

G. Curve Fits for HF_2^- :

The sets of curves $\{C_{ij}(R)\}$, $\{U_n(R)\}$ and $\{I_{KJ}(R)\}$ have all been calculated pointwise in R, at 0.05 a.u. intervals, from 3.80 a.u. to 7.00 a.u. It is necessary

to have continuous representations of these functions throughout the region of R in which numerical solutions to (5.1) are generated.

Expansion of the operator $(d/dR + \underline{C}(R))^2$, of equation (5.1), leads to a term involving $\underline{C}'(R)$. For this reason, it is convenient to represent each matrix element by a single, differentiable, functional form, throughout R .

Since, however, a knowledge of the derivatives of $\{U_n(R)\}$, and $\{I_{KJ}(R)\}$, is not explicitly required, they have been represented in a "piecewise" manner; first derivatives are matched at the boundaries of each region.

1. Matrix Elements.

For three channel coupling, it can be seen from figures 4.3 to 4.8 that the curves $\{C_{ij}(R)\}$ fall into two classes:

(i) adjacent state coupling.

Curves C_{02} , C_{24} , C_{13} and C_{35} all remain positive, and are essentially distorted single peaks. The Gaussian form, $A \exp(B(R-R_0)^2)$, has been found to decay too rapidly at large $|R-R_0|$, but a hyperbolic secant form, $A \operatorname{sech}^2(B(R-R_0))$, is quite satisfactory. An asymmetric curve, $C_{ij}(R)$ ($j = i + 2$), may be fitted to the polynomial-modified form:

$$C_{ij}(R) \simeq Y(R) \equiv P_L(R-R_0) \operatorname{sech}^2(B(R-R_0)) \quad (5.34)$$

where:

$$P_L(R-R_0) \equiv \sum_{\ell=0}^L a_{\ell} (R-R_0)^{\ell}$$

The constants R_0 and B are initially estimated from the position of the maximum of $C_{ij}(R)$, and the width at half the height, respectively. For a given order L , the coefficients $\{a_{\ell}\}$, of the polynomial P_L , are then obtained by a least-squares procedure, that is by minimizing S defined by:

$$S \equiv \sum_{k=1}^M [C_{ij}(R_k) - Y(R_k)]^2 \quad (5.35)$$

where M is the number of points.

S is then further minimized by varying B (for a fixed R_0), and recalculating the polynomial. Finally, S is minimized by varying R_0 , and iterating through B and P_L . In principle, higher order polynomials will also reduce S , but in practice, of course, round-off error limits the improvement. Polynomials of order eight to ten have been used.

(ii) Second neighbour coupling.

The shape of the curves C_{04} and C_{15} resembles that of the derivative of a single peak, and the curves may be fitted to the polynomial-modified derivative of (5.34):

$$C_{ij}(R) \simeq Y(R) \equiv P_L(R-R_0) \operatorname{sech}^2(B(R-R_0)) \tanh(B(R-R_0)) \quad (5.36)$$

Again the parameters B and R_0 are initialized, the least-squares polynomial obtained, and S minimized by varying B and R_0 .

2. $\{U_n\}$ and $\{I_{KJ}\}$:

Let $q_n(R)$ represent any one of these functions. The $\{q_n\}$ are all smoothly varying, non-oscillatory functions, and have all been approximated by the quadratic spline-fit method.

In this method, the region $R_1 \leq R \leq R_M$, in which the function $q(R)$ is known pointwise as $\{q(R_i); R_i = 1, 2, \dots, M\}$, is divided into sub-regions. In each of these regions, $q(R)$ is approximated by a different quadratic polynomial, with the continuity requirement that the first derivatives are matched at the boundaries between each region.

The procedure is initiated using three points, in a region where the curvature of $q(R)$ is small, to define the coefficients of a quadratic for region 1, $Q_1(R)$:

$$Q_1(R) \equiv \sum_{i=1}^3 a_i \left\{ \prod_{\substack{j=1 \\ j \neq i}}^3 (R-R_j) \right\} \quad (5.37)$$

whence

$$a_i = q(R_i) \prod_{\substack{j=1 \\ j \neq i}}^3 (R_i - R_j)^{-1} \quad (5.38)$$

$$\text{Thus } q(R) \simeq Q_1(R) \quad (R \leq R_3) \quad (5.39)$$

For all the curves $\{q_n(R)\}$, the first three points, $R = 3.80, 3.85, 4.00$ a.u., have been used to define region 1.

All subsequent regions are bounded by two points. The quadratic applicable to any region is defined by these two points, and the additional, derivative matching, constraint. For example:

$$Q_2(R_3) = Q_1(R_3) = q(R_3)$$

$$Q_2(R_4) = q(R_4)$$

$$\text{and } Q_2'(R_3) = Q_1'(R_3) \quad (5.40)$$

This procedure provides a representation of $q(R)$, which passes through all the points, R_1 to R_M , and has a continuous first derivative.

CHAPTER SIX

RESULTS AND DISCUSSION FOR HF_2^-

A. Eigenvalues and Eigenfunctions.

1. Uncoupled States:

In this one-channel case, there is only one term in the expansion (equation (5.12)) of the eigenfunction $\psi_j(z, R)$, corresponding to an eigenvalue E_j . Consequently, the eigenstate may be characterized by an additional index, n , referring to the potential curve $U_n(R)$, to which it belongs. Thus:

$$|j, n\rangle \equiv \psi_{jn}(z, R) = f_{jn}(R) \alpha_n(z; R) \quad (j=0, 1, 2, \dots) \quad (6.1)$$

The uncoupled eigenvectors $\{\underline{f}_{jn}(R)\}$, which satisfy equation (5.1), are, with parity separation ($P=0, 1$):

$$\underline{f}_{jp} = \begin{bmatrix} f_{jp}^{(R)} \\ 0 \\ 0 \\ \vdots \\ \vdots \end{bmatrix} ; \quad \underline{f}_{jp+2} = \begin{bmatrix} 0 \\ f_{jp+2}^{(R)} \\ 0 \\ \vdots \\ \vdots \end{bmatrix} ; \quad \underline{f}_{jp+4} = \begin{bmatrix} 0 \\ 0 \\ f_{jp+4}^{(R)} \\ \vdots \\ \vdots \end{bmatrix} \quad (6.2)$$

Each curve $U_n(R)$ has, therefore, associated with it a set of eigenvectors and eigenvalues $\{\underline{f}_{jn}(R); E_{jn}; j = 0, 1, 2, \dots\}$, which have no dependence on any other curve $U_m(R)$.

Figures 6.1 and 6.2 show, for HF_2^- , the series of eigenvalues calculated for even and odd parity curves $\{U_n\}$.

For a particular value of n , the assignment of an eigenvalue E_{jn} to the curve $U_n(R)$ is unambiguous, even in the case of the near degeneracy of E_{03} and E_{71} (figure 6.2). E_{03} is clearly associated with U_3 , because it is generated by the vector $\begin{pmatrix} 0 \\ f_{03}(R) \end{pmatrix}$, whereas E_{71} is generated by $\begin{pmatrix} f_{71}(R) \\ 0 \end{pmatrix}$.

This may seem painfully obvious, but it has an important conceptual consequence: the one-channel approximation asserts that the observation of a transition $|0,0\rangle \rightarrow |j,n\rangle$, allows a definite statement to be made concerning the change in the vibrational Born-Oppenheimer state of the proton (actually the reduced mass m). With final state $|0,1\rangle$, the proton is said to be in its first excited state; a 'fundamental' transition, with frequency ν_3 , corresponding to an excitation of the 'H-F stretching mode', is said to have occurred. [Actually, of course, the change in state of the system is not quite the same as a simple excitation of the proton, because the function $f_{00}(R)$ is not the same as $f_{01}(R)$: they are both ground state wavefunctions for the reduced mass μ , but in different potential wells]. Similarly the transition $|0,0\rangle \rightarrow |0,3\rangle$ is referred to as an 'overtone' of the H-F stretching frequency: ' $3\nu_3$ '.

FIGURE 6.1

EVEN PARITY UNCOUPLED EIGENSTATES

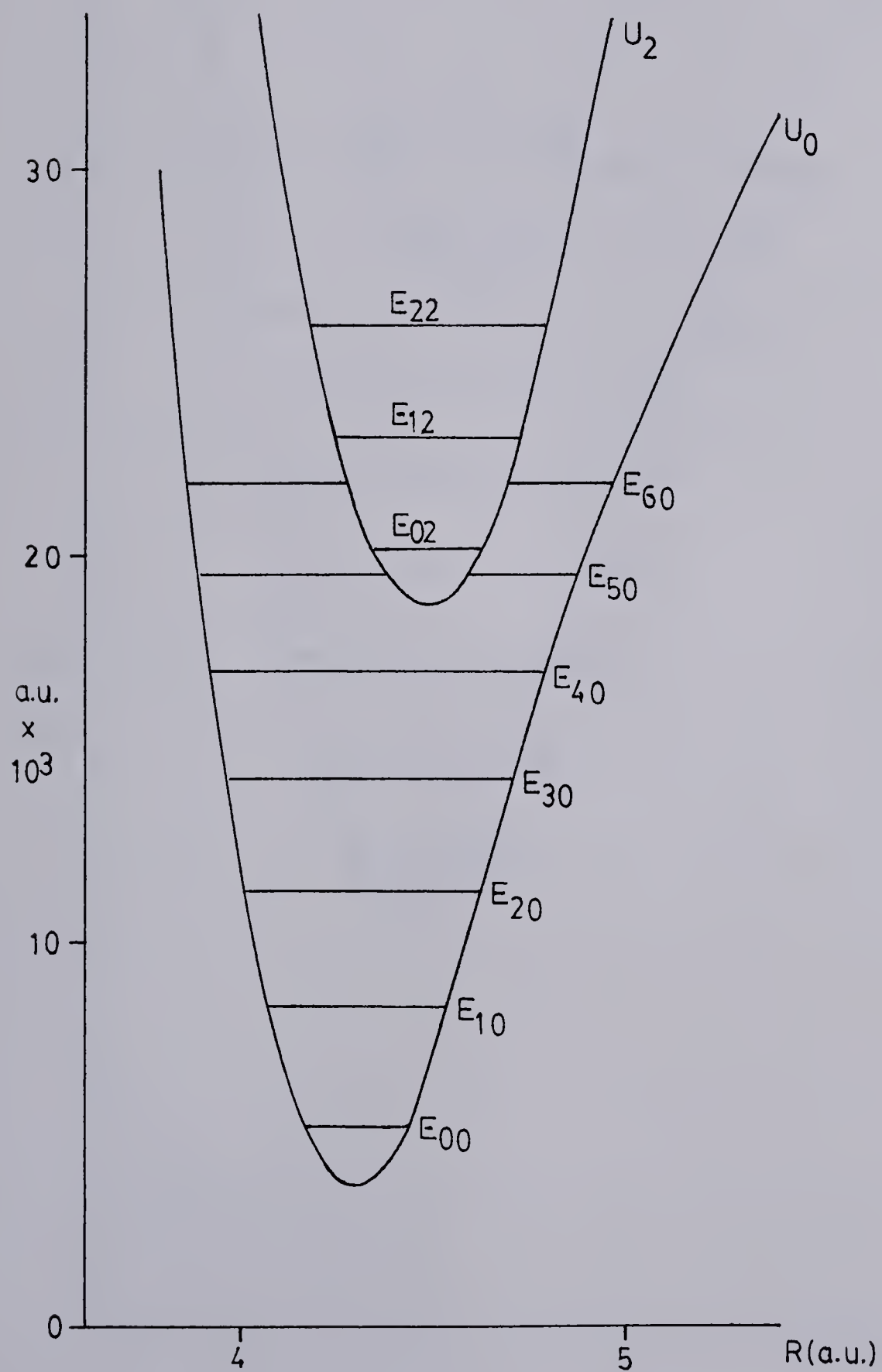
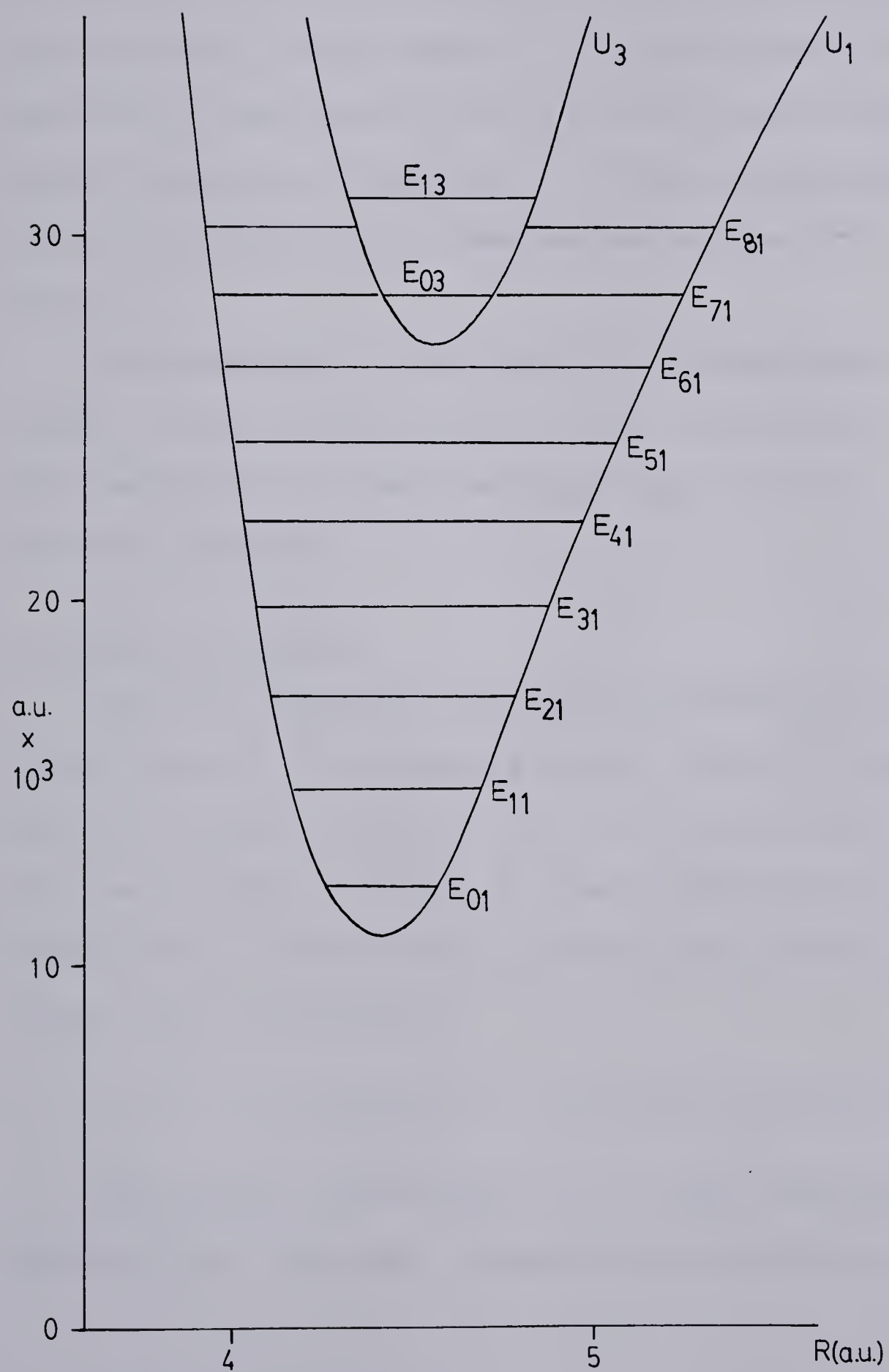


FIGURE 6.2

ODD PARITY UNCOUPLED EIGENSTATES



In this way, the line due to the transition $|0,0\rangle \rightarrow |j,1\rangle$, may, with some validity, be referred to as a 'combination band', of the form: $\nu_3 + j'\nu_1$ '. Again, the frequency ν_1 has been written within quotation marks because the spacing of levels (corresponding to energy states of the reduced mass μ , in the one-channel approximation) in the curve $U_1(R)$ is not the same as the Raman active transition frequency ν_1 : this corresponds to the transition $|0,0\rangle \rightarrow |1,0\rangle$ (excitation of the 'F-F stretching mode').

To summarize, in the one-channel approximation, the terms: 'state of the proton', and 'combination bands of the fundamental ν_3 (and overtone ' $3\nu_3$ ') with ν_1 ', have definite meaning.

2. Coupling Effects:

For $N(>1)$ -channels, the total wavefunction $\psi_j(z,R)$ cannot be said to correspond to any *definite* vibrational state of either the proton, or the reduced mass μ . It is not now strictly possible to characterize the state ψ_j by an index n , referring to a particular curve $U_n(R)$, since, for two channels:

$$\psi_j^{(P)} = f_{jP}(R)\alpha_P(z;R) + f_{jP+2}(R)\alpha_{P+2}(z;R) \quad . \quad (6.3)$$

(the parity superscript, P , is only possible for a symmetric, AHA, system). Eigenvectors satisfying (5.1) are:

$$\underline{f}_j^{(P)} = \begin{bmatrix} f_{jP}(R) \\ f_{jP+2}(R) \end{bmatrix}$$

for example:

$$\underline{f}_0^{(0)} = \begin{bmatrix} f_{00} \\ f_{02} \end{bmatrix} ; \quad \underline{f}_0^{(1)} = \begin{bmatrix} f_{01} \\ f_{03} \end{bmatrix} \quad (6.4)$$

If the coupling between Born-Oppenheimer states P and $P+2$ were *strong*, the contributions of $f_{jP}(R)$ and $f_{jP+2}(R)$, to the state vector $\psi_j^{(P)}(z, R)$, could be comparable, and it would not be possible to describe a transition from $\psi_0^{(0)}$ to $\psi_j^{(1)}$ as a combination band, $\nu_3 + j'\nu_1$, or as an overtone ' $3\nu_3$ ' + $j'\nu_1$ '. It would be meaningless to talk of the 'vibrational state of the proton' or 'the vibrational state of the reduced mass μ '.

The vibrational state of a closely coupled system would, therefore, be completely characterized by the function $\psi_j^{(P)}$, without reference to the isolated states of excitation of the symmetric (F-F), and asymmetric (H-F), stretching modes. It would only be possible to describe a transition as symmetric ($\psi_j^{(P)} \rightarrow \psi_k^{(P)}$), or asymmetric ($\psi_j^{(0)} \rightarrow \psi_k^{(1)}$), but it would *not* be possible to ascribe to that transition an excitation of *only* the H-F, or *only* the F-F, mode. In this case, the idea of isolated stretching modes becomes invalid, and the motions are truly inseparable.

Fortunately, the non-adiabatic coupling turns out to be weak, and a one-to-one mapping of the uncoupled to coupled eigenvalues is possible. The double index notation, $|j,n\rangle$, remains valid, with the understanding that the proton is 'almost' purely in the n th Born-Oppenheimer state.

For weak coupling, the index n defines the dominant channel. For example, with two channels, *either*:

$$\int_0^\infty (f_{jP}(R))^2 dR \gg \int_0^\infty (f_{jP+2}(R))^2 dR \Rightarrow |j,P\rangle \quad (6.5)$$

indicates the *lower* channel dominates, or the reverse of the inequality indicates the *upper* channel dominates:

$$\int_0^\infty (f_{jP+2}(R))^2 dR \gg \int_0^\infty (f_{jP}(R))^2 dR \Rightarrow |j,P+2\rangle \quad (6.6)$$

If (6.5) holds, the wavefunction may be characterized by the double index $|j,P\rangle$, and the eigenvalue by E_{jP} . This is *always* the case, for HF_2^- , when the upper channel is *closed* (states E_{00} to E_{40} , figure 6.1; E_{01} to E_{61} , figure 6.2).

A more interesting situation occurs when both channels are *open*. Upon finding an energy $E = E_j^{(P)}$, for which the generalized Wronskian ($W(E)$ (equation (5.5))), is zero, it is then only by an examination of the components of the eigenvector $\underline{f}_j^{(P)}(R)$, that an appropriate second index may be assigned, using the criteria (6.5) and (6.6).

In particular, the states $|7,1\rangle$ and $|0,3\rangle$, which are very nearly degenerate in the one-channel approximation, are noticeably separated by the introduction of coupling:

N Channels:	$(E_{30}-E_{71}) \text{ cm}^{-1}$	
1	-2.2	
2	+37.2	
3	+55.5	(6.7)

Figure (6.3) shows, for two channels, the behaviour of $W(E)$ in the region of these closely spaced eigenvalues.

Even and odd parity eigenvalues (E_{jP}, E_{jP+2}) , obtained from calculations using one to three channels, are shown in tables one and two respectively.

The effect of non-adiabatic coupling is clearly quite small for all cases in which the upper channel is closed (less than 1/2%), and as expected, the higher eigenvalues (upper channel open) are more noticeably affected (for example, E_{02} and E_{03} change by about 1%).

The convergence of the eigenvalues is excellent, particularly for those associated with the lower channel of each parity.

The weaker convergence of the eigenvalues (E_{03} and E_{13}) associated with the upper surface $U_3(R)$, is expected: for such states the three-channel approximation links only one higher surface ($U_5(R)$). It would require a

FIGURE 6.3

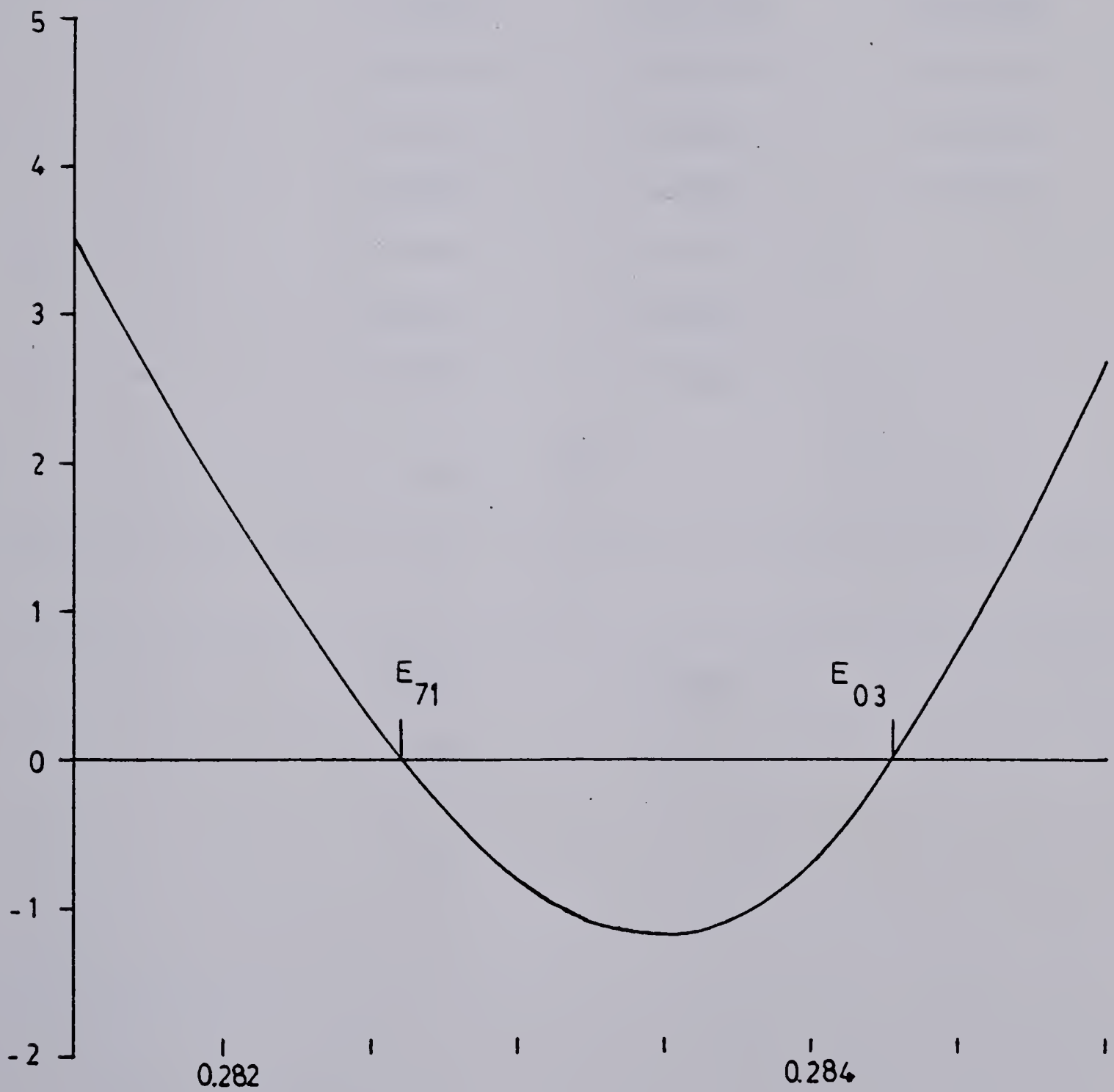
 $W(E) \times 10^2$ VS. $E \times 10$ (A.U.)2 CHANNELS : E_{71} ; E_{03} 

TABLE ONE

EVEN PARITY EIGENVALUES (HF_2^-)
(ATOMIC UNITS)

$E_{j0} \times 10^2$			
j	1 Chan.	2 Chan.	3 Chan.
0	0.524433	0.526146	0.526148
1	0.832564	0.834527	0.834538
2	1.13347	1.13555	1.13560
3	1.42397	1.42511	1.42531
4	1.69966	1.69672	
5	1.95641	1.94562	
6	2.19363	2.17827	
$E_{j2} \times 10^2$			
j			
0	2.01665	2.03001	
1	2.30661	2.32513	

TABLE TWO

ODD PARITY EIGENVALUES (HF_2^-)
(ATOMIC UNITS)

$E_{j1} \times 10^2$			
j	1 Chan.	2 Chan.	3 Chan.
0	1.21456	1.21878	1.21879
1	1.48124	1.48488	1.48492
2	1.73719	1.73937	1.73952
3	1.98096	1.98057	1.98089
4	2.21185	2.20857	2.20895
5	2.43015	2.42493	2.42514
6	2.63689	2.63055	2.63061
7	*2.83334	2.82596	2.82601
8	3.02071	3.01274	3.01268
$E_{j3} \times 10^2$			
j			
0	*2.83233	2.84289	2.85131
1	3.09917	3.11243	3.11734

* Near degeneracy: $E_{71}; E_{03}$.

four-channel calculation to match the convergence of the lower surface eigenvalues. Considering this convergence, however, it can be expected with confidence that a four-channel calculation would not significantly alter the three-channel upper eigenvalues shown.

Three-channel calculations have not been performed for the higher states of even parity (Table one) for two reasons: (i) they are not involved in the IR-active vibrational transitions; (ii) the effects of three-channel coupling can be inferred from the odd parity set (Table two).

Figures 6.4 to 6.15 show the components (from calculations using one to three channels) of eigenvectors $\{f_{jn}(R)\}$, associated with wavefunctions $\{\psi_{jn}(z,R)\}$. Each figure has six numbered graphs: '1' shows the single component $f_{jn}(R)$ (either f_{jp} or f_{jp+2} , depending on the curve $U_n(R)$ to which it belongs) obtained from a one-channel calculation; '2', and '3' show components $f_{jp}(R)$, and $f_{jp+2}(R)$ from a two-channel calculation; '4', '5', and '6' show components $f_{jp}(R)$, $f_{jp+2}(R)$, and $f_{jp+4}(R)$ from a three-channel calculation.

These pictures clearly illustrate the concept of 'weak' coupling (compare the relative magnitudes of the components of an $(N>1)$ -channel eigenvector), and the consequent assignment of the second index, n , indicating the dominant channel, or as an alternative viewpoint: the uncoupled

FIGURE 6.4
PSI 00

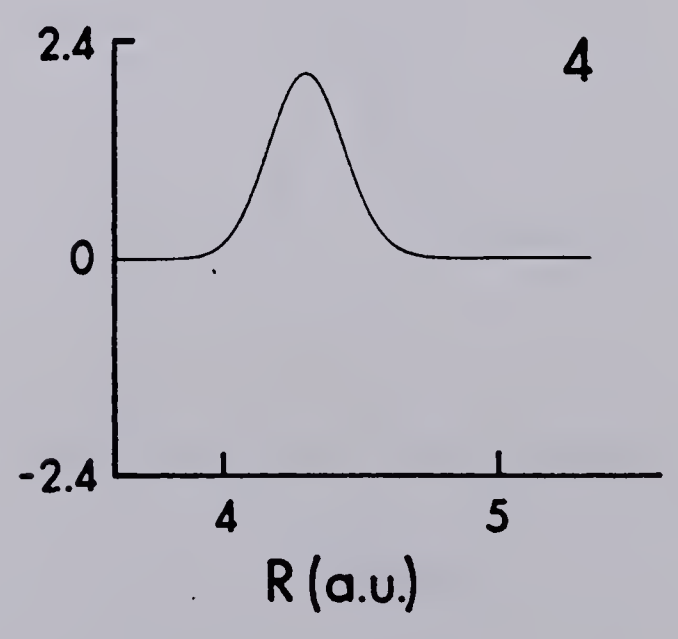
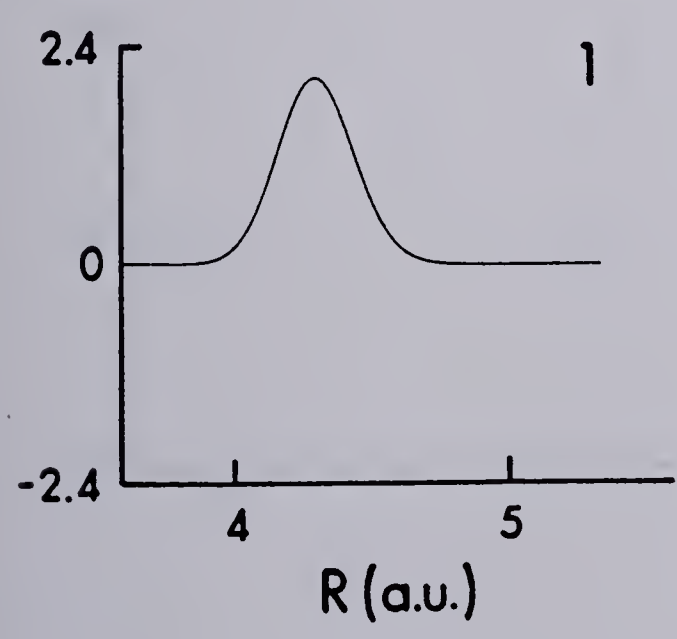
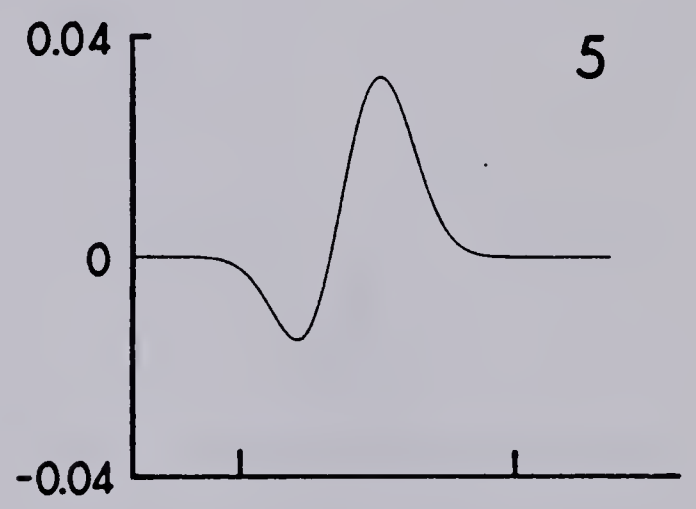
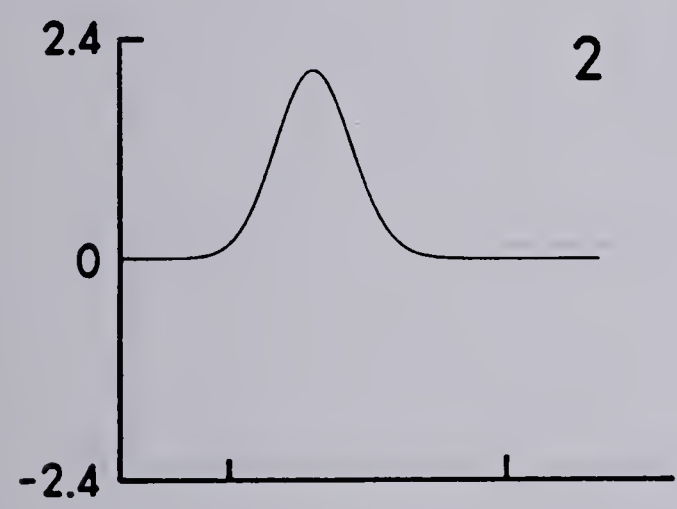
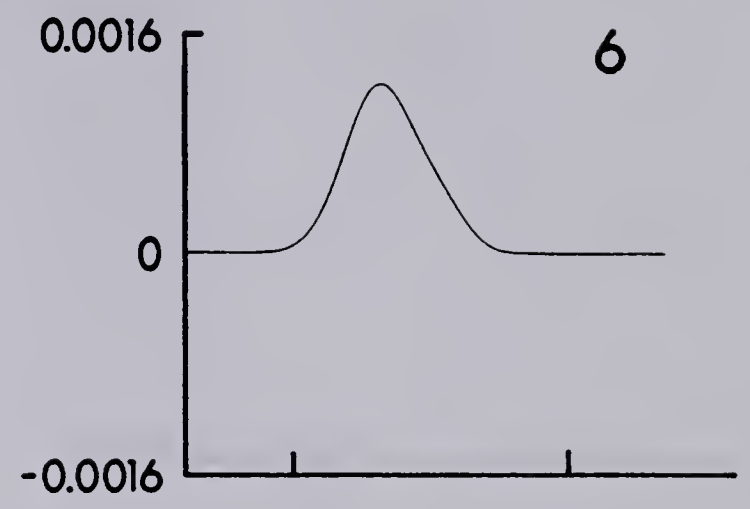
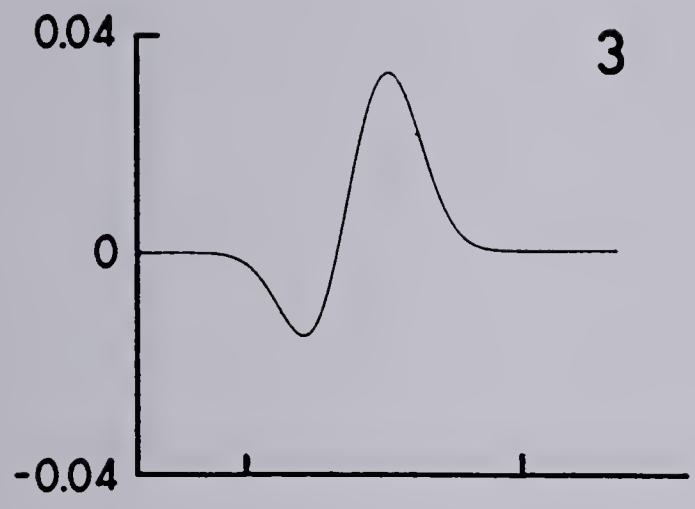


FIGURE 6.5
PSI 01

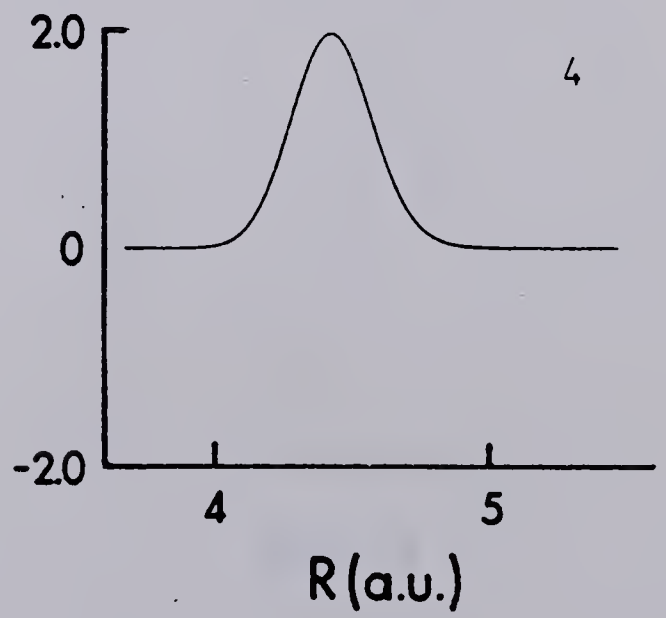
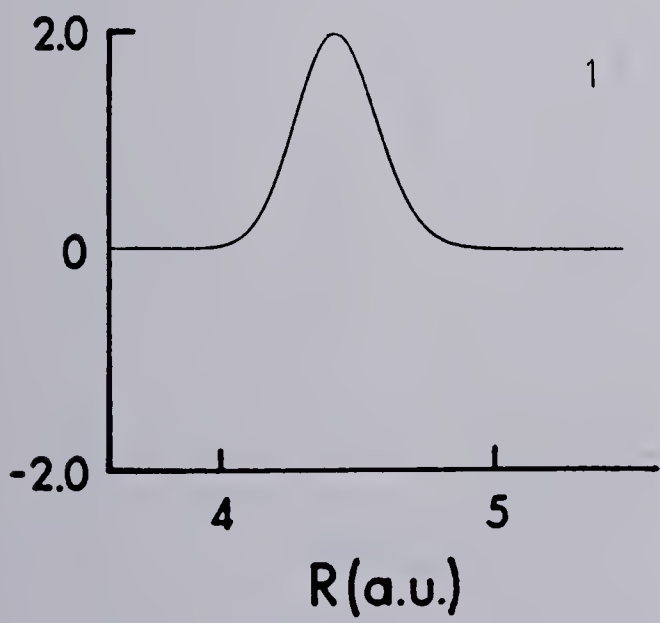
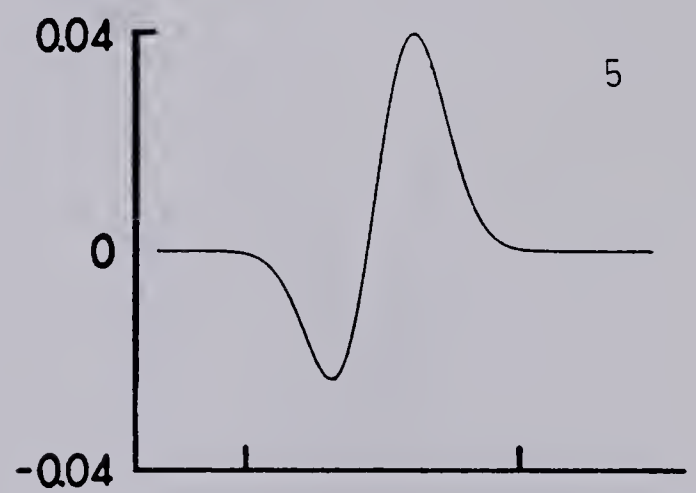
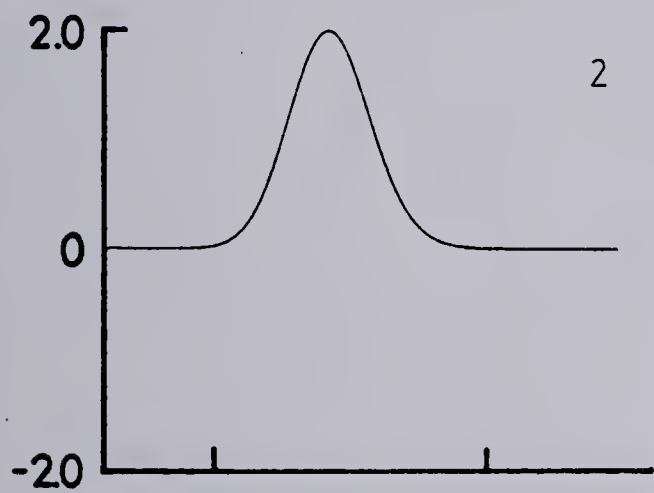
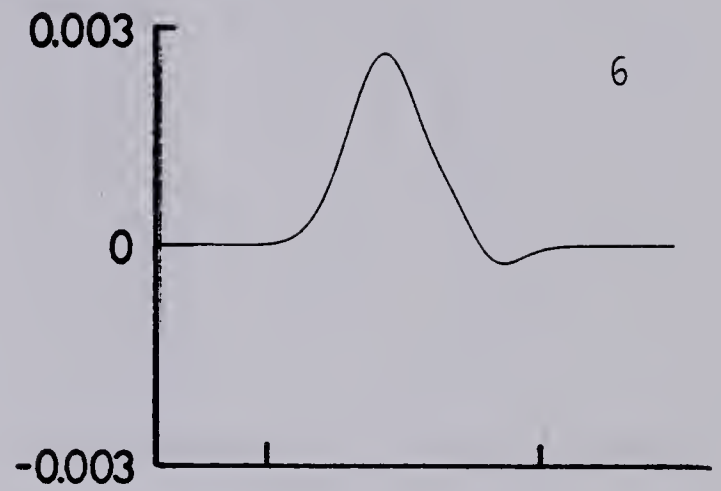
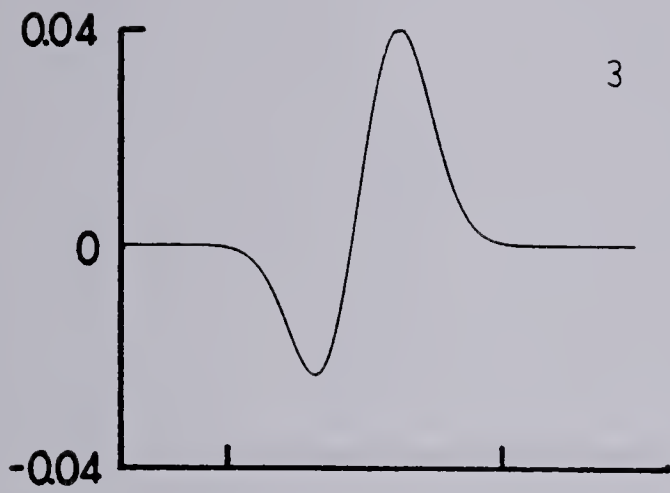


FIGURE 6.6
PSI 11

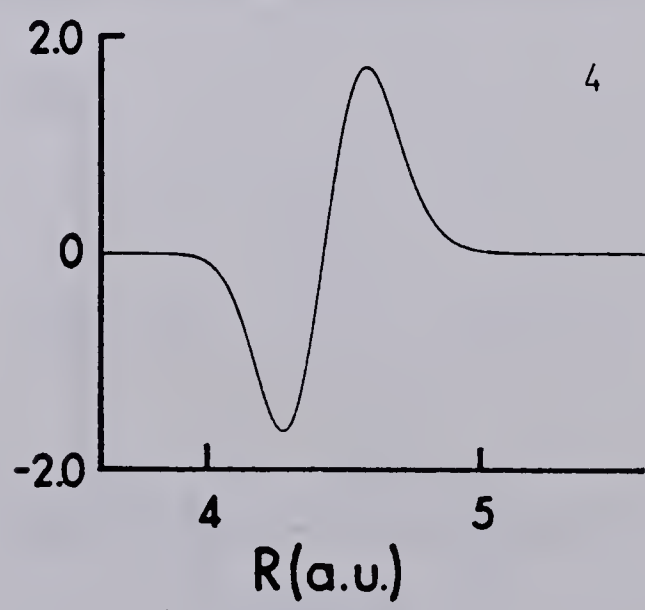
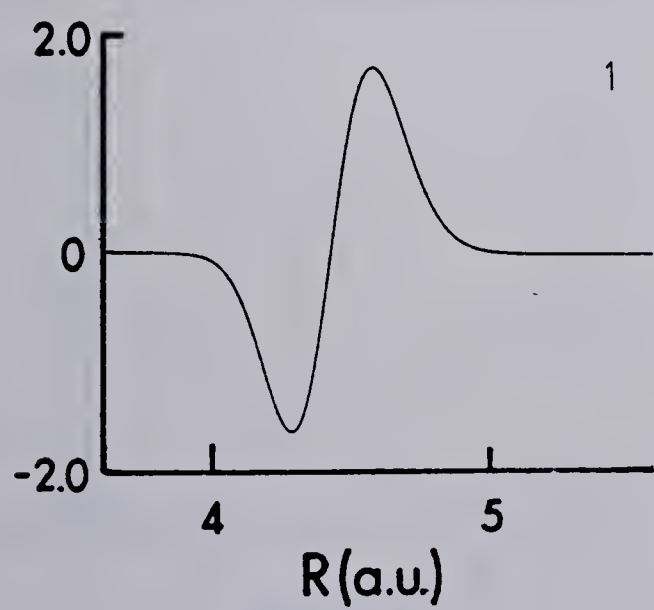
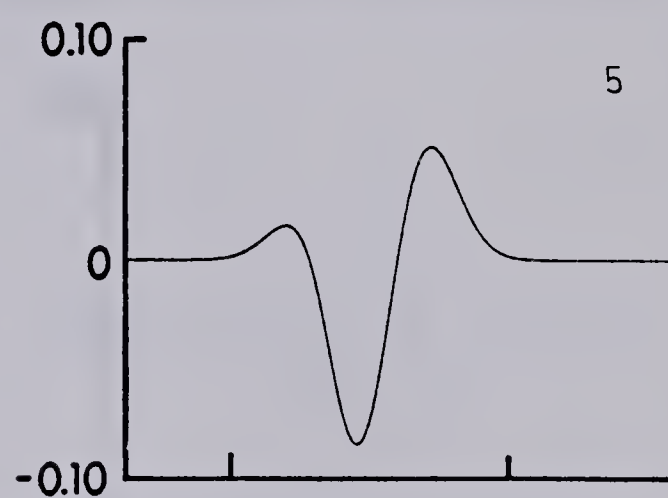
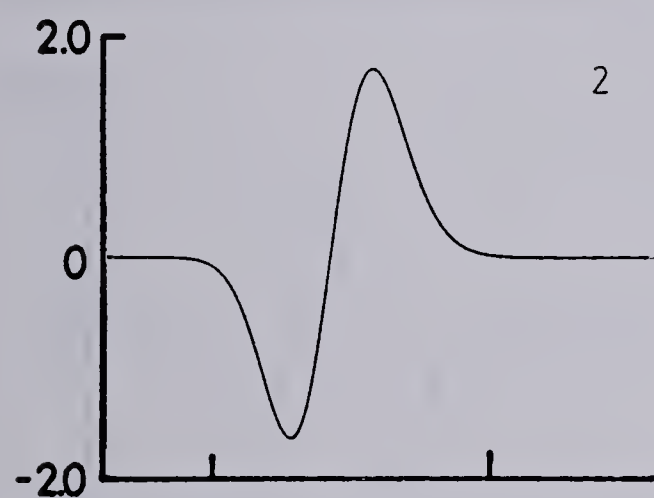
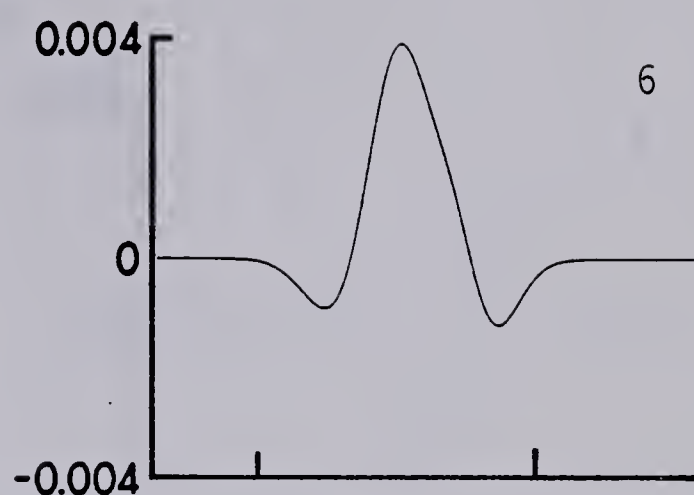
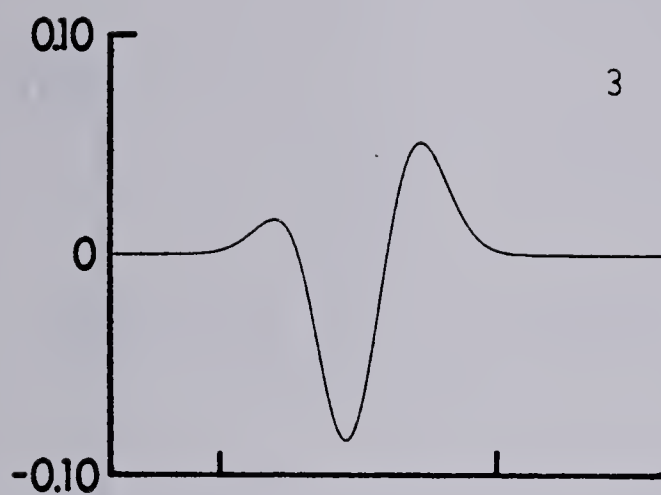


FIGURE 6.7
PSI 21

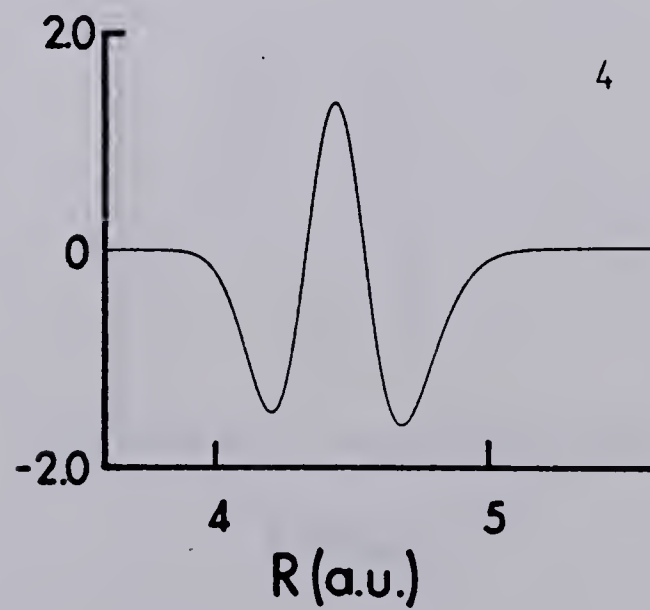
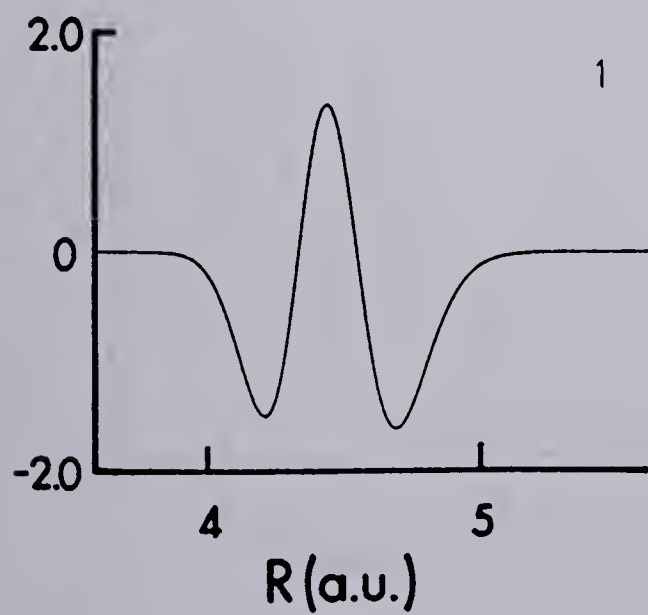
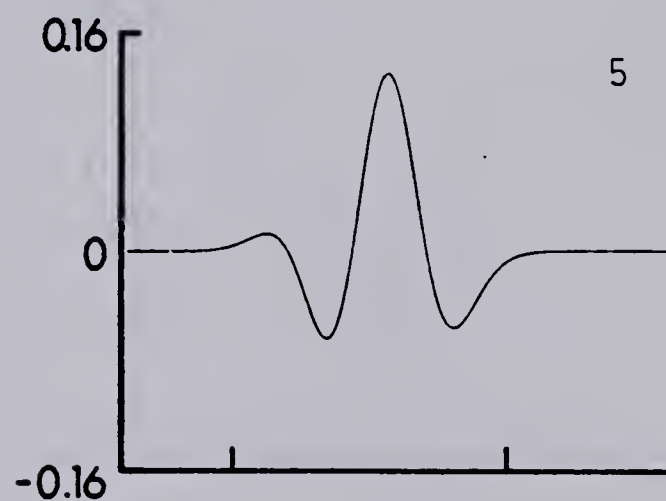
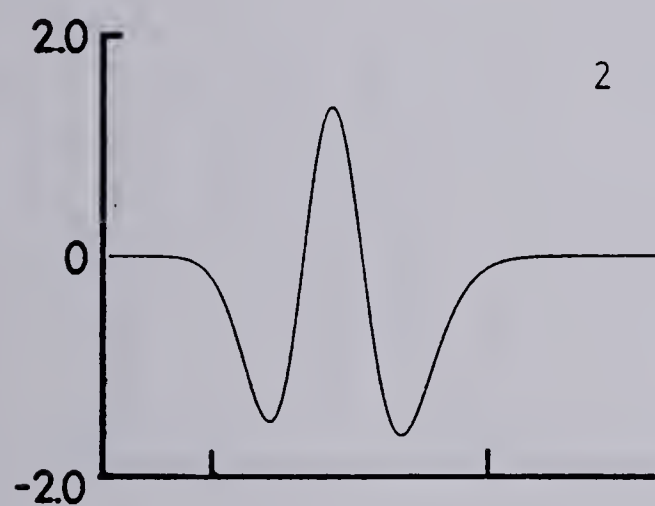
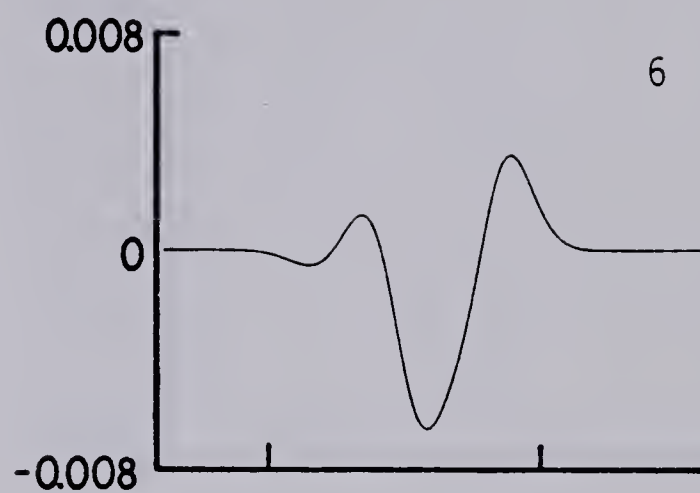
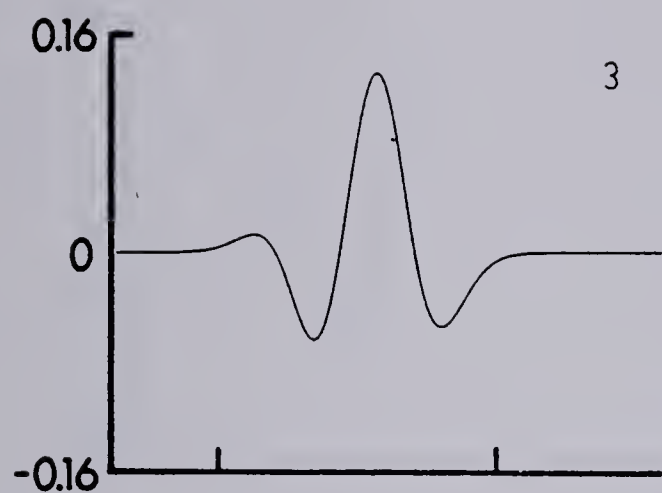


FIGURE 6.8
PSI 31

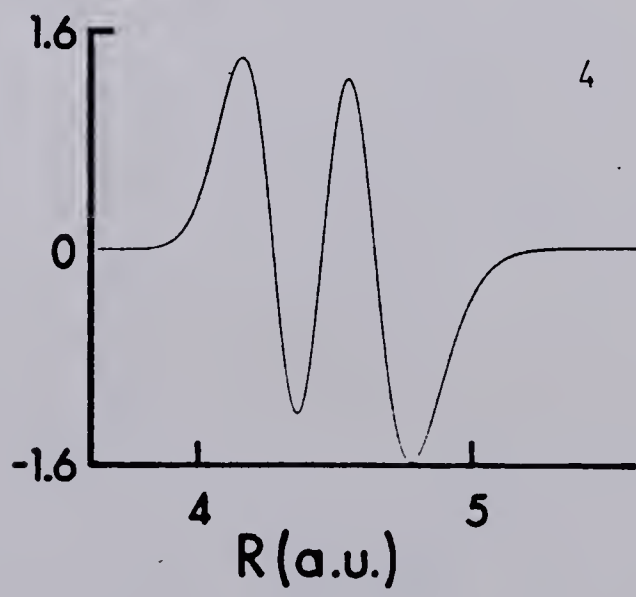
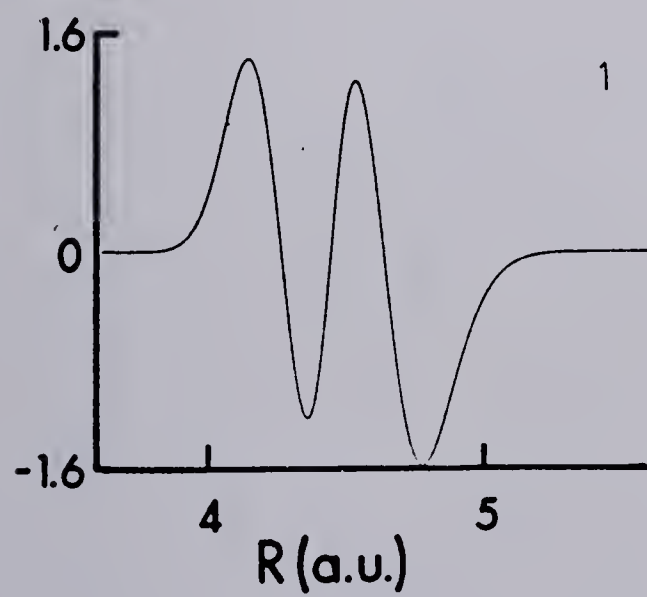
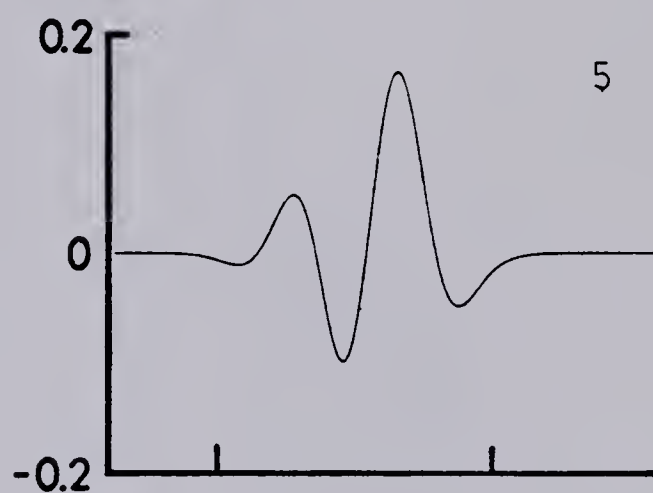
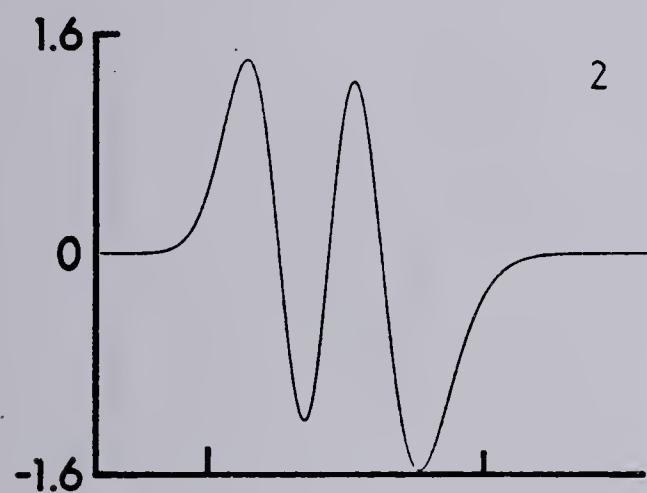
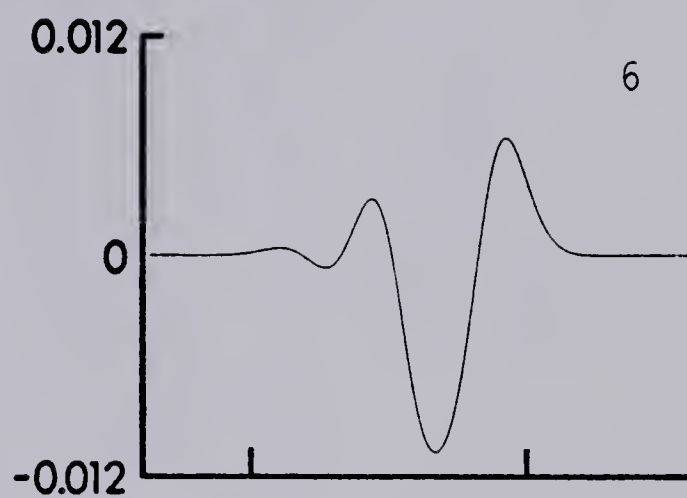
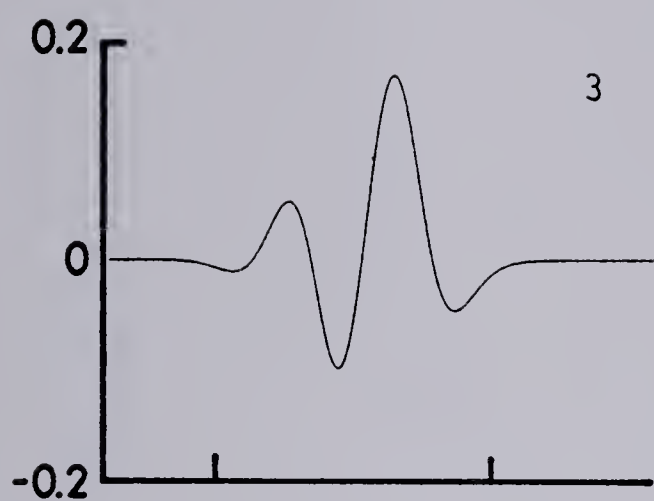


FIGURE 6.9
PSI 41

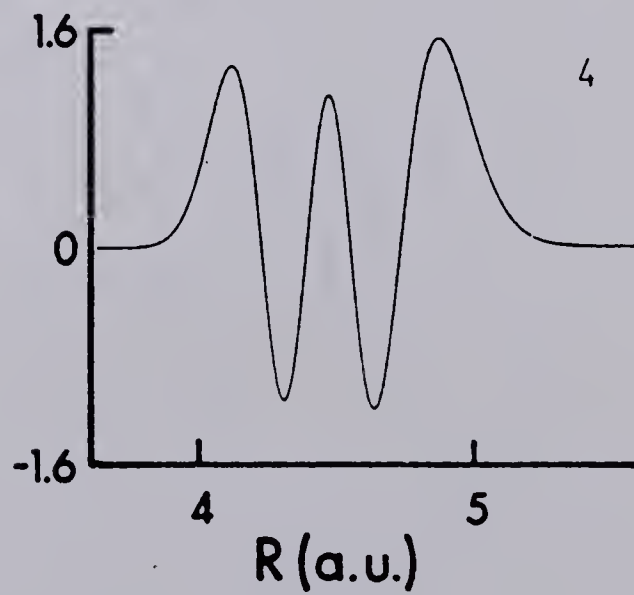
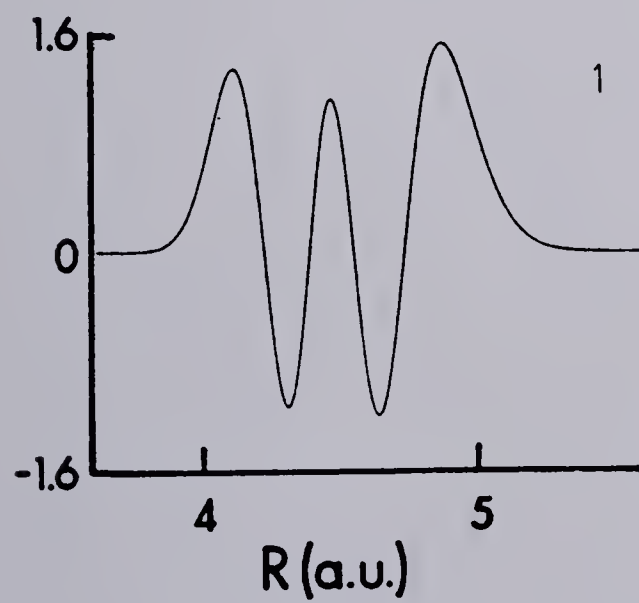
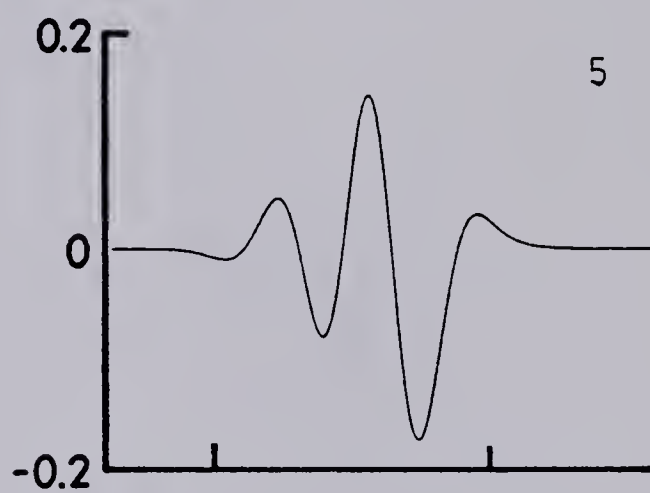
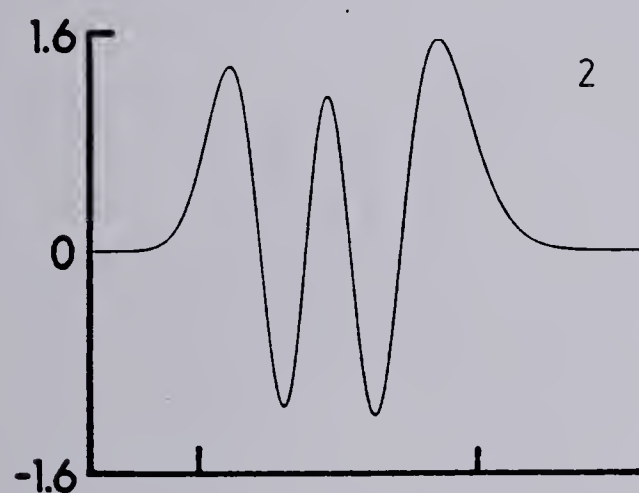
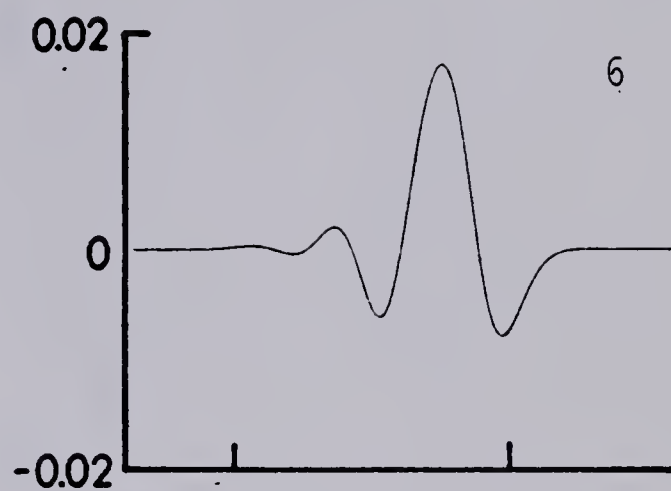
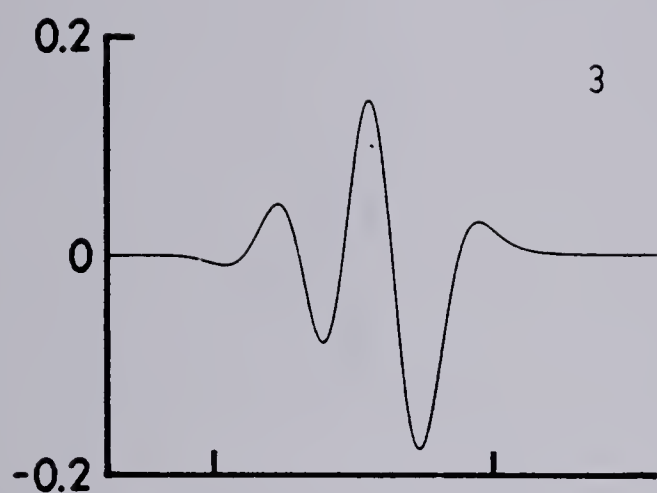


FIGURE 6.10
PSI 51

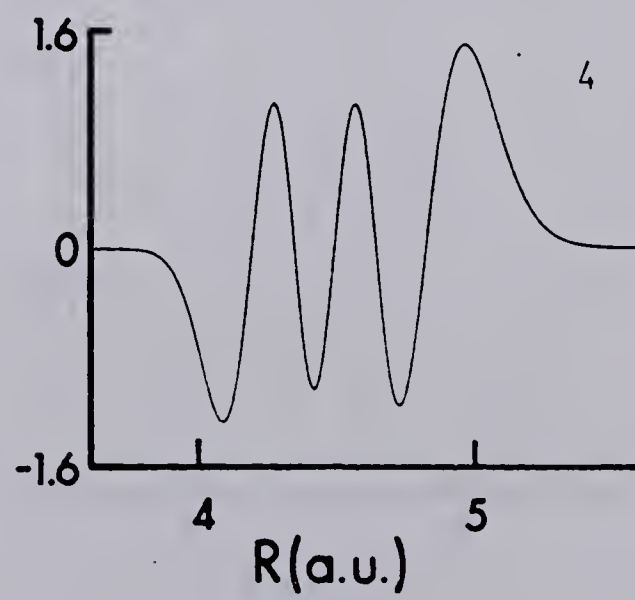
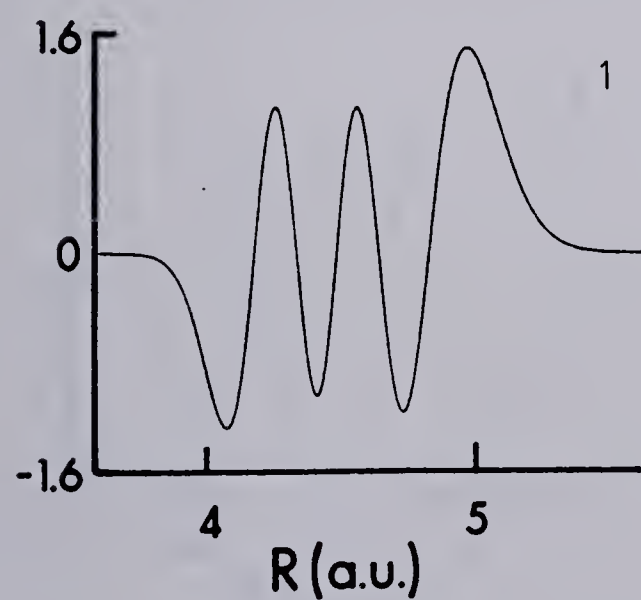
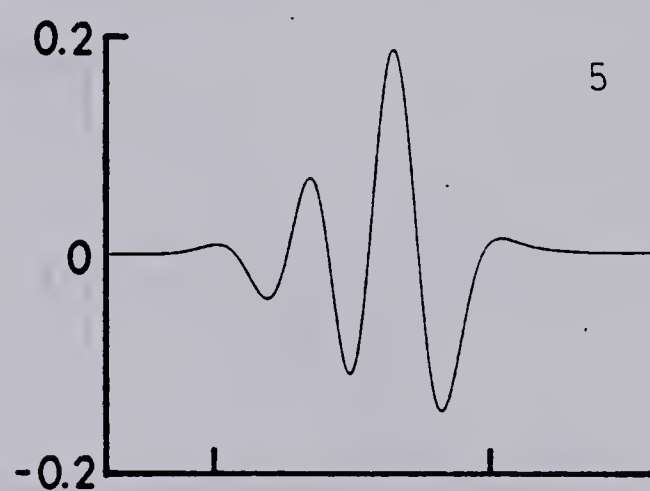
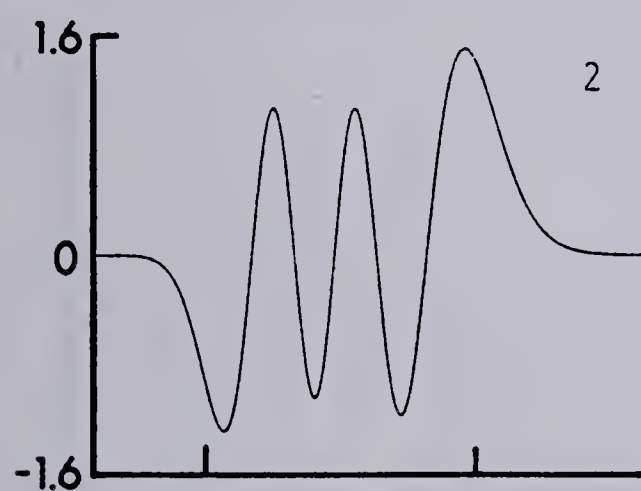
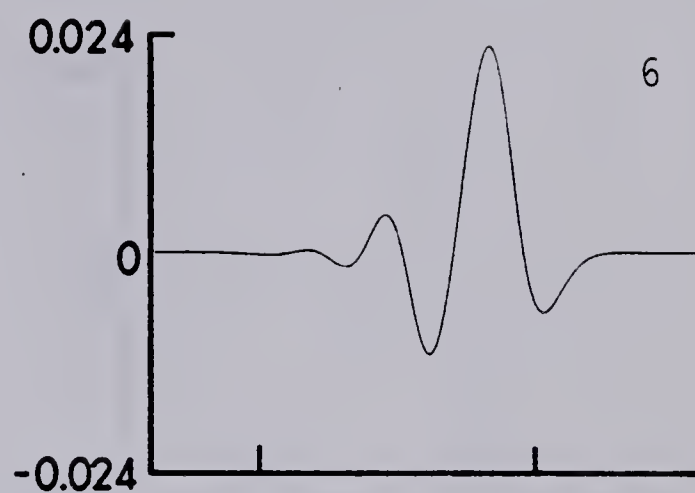
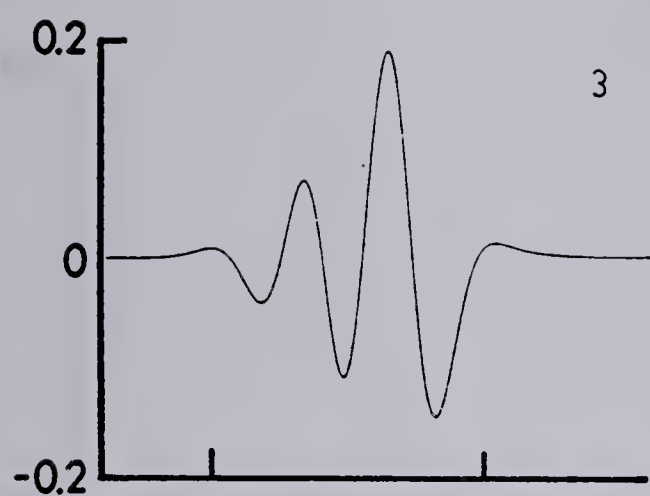


FIGURE 6.11
PSI 61

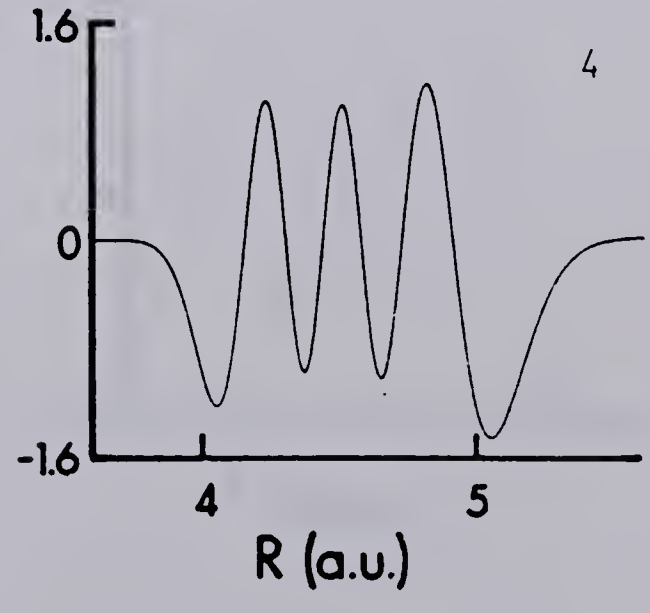
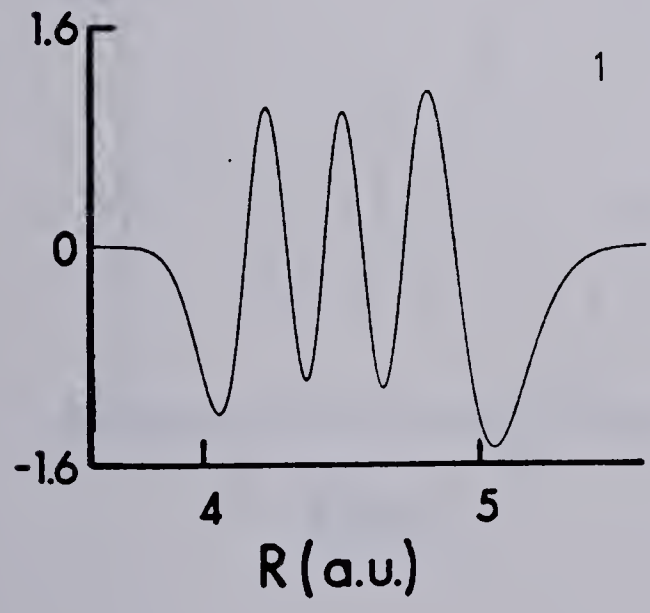
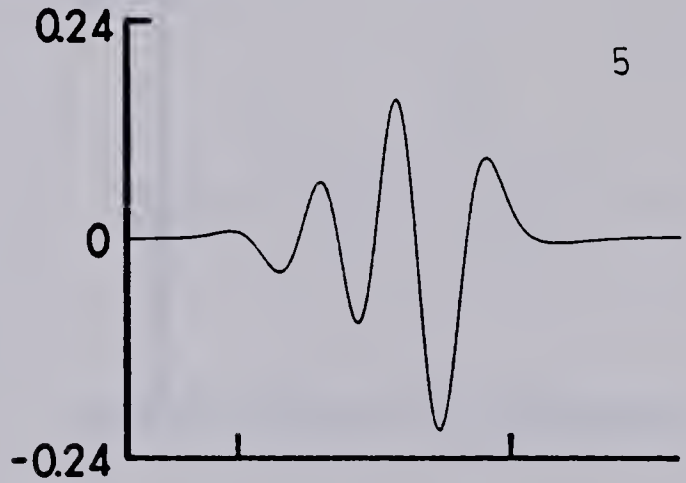
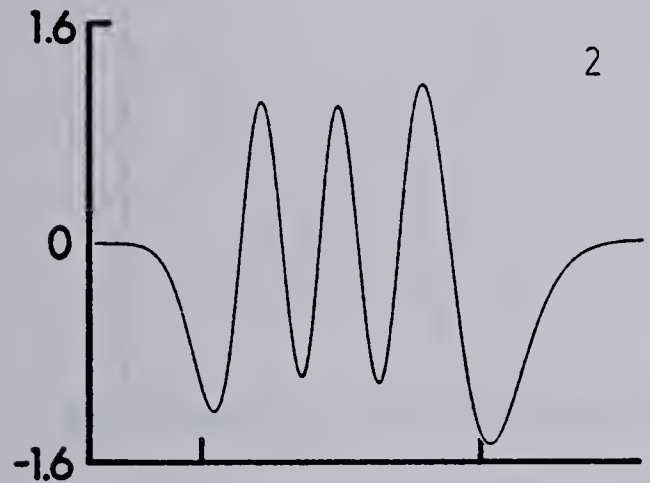
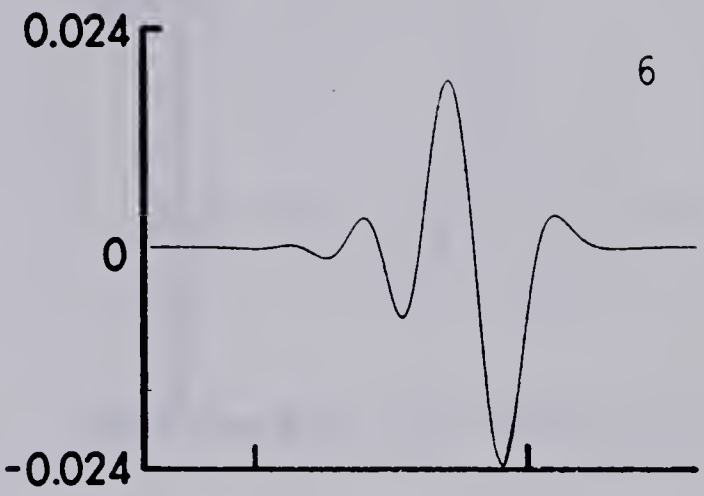
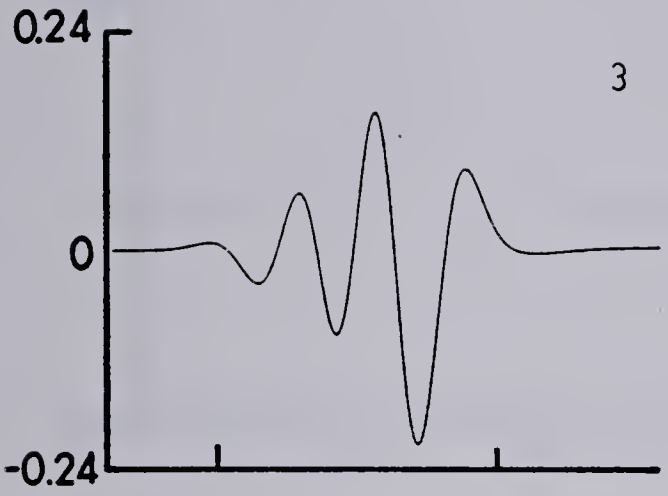


FIGURE 6.12
PSI 71

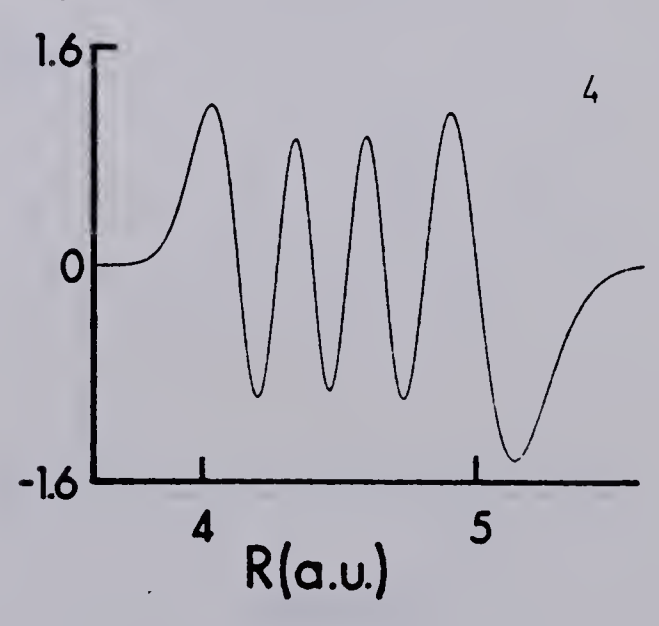
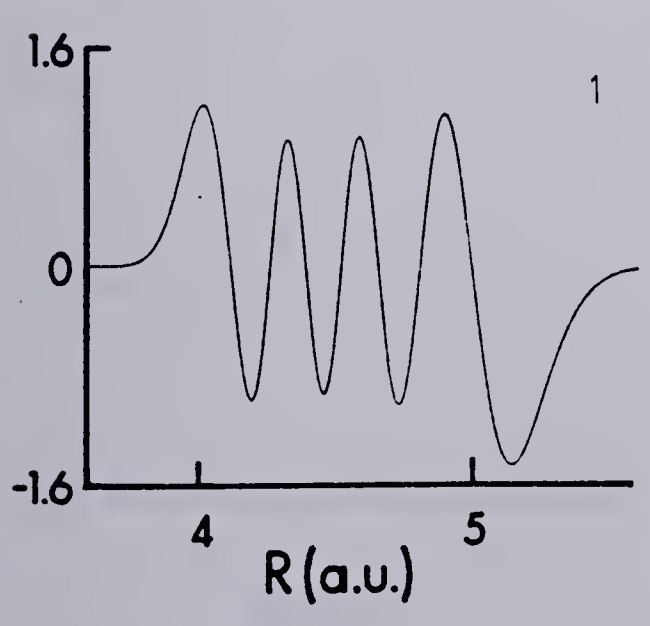
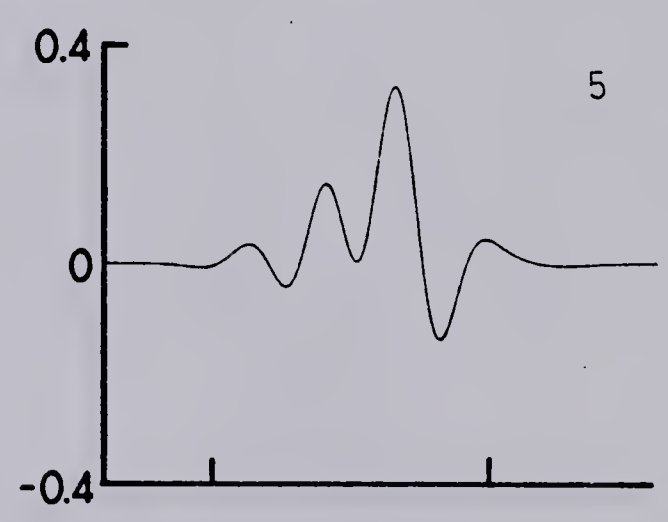
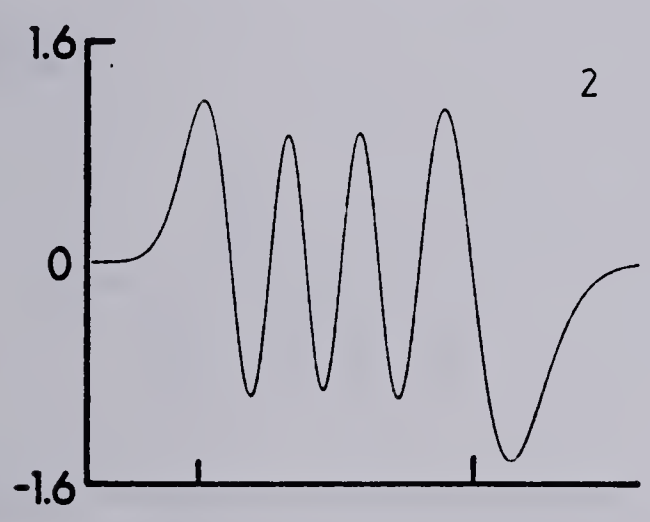
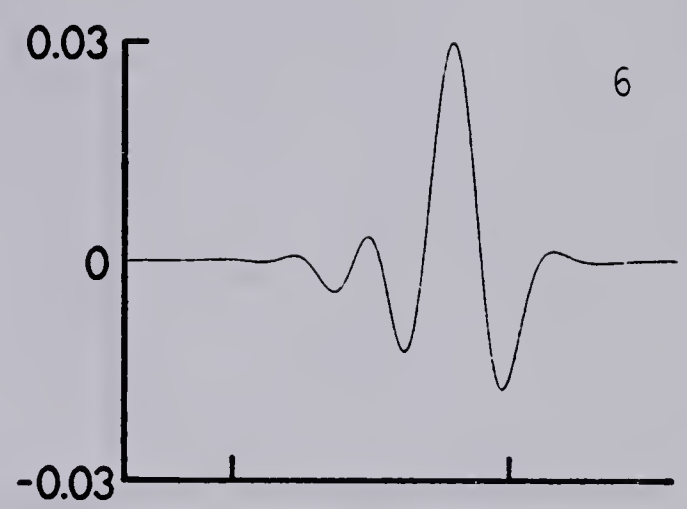
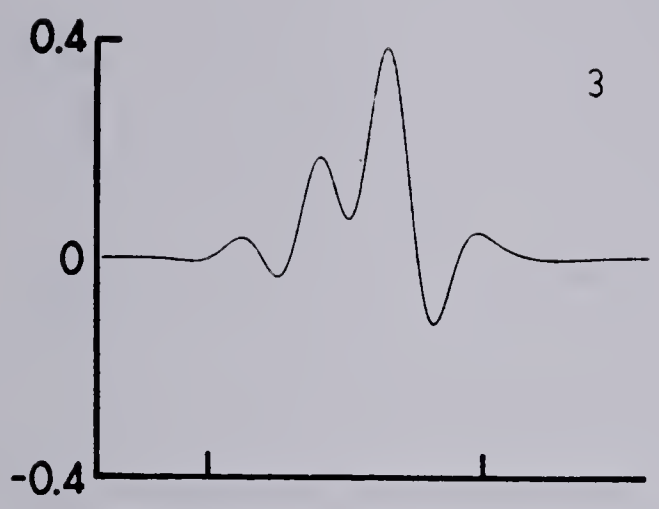


FIGURE 6.13
PSI 03

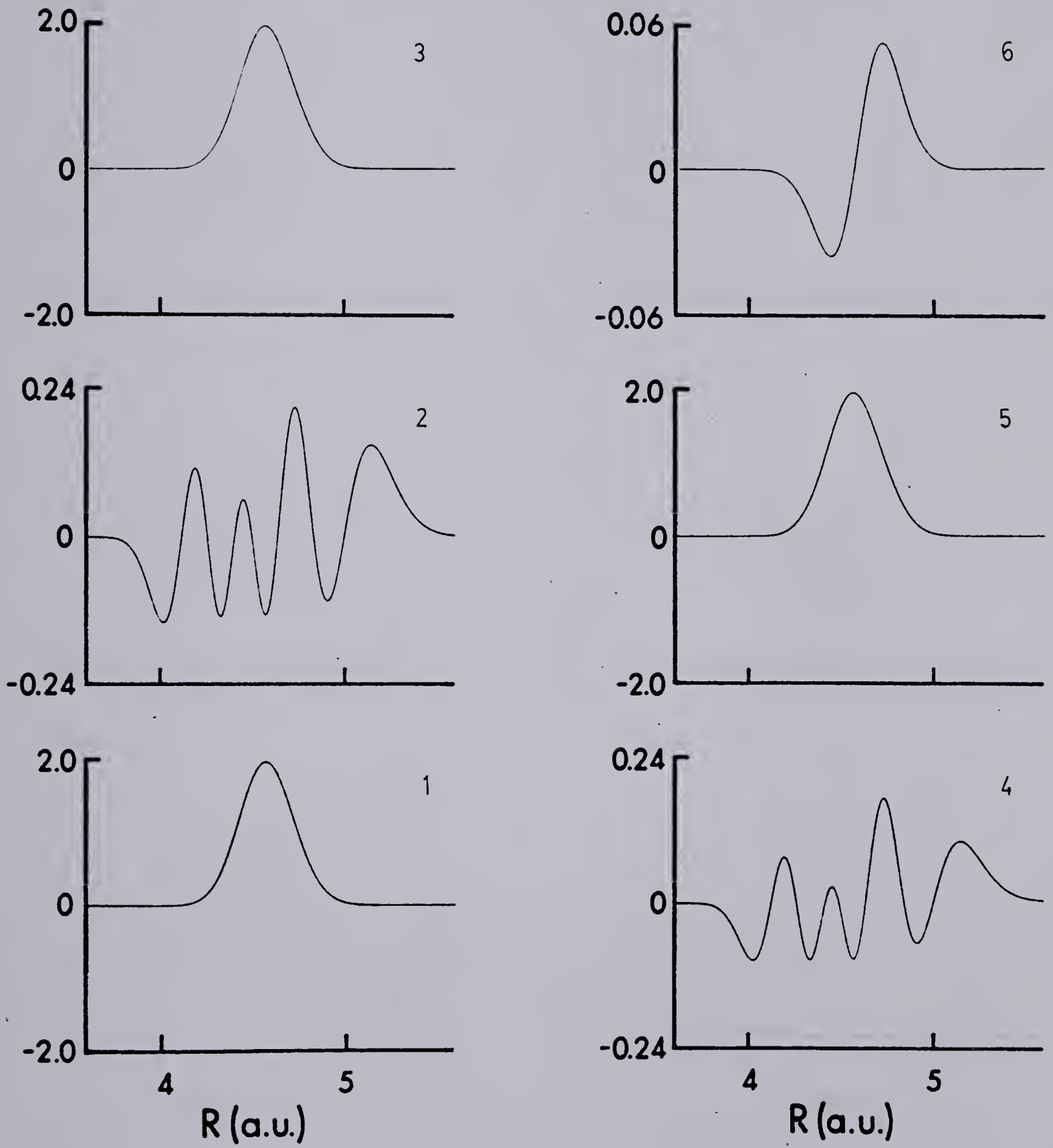


FIGURE 6.14
PSI 81

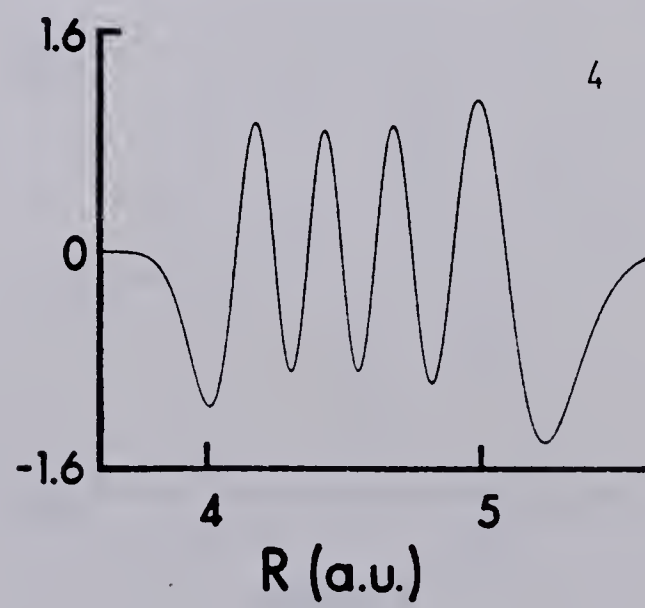
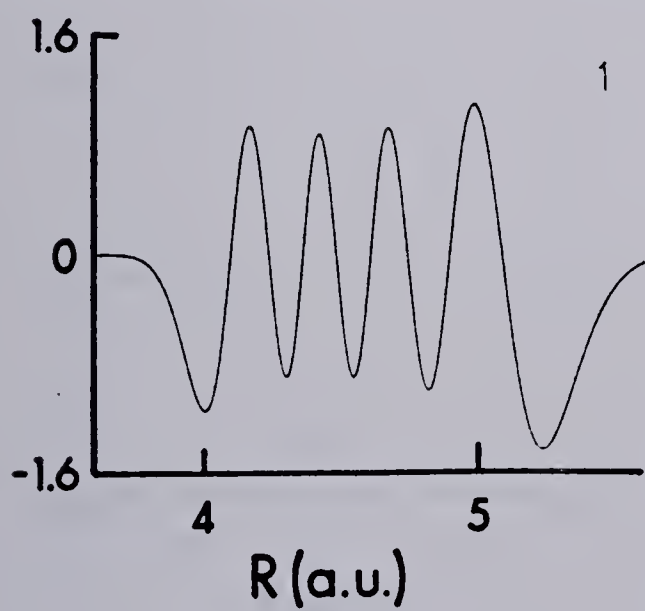
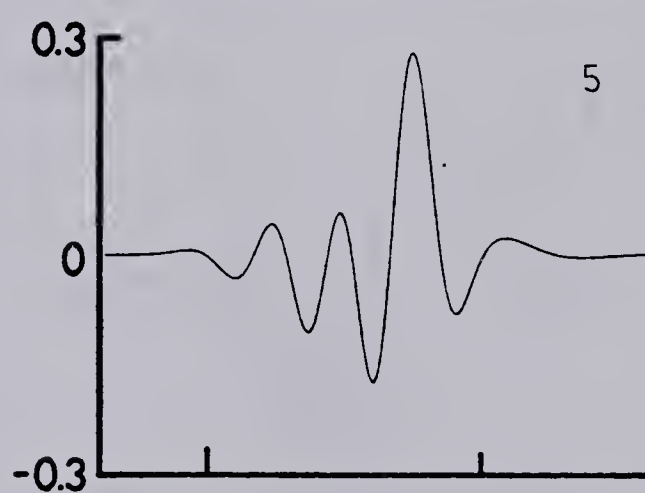
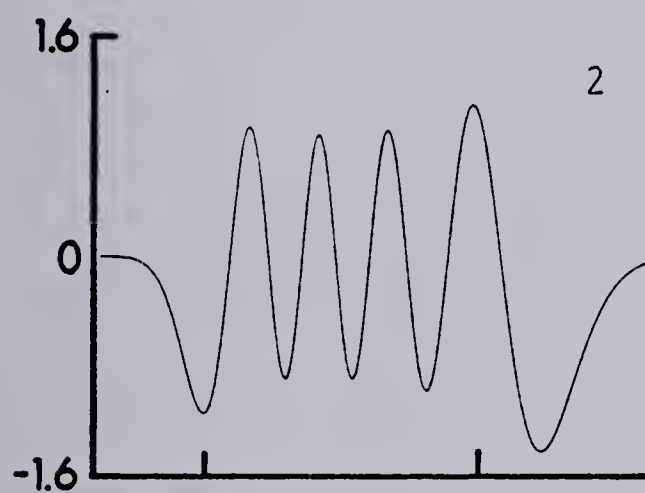
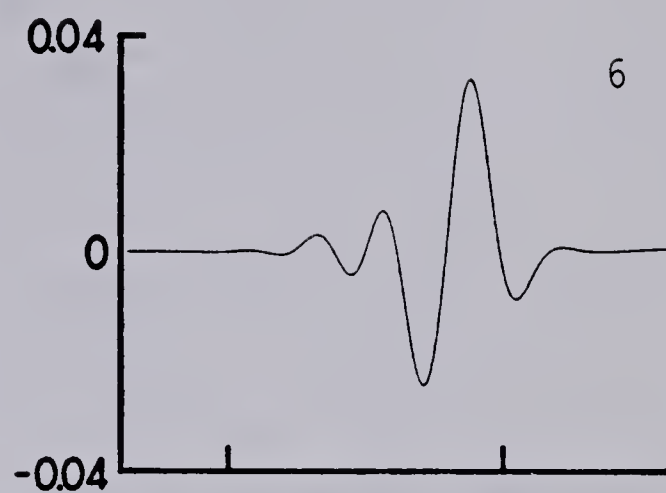
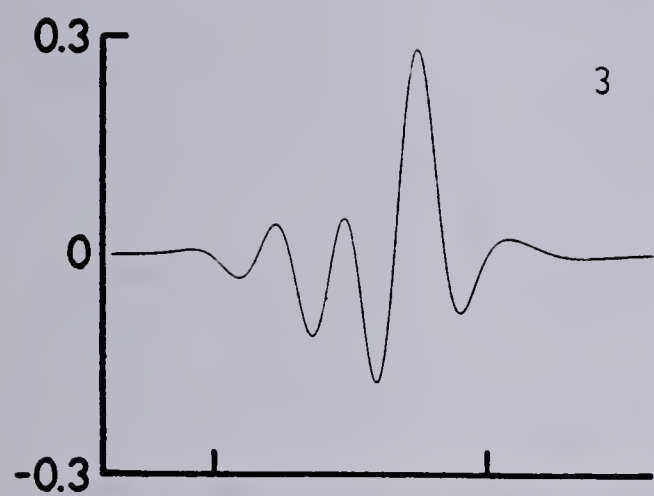
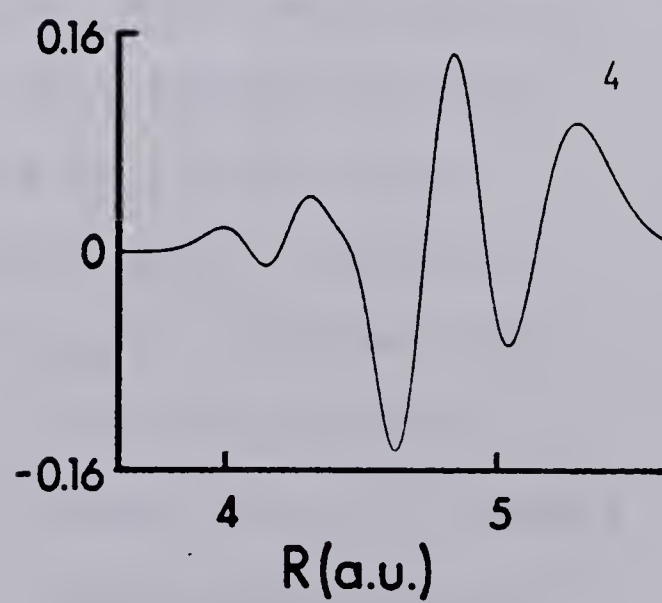
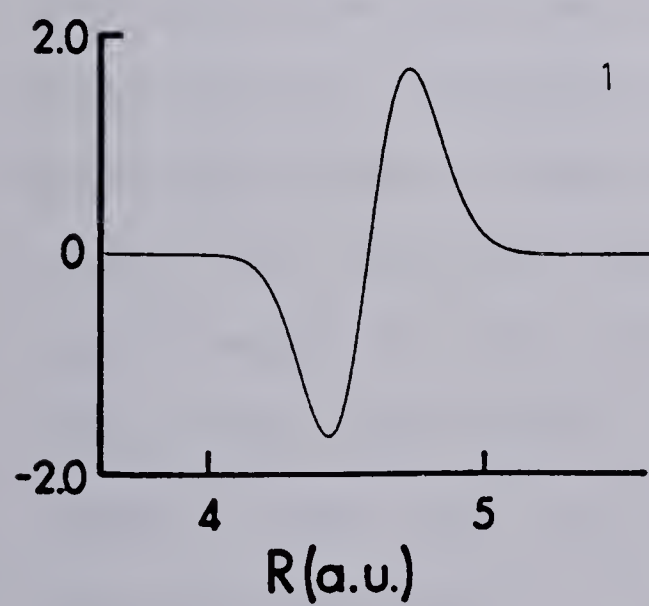
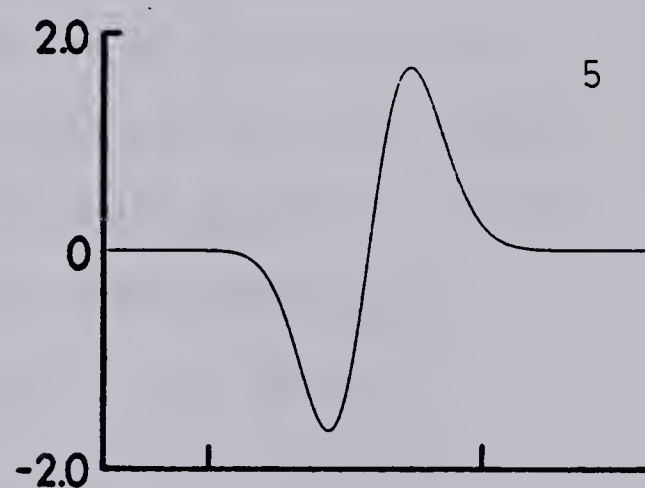
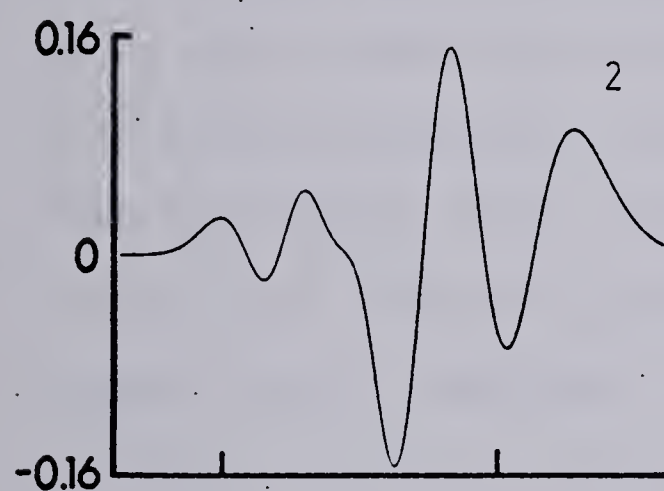
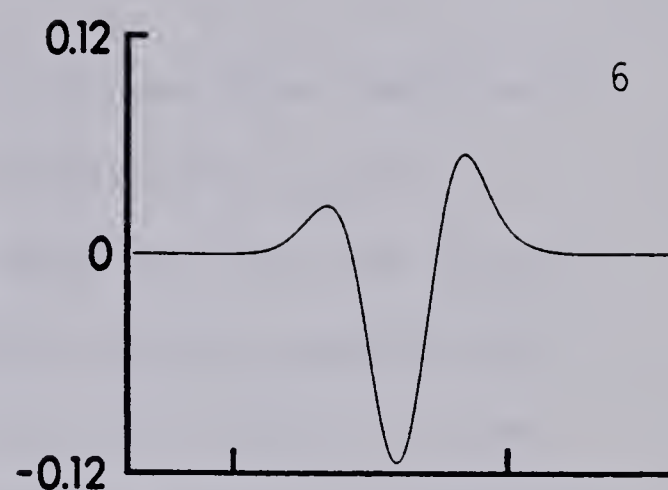
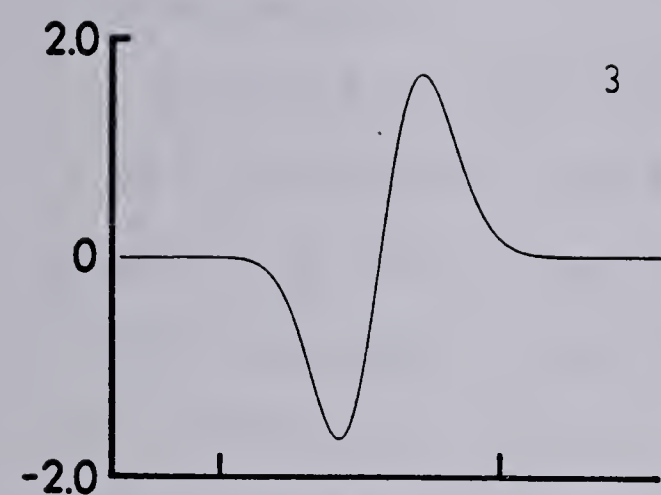


FIGURE 6.15
PSI 13



eigenstate $|j,n\rangle$, from which the coupled state is 'derived' (compare the functional forms of the dominant and uncoupled components).

It is worth discussing these wavefunction pictures in some detail.

Figure 6.4, labelled 'PSI 00', shows the components of the even parity ground state eigenvector $f_{00}(R)$. Graphs 1, 2, and 4 show the open channel function $f_{00}(R)$, in the one-, two-, and three-channel cases respectively. This function is evidently very similar to that of the ground state of an harmonic oscillator, and it is significant, as an indication of the weakness of the coupling, that the introduction of coupling does not visibly alter this functional form. It has a very much greater maximum value (~ 2.0) than the closed channel functions $f_{02}(R)$, graphs 3 and 5 (maximum ~ 0.03), and $f_{04}(R)$, graph 6 (maximum ~ 0.0012). In this case, there can be little doubt that the state may be labelled $|0,0\rangle$, and that the proton may be considered to be 'almost totally' in the Born-Oppenheimer ground state. Graphs 3 and 5, for $f_{02}(R)$ (two- and three-channel cases) show a 'dip' as $f_{00}(R)$ begins to grow, after which $f_{02}(R)$ 'follows' the form of the open channel function, but with a slight 'delay'. This 'dip' followed by 'delayed mimicry' appears to be *characteristic* of the first *closed* channel for all subsequent states: $|0,1\rangle$ to $|6,1\rangle$; the oscillatory

behaviour of the closed channel function is essentially determined by that of the open channel function (a "driven oscillator" response).

Figure 6.5 justifies the odd parity ground state labelling $|0,1\rangle$. It is very similar to the diagram for $|0,0\rangle$, and requires no further comment.

The states $|1,1\rangle$ to $|6,1\rangle$, figures 6.6 to 6.11, have in common that the upper channels are *closed*. The lower channel function $f_{j1}(R)$, dominates in all cases, and has the form of the j th state of a perturbed harmonic oscillator. Note the characteristic 'mimicry' of the upper channels.

Figures 6.12 and 6.13 show the first cases in which the first upper channel is *open*. These two also correspond to the case of near degeneracy in the one-channel calculation: $|7,1\rangle$ and $|0,3\rangle$. Consider the two-channel situation. The functional form of the dominant channel (figure 6.12, graph 2: lower channel for $|7,1\rangle$; figure 6.13, graph 3: upper channel for $|0,3\rangle$) clearly indicates the appropriate pair of indices. Once again, these functional forms are not visibly altered by the introduction of two- or three-channel coupling. There is, however, a strikingly different behaviour in the, now *open*, weaker channel (graph 3: upper channel for $|7,1\rangle$; graph 2: lower channel for $|0,3\rangle$). The dominated function now exhibits an independent form, rather than merely mimicking

the behaviour of the dominant channel (as in the case of a closed upper channel). For $|7,1\rangle$, the *lower* channel imposes some oscillation upon the ground state form of the upper channel, while for $|0,3\rangle$ the *upper* channel significantly perturbs the seventh harmonic oscillator functional form of the lower channel, but the characteristics of the weaker channel are maintained. In the three-channel calculations (graphs 4 to 6 of both figures) the weaker open channel function is visibly perturbed by the coupling to a higher channel. The closed (third) channel again essentially mimics the behaviour of the channel immediately below it. The significant 'mixing' of the open channel functions for the closely degenerate states $|7,1\rangle$ and $|0,3\rangle$, leads to a 'Fermi resonance',¹⁴ effect, which will be discussed in greater detail in section B of this chapter.

Figures 6.14 and 6.15, for $|8,1\rangle$ and $|1,3\rangle$, also have two open channels. One is clearly dominant, allowing the distinct labelling. The weaker open channel again evolves independently, but with superimposition of the dominant channel form, and the closed channel mimics its immediately inferior neighbour.

3. Summary.

Calculations using one to three channels have been shown to produce convergent eigenvalues. This in itself implies that the coupling is weak, a conclusion which has been confirmed by a discussion of the relative magnitudes and functional forms of the components of the eigenvectors. The latter considerations have also justified retention of a double index notation for the eigenstates in the ($N > 1$)-channel situation. Hence the terms 'excitation of H-F and F-F modes' have been shown to adequately (but approximately) describe transitions between these eigenstates. A description of the IR spectrum of HF_2^- , using the concepts of combination bands and overtones of ν_1 and ν_3 , is therefore a reasonable physical approximation.

B. Transition Frequencies and Relative Intensities.

Table three shows a comparison of transition frequencies ($E_{jn} - E_{k0}$, cm^{-1}) obtained from this calculation, using one to three channels, with those observed,^{95-97,101-114} and calculated by Almløf.²⁴

The frequency (ν_1) calculated for the Raman active transition, $|0,0\rangle \rightarrow |1,0\rangle$, is about 10% higher than experimental values, but is within 3% of the value obtained by Almløf. This is probably a reflection of the fact that the *ab initio* calculation tends to overestimate the curvature of the potential surface near the equilibrium

TABLE THREE

TRANSITION FREQUENCIES (cm^{-1})

FROM INITIAL STATE PSI 0,0:

Final State	Assign.	# Channels			Observed ^a	Almløf ^b
		1	2	3		
1,0	ν_1	676.3	676.8	676.8	600,631	660
0,1	ν_3	1514.6	1520.2	1520.2	1425-1550	1497
1,1	$\nu_3 + \nu_1$	2099.9	2104.2	2104.3	2045-2060	2070
2,1	$\nu_3 + 2\nu_1$	2661.7	2662.7	2663.0	2610-2670	2632
3,1	$\nu_3 + 3\nu_1$	3196.7	3192.1	3192.8	3166-3240	3226
4,1	$\nu_3 + 4\nu_1$	3703.4	3692.5	3693.3		3916?
5,1	$\nu_3 + 5\nu_1$	4182.6	4167.3	4167.8		?
6,1	$\nu_3 + 6\nu_1$	4636.3	4618.6	4618.7		4750?
7,1	$\nu_3 + 7\nu_1$	5067.5	5047.5	5047.6		
0,3	$3\nu_3$	5065.2	5084.7	5103.1	5085-5099	5157
8,1	$\nu_3 + 8\nu_1$	5478.7	5457.4	5457.3		
1,3	$3\nu_3 + \nu_1$	5650.9	5676.2	5687.0	5590-5650	

FROM INITIAL STATE PSI 1,0:

0,1	$\nu_3 - \nu_1$	838.4	843.3	843.3	880,855	837
-----	-----------------	-------	-------	-------	---------	-----

^aReferences 95-97, 101-114.^bReference 24.

value,^{7,24} and also considers an isolated ion with no crystal field effect.

Frequencies calculated for the lower combination bands ($\nu_3 + j'\nu_1$; $j = 0, \dots, 3$) agree well with both observed lines, and the values of Almløf. The higher combination bands ($j = 4 \dots 6$) do not, however, correspond in a 1:1 way with those reported by Almløf, a fact which is not surprising considering the behaviour of his potential function (Chapter three).

Tables four to six show relative intensities calculated using equations (5.32) and (5.33), and incorporating the 'electrical anharmonicity parameter' B (defined in equations (5.31)). It is evident from these tables that electrical anharmonicity is not a primary cause for the relatively high intensities of the combination bands of the fundamental ($\nu_3 + j'\nu_1$) and overtone ($'3\nu_3' + j'\nu_1'$). In general, a negative B increases the relative intensities of combination bands while decreasing the overtone intensity, and a positive B decreases combination band intensity while increasing the intensity of the overtone. The unusually large relative intensities are due to a vibrational Franck-Condon effect, that is, the overlap of the functions $\{f_{0K}(R), f_{nJ}(R)\}$.

For a consideration of the effects on the intensities due to coupling, the case in which B is zero (Table four) is quite representative. The relative intensity of a

TABLE FOUR

RELATIVE INTENSITIES: B = ZERO

Final State	# Channels		
	1	2	3
0,1	0.1000E+1	0.1000E+1	0.1000E+1
1,1	0.2849E+0	0.3148E+0	0.3148E+0
2,1	0.5514E-1	0.5979E-1	0.5976E-1
3,1	0.8067E-2	0.8636E-2	0.8623E-2
4,1	0.9335E-3	0.1089E-2	0.1084E-2
5,1	0.1036E-3	0.1336E-3	0.1347E-3
6,1	0.1375E-4	0.1496E-4	0.1529E-4
7,1	0.1792E-5	0.2754E-4	0.9730E-5
0,3	0.6026E-2	0.3666E-2	0.3857E-2
8,1	0.1136E-6	0.3194E-5	0.2399E-5
1,3	0.3545E-2	0.3468E-2	0.3571E-2

TABLE FIVE

RELATIVE INTENSITIES: B NEGATIVE

B = -0.2			
Final	# Channels		
State	1	2	3
<hr/>			
0,1	0.1000E+1	0.1000E+1	0.1000E+1
1,1	0.3101E+0	0.3405E+0	0.3404E+0
2,1	0.6388E-1	0.6920E-1	0.6916E-1
3,1	0.9979E-2	0.1071E-1	0.1069E-1
4,1	0.1253E-2	0.1446E-2	0.1440E-2
5,1	0.1497E-3	0.1908E-3	0.1897E-3
6,1	0.2036E-4	0.2268E-4	0.2308E-4
7,1	0.2746E-5	0.2333E-4	0.7377E-5
0,3	0.5723E-2	0.3611E-2	0.3796E-2
8,1	0.2235E-6	0.2764E-5	0.2020E-5
1,3	0.3568E-2	0.3565E-2	0.3670E-2
B = -0.5			
0,1	0.1000E+1	0.1000E+1	0.1000E+1
1,1	0.3515E+0	0.3824E+0	0.3824E+0
2,1	0.7879E-1	0.8519E-1	0.8515E-1
3,1	0.1337E-1	0.1437E-1	0.1435E-1
4,1	0.1845E-2	0.2104E-2	0.2095E-2
5,1	0.2384E-3	0.2954E-3	0.2939E-3
6,1	0.3326E-4	0.3789E-4	0.3836E-4
7,1	0.4638E-5	0.1746E-4	0.4362E-5
0,3	0.5266E-2	0.3527E-2	0.3702E-2
8,1	0.4681E-6	0.2156E-5	0.1495E-5
1,3	0.3604E-2	0.3719E-2	0.3827E-2

TABLE SIX

RELATIVE INTENSITIES: B POSITIVE

B = +0.2

Final State	# Channels		
	1	2	3
0,1	0.1000E+1	0.1000E+1	0.1000E+1
1,1	0.2615E+0	0.2908E+0	0.2908E+0
2,1	0.4728E-1	0.5131E-1	0.5128E-1
3,1	0.6405E-2	0.6837E-2	0.6826E-2
4,1	0.6684E-3	0.7898E-3	0.7860E-3
5,1	0.6700E-4	0.9095E-4	0.9030E-4
6,1	0.8565E-5	0.8986E-5	0.9257E-5
7,1	0.1060E-5	0.3197E-4	0.1233E-4
0,3	0.6328E-2	0.3719E-2	0.3917E-2
8,1	0.4220E-7	0.3642E-5	0.2798E-5
1,3	0.3523E-2	0.3374E-2	0.3477E-2

B = +0.5

0,1	0.1000E+1	0.1000E+1	0.1000E+1
1,1	0.2294E+0	0.2577E+0	0.2577E+0
2,1	0.3697E-1	0.4017E-1	0.4015E-1
3,1	0.4342E-2	0.4604E-2	0.4596E-2
4,1	0.3633E-3	0.4418E-3	0.4393E-3
5,1	0.2811E-4	0.4205E-4	0.4166E-4
6,1	0.3232E-5	0.3022E-5	0.3188E-5
7,1	0.3401E-6	0.3897E-4	0.1663E-4
0,3	0.6778E-2	0.3798E-2	0.4004E-2
8,1	0.2300E-9	0.4343E-5	0.3431E-5
1,3	0.3491E-2	0.3241E-2	0.3342E-2

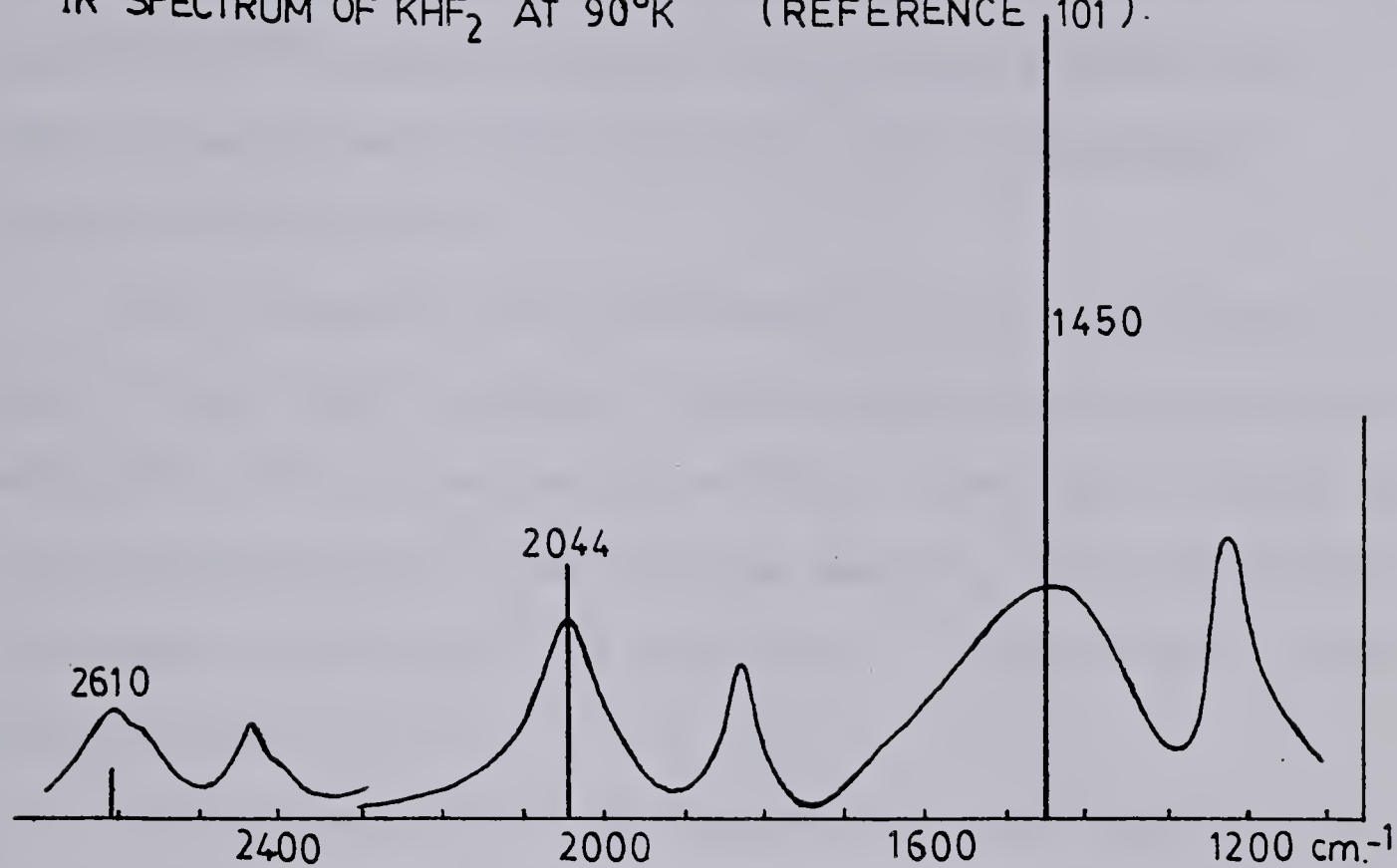
combination band $\nu_3 + j'\nu_1$ ($j = 1$ to 4), is increased by about 10% in going from one to two channels (compared to a change of less than 1% in the eigenvalues), and is virtually unaltered ($j = 1$ to 5) by the expansion to three channels. This behaviour is a good indication of the convergence of the wavefunctions for these lower states.

There is a strong 'Fermi resonance' effect for the closely degenerate pair $|7,1\rangle$ and $|0,3\rangle$: the combination band $\nu_3 + 7'\nu_1$ shows an approximately five-fold increase in intensity, accompanied by about a 30% decrease in intensity for the overtone $'3\nu_3'$. This degeneracy is 'accidental': it is a consequence of the particular form used as a model for the true potential function, and in the following discussion of the IR spectrum of KHF_2 , it will be argued that the degeneracy is not in fact 'real'. The existence of such Fermi resonances in the spectrum of a hydrogen bonded system is, however, highly probable, even if so far unobserved.

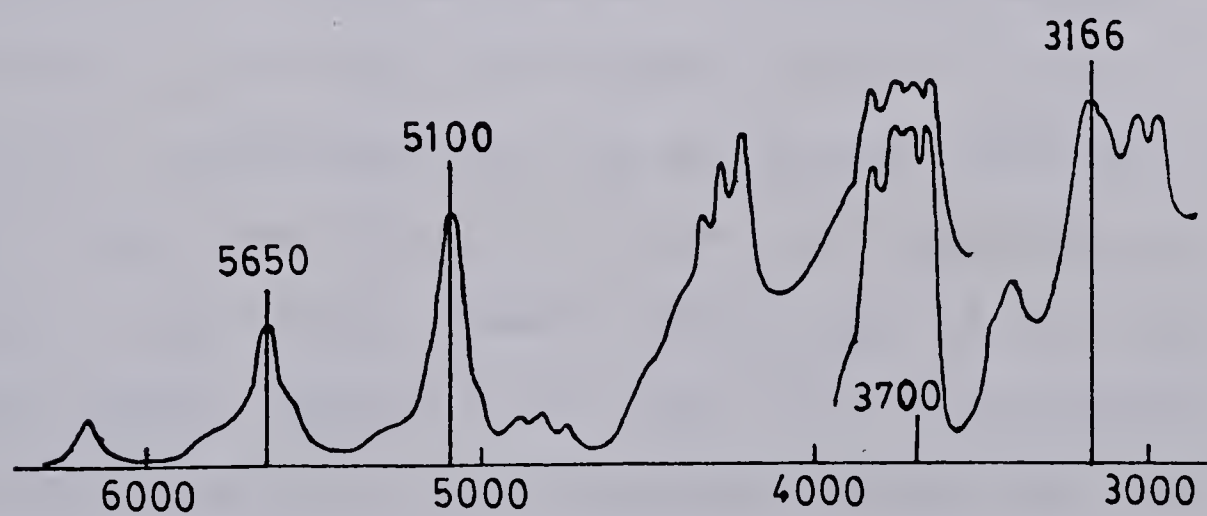
The IR transmission spectrum of KHF_2 at 90°K , obtained by Coté and Thompson¹⁰¹ (C&T henceforth) is shown in figure 6.16.

The upper curve (1100 to 2700 cm^{-1}) shows vertical lines placed at the maxima of the bands assigned by C&T to $\nu_3 + j'\nu_1$, for $j = 0,1,2$. The height of each line is proportional to the calculated relative intensity of the corresponding transition for the two (or three) channel

FIGURE 6.16

IR SPECTRUM OF KHF_2 AT 90°K (REFERENCE 101).

Vertical lines show calculated relative intensities.



case, listed in Table four. Although it has been established from reflectance studies¹¹⁰⁻¹¹² that the strong ν_3 band seen in transmission has a greatly broadened contour, a crude estimate of the areas under the C&T bands at 1450 and 2044 cm^{-1} gives a ratio 1:0.34 ($\pm 20\%$), which is in good agreement with the intensity ratio calculated, 1:0.315 (Table four).

The calculation of the positions and intensities of these lines thus provides a strong confirmation of their assignment to the series $\nu_3 + j'\nu_1'$. The peak at 1225 cm^{-1} has been assigned to the bending mode ν_2 , and the remaining lines, at 1833 cm^{-1} and 2426 cm^{-1} , are evidently the combinations $\nu_2 + j'\nu_1'$, $j = 1, 2$.

In the lower curve of figure 6.16 (3000-6200 cm^{-1}), the vertical lines correspond to relative intensities calculated using *one* channel. It is clear from the calculated line positions of Table three, and relative intensities of Table four, that the lines at 5100, 5650, and 6185 cm^{-1} are combinations of ν_1 with the second overtone of ν_3 , that is, the series: ' $3\nu_3$ ' + $j'\nu_1'$ ($j = 0, 1, 2$). Experimentally, it can be seen that the intensities of ' $3\nu_3$ ' and ' $3\nu_3$ ' + ' ν_1 ' are *not* comparable in magnitude. Table four, however, shows that if the Fermi resonance effect, between $|0, 3\rangle$ and $|7, 1\rangle$, were present, these intensities *would* be of comparable magnitude, and it is concluded that the close degeneracy of the states

is an artifact of the potential model.

The relative intensity of the lines at 3166 cm^{-1} and 5100 cm^{-1} offers strong support for the labelling $\nu_3 + 3'\nu_1'$ and $'3\nu_3'$ respectively, in agreement with the assignment of C&T. There has been some disagreement about this assignment. Newman and Badger¹⁰² have assigned lines at 4240 and 4890 cm^{-1} , to $'3\nu_3'$ and $'3\nu_3' + '\nu_1'$ respectively, and subsequently 5085 and 5590 cm^{-1} , to $\nu_3 + 2\nu_2 + 2\nu_1$ and $\nu_3 + 2\nu_2 + 3\nu_1$. On the basis of a consideration of the deuterium spectrum (KDF_2) of Ketelaar,⁹⁵ Ibers²⁰ has argued in favour of the C&T assignment. This calculation strongly supports his conclusion.

A line at 3000 cm^{-1} has been assigned to $\nu_2 + '3\nu_1'$ by Dawson *et al.*,¹¹⁰ and the line at about 3400 cm^{-1} is probably due to $\nu_2 + '4\nu_1'$.

The absorption region $3600\text{--}5000\text{ cm}^{-1}$ is evidently due primarily to overtones and combinations of the bending modes (C&T discuss this in detail), although the combination $\nu_3 + '4\nu_1'$ will clearly contribute some intensity in the region of 3700 cm^{-1} . Higher combinations, $\nu_3 + j'\nu_1'$ ($j = 5, 6, \dots$), will not contribute significantly in this region, except perhaps through Fermi resonance with the bending overtones and combinations.

The comparison by Almløf,²⁴ of the lines he calculated at 3916 and 4750 cm^{-1} , with experimental lines in the region $3800\text{--}4800\text{ cm}^{-1}$ is invalid, for the following reasons.

Since his potential surface (being only a function of the linear coordinates Q_1 and Q_2) can only estimate stretching frequencies, his assignment implies the experimental lines are 'stretching' in origin, whereas it has been shown here that the relative intensities for these stretching transitions are much too low to account for the intensity observed in this region. Almløf did not calculate relative intensities.

C. Conclusions.

1. Stepanov Approximation.

In the absence of near-degeneracy between adiabatic protonic states (e.g., ν_3 and $2\nu_2$ treated by Witkowski and Wojcik¹⁵), the Stepanov approximation has been shown to give acceptable accuracy ($\sim 1\%$) for the prediction of vibrational eigenvalues. The inclusion of non-adiabatic coupling between adjacent adiabatic protonic states (2 channel coupling for most IR transitions) yields essentially *exact* solutions.

It does not appear to be necessary to invoke the mechanism of "electrical anharmonicity" *explicitly* in order to explain the abnormally high relative intensities of combination bands and overtones which together produce the unusually broad, structured " ν_3 band" so characteristic of the IR spectrum of an H-bonded species. Relative intensities calculated within the Stepanov approximation,

and with a zero electrical anharmonicity parameter, are of the same order of magnitude as those observed experimentally. Inclusion of adjacent state non-adiabatic coupling may lead to about a 10% increase in combination band intensity, again in the absence of degeneracy. The combination bands have thus been shown to occur as a vibrational analogue of the Franck-Condon principle.

For the case of isolated "Fermi resonance", $|7,1\rangle$ and $|0,3\rangle$ in the model problem, it is clearly necessary to go beyond the Stepanov approximation. A perturbation treatment in the two-dimensional subspace could not have predicted the energy level *reversal of order* which is obtained by exact solution with the non-adiabatic couplings, and of course the Stepanov eigenvalues and wavefunctions are seriously in error for this case.

These conclusions are not restricted to the particular model problem (HF_2^-) investigated, because this model represents the strongest case of non-adiabatic coupling likely to occur in any hydrogen bond: the potential $V_1(z;R)$ has strong anharmonic interaction of the two stretching coordinates, leading to strong deformation of the protonic states with R ; the reduced mass ratio (m/μ), and adiabatically separated frequency ratio (ν_1/ν_3), are unusually large.

It seems likely, therefore, that the Stepanov approximation provides a useful basis for the interpretation

of the vibrational spectra of most H-bonded systems (where no degeneracy-mediated couplings occur). Even for the cases of isolated "Fermi resonance", where non-adiabatic couplings must be included, the adiabatic representation still provides a significant advantage over the "matrix expansion" methods (Chapter one, section B2) in terms of the clarity of interpretation (the "dominant channel" concept).

2. Vibrational Spectrum of the Bifluoride Ion.

Absolute values for ν_3 and ν_1 , for an *isolated* HF_2^- ion, are not available. Experimental measurements of ν_3 vary from 1425¹¹⁰ to 1600¹⁰³ cm^{-1} depending upon the cation (K^+ , Na^+ or NH_4^+ generally), and the environment (Ketelaar *et al.*¹⁰³ have measured $\nu_3 \sim 1599, 1570, 1527, 1478 \text{ cm}^{-1}$ for KHF_2 in NaBr, KCl, KBr, KI respectively; Salthouse and Waddington¹⁰⁴ have $\nu_3 \sim 1560 \text{ cm}^{-1}$ for KHF_2 in KCl). Also ν_1 has been observed at 600 and 610 cm^{-1} ^{97,106-110} for KHF_2 (with a correlation field splitting due to the crystal site symmetry), and at $\sim 630 \text{ cm}^{-1}$ for NaHF_2 (no splitting). Azman and Ocvirk¹⁰⁵ have also reported $\nu_1 \sim 675 \text{ cm}^{-1}$ for NaHF_2 .

The values calculated in this work ($\nu_3 \sim 1520 \text{ cm}^{-1}$; $\nu_1 \sim 677 \text{ cm}^{-1}$) strongly suggest that the potential function used is at least a close model of the physical reality.

Keeping in mind that the weak dependency of the stretching eigenvalues on the state of excitation of the

bending mode has been ignored, the interpretation of the IR spectrum of crystalline KHF_2 essentially confirms that of Côté and Thompson.¹⁰¹

Though the bending modes have not been explicitly calculated here, it is possible to discuss them on the basis of the separation given in Chapter two, section C1 (equation 2.15).

Unfortunately, the experimental situation with respect to ν_2 is rather unclear. Côté and Thompson¹⁰¹ appear to have observed a $\sim 50 \text{ cm}^{-1}$ splitting (static field splitting) in KHF_2 between bending frequencies perpendicular (1225 cm^{-1}) and parallel (1274 cm^{-1}) to the tetragonal axis, but the polarized single crystal transmission spectra of Newman and Badger¹⁰² show the splitting to be only 10 cm^{-1} . Analyses of the reflectance spectrum^{111,112} of KHF_2 have given a splitting of $4\text{--}7 \text{ cm}^{-1}$, with $\nu_2 \sim 1227$ and 1235 cm^{-1} . In the sodium salt there is no splitting, and the frequency is only slightly smaller:^{109,112} 1210 to 1223 cm^{-1} , while Ault¹¹⁵ finds 1217 cm^{-1} for HF_2^- in an argon matrix (CsF/HF). Cooke *et al.*¹¹² have reported a splitting of 25 cm^{-1} for isotopically isolated HF_2^- in KDF_2 (and 17 cm^{-1} for DF_2^- in KHF_2), and have interpreted this as a measure of the true local anisotropy of the bending force field in the lattice of the potassium salt.

As mentioned in Chapter two, section C1, however, the model involving cylindrical symmetry is easily modified to allow for non-degenerate bending modes. The essential feature is the R -dependence of the force constants for these motions. This leads, *via* the analogous Franck-Condon principle to the series of combination bands $\nu_2 + j\nu_1$, which is clearly present in the spectrum of Côté and Thompson¹⁰¹ (Figure 6.16). A monotonic R -dependence of the force constant would mainly displace the minimum of the potential curve for the first excited state of the bending motion (relative to the ground state curve), rather than strongly modifying the "force constant for R motion" in that curve.

It is probable that the moderately intense features in the regions $3660\text{--}3830\text{ cm}^{-1}$, and $4200\text{--}4500\text{ cm}^{-1}$, observed by Côté and Thompson¹⁰¹ and Newman and Badger,¹⁰² are *not* due to the bands " $3\nu_2$ " and " $3\nu_2 + \nu_1$ " as C&T have supposed. The dipole moment integral in ρ space (analogous to equation (5.33), for $I_{KJ}(R)$ in z space) for the second overtone transition " $3\nu_2$ ", has appreciable value at any R point only if the potential function for bending motion is strongly anharmonic in ρ . Since this is unlikely, it would be expected that the intensity of " $3\nu_2$ " should be very much less than the intensity of " $3\nu_3$ " (for which the potential function in z space is *highly* anharmonic); yet the band at $3660\text{--}3830$ is in fact stronger than " $3\nu_3$ ".

An alternative assignment is possible.¹¹⁶ Cooke, Pastorek, Carlson and Decius¹¹² have pointed out that in KHF_2 (but not in NaHF_2) intermode coupling between ν_2 and ν_3 may occur (they have components of the same unit cell symmetry). It is possible that the potential surface (for bending in one molecule, and simultaneous protonic stretching in its neighbour) could have significant anharmonic interaction terms, leading to the appearance of the bands " $2\nu_2 + \nu_3$ " and " $2\nu_3 + \nu_2$ " with relatively high intensity.

It is therefore proposed that the band at 3600-3830 cm^{-1} should be associated with the transition " $2\nu_2 + \nu_3$ ", and that at 4200-4500 cm^{-1} with " $2\nu_3 + \nu_2$ ". If such an intermolecular interpretation is correct, then (i) the bands should not appear in the spectrum of NaHF_2 (where the unit cell contains only one HF_2^- ion), and (ii) isotopically isolated spectra of HF_2^- in KDF_2 (and DF_2^- in KHF_2) should give different locations for these bands (compared to pure salts).

REFERENCES

1. P. Schuster, G. Zundel, and C. Sandorfy, editors, *The Hydrogen Bond*, (North Holland, Amsterdam, 1976), Vols. I to III.
2. M.D. Joesten, and L.J. Schaad, *Hydrogen Bonding* (Marcel Dekker, N.Y., 1974).
3. S.N. Vinogradov, and R.H. Linnell, *Hydrogen Bonding* (Van Nostrand Reinhold, N.Y., 1971).
4. G.C. Pimentel, and A.L. McClellan, *The Hydrogen Bond* (Freeman, San Francisco, 1960).
5. W.C. Hamilton, and J.A. Ibers, *Hydrogen Bonding in Solids* (Benjamin, N.Y., 1968).
6. D. Hadzi, and H.W. Thompson, editors, *Hydrogen Bonding* (Pergamon Press, London, 1959).
7. P.A. Kollman, in *Modern Theoretical Chemistry*, Vol. 4 (Ed. H.F. Schaeffer; Plenum Press, N.Y., 1977), p. 109.
8. N. Sheppard, reference 6, p. 85.
9. B.I. Stepanov, *Zh. Fiz. Khim.*, 19, 507 (1945); 20, 408 (1946); *Nature*, 157, 808 (1946).
10. M. Born, and J.R. Oppenheimer, *Ann. der Phys.*, 84, 457 (1927).
11. M. Born, and K. Huang, *Dynamical Theory of Crystal Lattices* (Clarendon Press, Oxford, 1954), p. 166ff, and p. 402.
12. J. Franck, *Trans. Far. Soc.*, 21, 536 (1925).

13. E.U. Condon, Phys. Rev., 32, 858 (1928).
14. E. Fermi, Z. Physik, 71, 250 (1931).
15. A. Witkowski, and M. Wójcik, Chem. Phys., 1, 9 (1973).
16. W.R. Thorson, and J.B. Delos, Phys. Rev. A, 18, 135 (1978).
17. R. Janoschek, reference 1, vol. I, p. 165.
18. C.A. Coulson, and G.N. Robertson, Proc. R. Soc. Lond. A, 337, 167 (1974).
19. D. Hadzi, and S. Bratos, reference 1, vol. II, p. 594.
20. J.A. Ibers, J. Chem. Phys., 41, 25 (1964).
21. T.R. Singh, and J.L. Wood, J. Chem. Phys., 48, 4567 (1968).
22. R. Janoschek, E.G. Weidemann, and G. Zundel, Faraday Trans. II, 69, 505 (1973).
23. R. Janoschek, Theoret. Chim. Acta, 29, 57 (1973).
24. J. Almløf, Chem. Phys. Lett., 17, 49 (1972).
25. A. Hayd, E.G. Weidemann, and G. Zundel, J. Chem. Phys., 70, 86 (1979).
26. T.R. Singh and J.L. Wood, J. Chem. Phys., 50, 3572 (1969).
27. J.A. Ibers, and R.G. Delaplane, J. Chem. Phys., 48, 539 (1968).
28. B.L. McGaw, and J.A. Ibers, J. Chem. Phys., 39, 2677 (1963).
29. A.R. Ubbelohde, Proc. R. Soc. Lond. A, 173, 417 (1939).
30. K.J. Gallagher, reference 6, p. 45.

31. A. Witkowski, J. Chem. Phys., 47, 3645 (1967).
32. Y. Marechal, and A. Witkowski, Theor. Chim. Acta, 9, 116 (1967).
33. Y. Marechal, and A. Witkowski, J. Chem. Phys., 48, 3697 (1968).
34. J.L. Leviel, and Y. Marechal, J. Chem. Phys., 54, 1104 (1971).
35. J. Bournay, and Y. Marechal, J. Chem. Phys., 55, 1230 (1971).
36. Y. Marechal, Chem. Phys. Lett., 13, 237 (1972).
37. P. Excoffon, and Y. Marechal, Spectrochim. Acta, 28A, 269 (1972).
38. A. Witkowski, and M. Wojcik, Chem. Phys. Lett., 20, 615 (1973).
39. A. Witkowski, and M. Wojcik, Chem. Phys. Lett., 26, 327 (1974).
40. J. Bournay, and Y. Marechal, Chem. Phys. Lett., 27, 180 (1974).
41. M. Wojcik, Int. J. Quantum Chem., X, 747 (1976).
42. A. Witkowski, and M. Wojcik, Chem. Phys., 21, 385 (1977).
43. H.R. Zelsmann, and Y. Marechal, Chem. Phys., 20, 445 (1977); 20, 459 (1977).
44. Y. Marechal, J. Mol. Struct., 47, 291 (1978).
45. M. Wojcik, J. Mol. Struct., 47, 303 (1978).
46. C. Reid, J. Chem. Phys., 30, 182 (1959).

47. E.R. Lippincott, and R. Schroeder, J. Chem. Phys., 23, 1099 (1955); J. Am. Chem. Soc., 78, 5171 (1956).
48. G.L. Hofacker, Y. Marechal, and M.A. Ratner, reference 1, vol. I, Chapter 6.
49. N.D. Sokolov, and V.A. Savel'ev, Chem. Phys., 22, 383 (1977).
50. C.A. Coulson, and G.N. Robertson, Proc. R. Soc. Lond. A, 342, 289 (1975).
51. G.N. Robertson, Phil. Trans. R. Soc. Lond. A, 286, 25 (1977).
52. G.R. Anderson, and E.R. Lippincott, J. Chem. Phys., 55, 4077 (1971).
53. G.J. Jiang, and G.R. Anderson, J. Phys. Chem., 77, 1764 (1973).
54. G.R. Anderson, and G.J. Jiang, J. Phys. Chem., 77, 2560 (1973).
55. G.J. Jiang, and G.R. Anderson, J. Chem. Phys., 60, 3258 (1974).
56. D.I. Blokhintsev, *Principles of Quantum Mechanics* (Allyn and Bacon, Boston, 1964), p. 424.
57. E.B. Wilson, J.C. Decius, and P.C. Cross, *Molecular Vibrations* (McGraw-Hill, New York, 1955), Chapter 11.
58. J.E. Bertie, and M.V. Falk, Can. J. Chem., 51, 1713 (1973).
59. R.K. Thomas, and H.W. Thompson, Proc. R. Soc. Lond. A, 316, 303 (1970).

60. B. Desbat, and J.C. Lassegues, J. Chem. Phys., 70, 1824 (1979).
61. M. Born, and K. Huang, reference 11, p. 406.
62. L. Pauling, and E.B. Wilson, *Introduction to Quantum Mechanics* (McGraw-Hill, New York, 1935), p. 105.
63. G. Hunter, and M. Kuriyan, Proc. R. Soc. Lond. A, 341, 491 (1975).
64. W.R. Thorson, and J.B. Delos, Phys. Rev. A, 18, 117 (1978).
65. J.P. Davis, and W.R. Thorson, Can. J. Phys., 56, 996 (1978).
66. M.H. Mittleman, Phys. Rev., 188, 221 (1969).
67. M.H. Mittleman, and H. Tai, Phys. Rev. A, 8, 1880 (1973).
68. M.H. Mittleman, Phys. Rev. A, 9, 704 (1974).
69. L.A. Pars, *A Treatise on Analytical Dynamics* (Heinemann, London, 1965), p. 537.
70. S. Glasstone, K.J. Laidler, and H. Eyring, *Theory of Rate Processes* (McGraw-Hill, New York, 1941), p. 100.
71. S.B. Schneiderman, and A. Russek, Phys. Rev., 181, 311 (1969).
72. S. Bratoz, and G. Bessis, C.R. Acad. Sci., Ser. C, 249, 1881 (1959).
73. G. Bessis, and S. Bratoz, J. Chim. Phys., 57, 769 (1960).
74. H. Hamano, Bull. Chem. Soc. Japan, 30, 741 (1957).

75. E. Clementi, and A.D. McLean, J. Chem. Phys., 36, 745 (1962).
76. E. Clementi, J. Chem. Phys., 34, 1468 (1961).
77. A.D. McLean, and M. Yoshimine, IBM J. Res. Dev., 11, 169 (1967).
78. P.A. Kollman, and L.C. Allen, J. Am. Chem. Soc., 92, 6101 (1970).
79. P. Noble, and R. Kortzeborn, J. Chem. Phys., 52, 5375 (1970).
80. W. van Gool, J. Bruinink, and P.H. Bottleberghs, J. Inorg. Nucl. Chem., 34, 3631 (1972).
81. H.L. Carell, and J. Donohue, Israel J. Chem., 10, 195 (1972).
82. J.A. Ibers, J. Chem. Phys., 40, 402 (1964).
83. T.R.R. McDonald, Acta Crystallogr., 13, 113 (1960).
84. J.M. Williams, and L.F. Schneemeyer, J. Am. Chem. Soc., 95, 5780 (1973).
85. D.G. Tuck, Prog. Inorg. Chem., 9, 161 (1968).
86. T.C. Waddington, Trans. Far. Soc., 54, 25 (1958).
87. S.A. Harrell, and D.H. McDaniel, J. Am. Chem. Soc., 86, 4497 (1964).
88. H.P. Dixon, H.D.B. Jenkins, and T.C. Waddington, J. Chem. Phys., 57, 4388 (1972).
89. A. Neckel, P. Kuzmany, and G. Vinek, Z. Naturforsch. A, 26, 569 (1971).
90. E.R. Lippincott, J. Chem. Phys., 21, 2070 (1953).

91. E.R. Lippincott, and R. Schroeder, J. Chem. Phys., 23, 1131 (1955).
92. A. Messiah, *Quantum Mechanics*, Volume I (North Holland, Amsterdam, 1965), p. 231.
93. G.F. Simmons, *Differential Equations* (McGraw-Hill, New York, 1972), p. 78.
94. (a) H. Hellmann, *Einführung in die Quantenchemie*, (Deuticke, Leipzig, 1937); (b) R.P. Feynman, Phys. Rev. 56, 340 (1939).
95. J.A.A. Ketelaar, Rec. Trav. Chim., 60, 523 (1941).
96. J.A.A. Ketelaar, and W. Vedder, J. Chem. Phys., 19, 654 (1951).
97. P. Dawson, J. Chem. Soc. Farad. Trans., 2, 68, 1448 (1972).
98. G. Herzberg, *Spectra of Diatomic Molecules* (Van Nostrand, New York, 1950).
99. M.E. Riley, and A. Kuppermann, Chem. Phys. Lett., 1, 537 (1968).
100. S. Wu, and R.D. Levine, Mol. Phys., 22, 881 (1971).
101. G.L. Coté, and H.W. Thompson, Proc. R. Soc. Lond. A, 210, 206 (1951).
102. R. Newman, and R.M. Badger, J. Chem. Phys., 19, 1207 (1951).
103. J.A.A. Ketelaar, C. Haas, and J. van der Elsen, J. Chem. Phys., 24, 624 (1956).
104. J.A. Salthouse, and T.C. Waddington, J. Chem. Phys., 48, 5274 (1968).

105. A. Azman, and A. Ocvirk, *Spectrochim. Acta*, 23A, 1597 (1967).
106. L. Couture, and J.P. Mathieu, *Compt. Rend. Acad. Sci.*, 228, 555 (1949).
107. J.P. Mathieu, and L. Couture, *Compt. Rend. Acad. Sci.*, 230, 1054 (1950).
108. Z. Iqbal, *J. Chem. Phys.*, 59, 6183 (1973).
109. J.J. Rush, L.W. Schroeder, and A.J. Melveger, *J. Chem. Phys.*, 56, 2793 (1972).
110. P. Dawson, M.M. Hargreave, and G.R. Wilkinson, *Spectrochim. Acta*, 31A, 1055 (1975).
111. G.R. Wilkinson, *Natl. Bur. Stand. Spec. Publ.*, 301, 107 (1969).
112. R.D. Cooke, C. Pastorek, R.E. Carlson, and J.C. Decius, *J. Chem. Phys.*, 69, 5 (1978).
113. E. Spinner, *Aust. J. Chem.*, 30, 1167 (1977).
114. S.D. Hamann, and M. Linton, *Aust. J. Chem.*, 29, 479 (1976).
115. B.S. Ault, *J. Phys. Chem.*, 82, 844 (1978).
116. The ideas expressed here, concerning the assignment of bands at $3660\text{--}3830\text{ cm}^{-1}$ and $4200\text{--}4500\text{ cm}^{-1}$, were conceived by Dr. W.R. Thorson.

B30258